

---

# ART3D

(version 1.0beta)

## Analytical Model for Simulating **R**eactive Multi-species **T**ransport in **3-D**imensional Groundwater Systems

By T. P. Clement and C. Quezada

---

**Draft report**  
**Please do not cite**

## **ART3D (An analytical tool for modeling coupled reaction in 3-Dimensional groundwater systems)**

### **1. Introduction**

Modeling the fate and transport of multiple reactive contaminants in groundwater aquifers has received considerable attention in recent years. Due this increased attention, several numerical codes have been developed for analysing different types of reactive transport problems [Rifai et al., 1990; Clement et al., 1998; Chilakapati et al., 1998]. However, due to numerical complexities, application of these codes to field-scale problems requires considerable time and effort. Analytical models, on the other hand, provide a simple alternative for analysing the fate and transport of reactive or non-reactive contaminants. They are particularly useful at the site-investigation stage for performing preliminary screening simulations to evaluate the impacts of contaminant plumes [Newell et al., 1996; Carol et al., 1999]. In addition, analytical models are also useful for testing the accuracy of complex numerical reactive transport codes.

Although numerous analytical solutions are available for solving single-species transport problems, they are of limited use for site remediation design applications, because most groundwater contamination problems involve multiple reactive species. For example, radioactive contaminants, which include multiple parent and daughter species, are common multi-species reactive contaminants observed at various nuclear waste disposal facilities. Chlorinated solvent contaminants, which include multiple dissolved chlorinated organic species such as PCE (tetrachloroethylene) and TCE (trichloroethylene) and their daughter products DCE (dichloroethylene) and VC vinyl chloride; TCA (trichloroethane) and its daughter products DCA (dichloroethane) and CA (chloroethane); and CCl<sub>4</sub> (carbon tetrachloride) and its daughter product chloroform are another class of common reactive contaminants observed at several hazardous waste sites throughout the United States. At these sites, use of single-species analytical models to analyze the fate-and-transport mechanisms of a (parent) species, may not be adequate to evaluate the overall impacts; some of the degradation daughter products (such as VC produced from TCE) might be more detrimental to the environment than the parent species. Hence, a detailed analysis of the entire decay chain is usually required to perform a comprehensive environmental impact assessment of these types of reactive contaminants.

Analytical solutions to multi-species reactive transport equations are currently available only for a limited number of first-order reactive transport problems. van Genuchten [1985] presented a one-dimensional analytical solution to a four-species transport problem. Lunn et al. [1996] used the Fourier transform method to derive an analytical solution to a first-order, three-species reactive transport system. Khandelwal and Rabideau [1999] presented an analytical solution to a sequentially decaying reaction chain (parent and three daughter products) influenced by linear non-equilibrium sorption; they also demonstrated the application of the new solution for evaluating permeable reactive barrier designs. However, almost all multi-species analytical models available in

the literature can only be used for solving one-dimensional problems, which greatly limits their use in realistic field-scale situations.

Sun et al. [1999 a] presented a transformation format to solve reactive transport equations that are coupled with sequential first-order reactions. The method is general enough to solve the reactive transport of any number of sequential reactive species in one, two, or three dimensions. Sun et al. [1999 b] extended the method to analyze serial and parallel reaction networks. Sun and Clement [1999] further generalized the solution strategy and proposed a numbering scheme for systematically representing and solving multiple serial-parallel reactions, and presented two- and three-dimensional validation results for the solution strategy under various initial and boundary conditions. However, in all of the above manuscripts, the basic solution format employed was simply presented (not derived) without any fundamental analysis. Although the validity of the transformation format was tested extensively by comparing it against numerical solutions [Sun and Clement, 1999], the fundamental principles behind the solution strategy were never discussed. Moreover, the approach discussed in Sun et al. [1999 a, b] and Sun and Clement [1999] cannot be used to solve complex reactions such as reversible reactions, converging reactions, and multi-parent reactions.

Clement (2001) presented a generalized singular value decomposition method for solving multi-species transport equations, which are coupled with any type of first-order reactions. ART3D is an analytical three-dimensional reactive transport model that was developed based on this solution strategy. ART3D is a Fortran code that the Clement (2001) method for solving any number of transport equations which are coupled with multi-parent, serial, parallel, converging, diverging, and/or reversible first-order reactions. Further, the code can be run in a batch mode to solve the reaction equations in a completely mixed reactor.

## Governing Equations

Considering that the velocity in the x direction is uniform, the three-dimensional transport equations that describe one-dimensional advection, three-dimensional dispersion, linear sorption, first-order biodegradation and multiple reactive contaminants are shown below.

$$R_i \frac{\partial c_i}{\partial t} + v \frac{\partial c_i}{\partial x} - D_x \frac{\partial^2 c_i}{\partial x^2} - D_y \frac{\partial^2 c_i}{\partial y^2} - D_z \frac{\partial^2 c_i}{\partial z^2} = \sum_{j=1}^{i-1} y_{i/j} k_j c_j - k_i c_i + \sum_{j=i+1}^n y_{i/j} k_j c_j, \quad \forall i = 1, 2, \dots, n \quad (1)$$

where  $c_i$  is the  $i$ th species concentration [ $\text{ML}^{-3}$ ];  $D_x$ ,  $D_y$ , and  $D_z$  are the hydrodynamic dispersion coefficients [ $\text{ft}^2/\text{yr}$ ];  $v$  is the contaminant transport velocity [ $\text{ft}/\text{yr}$ ];  $k$  is the first-order degradation coefficient [ $1/\text{yr}$ ];  $y$  is the yield coefficient [a dimensionless value];

for example,  $y_1$  would represent the mg of TCE produced per unit mg of PCE destroyed]; and  $R_1, R_2, R_3, R_4,$  and  $R_5$  are respective retardation factors.

Owing to the way in which this code was developed, the retardation factor values used by ART3D corresponds to "effective retardation factor,  $R$ ". This new effective factor is the average of retardation factor values of different species. An explanation more itemized of this consideration is found in the chapters that are shown later.

In whose case where there is not transport of contaminant, that is, only natural attenuation reactions are occurring (Batch reactor); equation (1) can be simplified as.

$$\frac{dc_i}{dt} = \sum_{j=1}^{i-1} y_{i/j} k_j c_j - k_i c_i + \sum_{j=i+1}^n y_{i/j} k_j c_j, \quad \forall i=1,2,\dots,n \quad (2)$$

The only difference between equation (1) and (2) is that in the second one the concentration of contaminant depends only on time and not on the position. The parameters showed in equation (2) have the same meaning as in equation (1).

ART3D was elaborated to solve both situations, transport (1) and Batch (2), but not simultaneously. Depending on the features of the problem, one of these must be chosen at the beginning of the simulation process.

## 1.2 Analytical Solution Strategy

The coupled reactive transport system described by equations (1) can be compactly represented by using matrix notation as:

$$\mathbf{R} \hat{\mathbf{c}}' + v \hat{\mathbf{c}}_x^1 - D_x \hat{\mathbf{c}}_x^2 - D_y \hat{\mathbf{c}}_y^2 - D_z \hat{\mathbf{c}}_z^2 = \mathbf{K} \hat{\mathbf{c}} \quad (3)$$

where bold letters are used to represent square matrices, and the symbol  $\hat{\mathbf{c}}$  is used to represent column matrices (or vectors);  $\hat{\mathbf{c}}$  is the concentration vector;  $\hat{\mathbf{c}}'$  is the temporal derivative of the concentration vector;  $\hat{\mathbf{c}}_x^1$  is the x component of the first spatial derivative of the concentration;  $\hat{\mathbf{c}}_x^2$  is the x component of the second spatial derivative of the concentration vector (similar notations are used for the y and z components);  $\mathbf{R}$  is the retardation matrix; and  $\mathbf{K}$  is the reaction coefficient matrix. Matrices in equation (3) can be explicitly assembled for any type of first-order reactive transport system having any number of species. As an example, for a four-component sequential reactive transport system (e.g.,  $\text{PCE} \rightarrow \text{TCE} \rightarrow \text{DCE} \rightarrow \text{VC}$ ), the matrix equation can be written as:

$$\begin{aligned}
& \begin{bmatrix} R_1 & 0 & 0 & 0 \\ 0 & R_2 & 0 & 0 \\ 0 & 0 & R_3 & 0 \\ 0 & 0 & 0 & R_4 \end{bmatrix} \begin{bmatrix} \frac{\partial c_1}{\partial t} \\ \frac{\partial c_2}{\partial t} \\ \frac{\partial c_3}{\partial t} \\ \frac{\partial c_4}{\partial t} \end{bmatrix} + \begin{bmatrix} v \frac{\partial c_1}{\partial x} \\ v \frac{\partial c_2}{\partial x} \\ v \frac{\partial c_3}{\partial x} \\ v \frac{\partial c_4}{\partial x} \end{bmatrix} - \begin{bmatrix} D_x \frac{\partial^2 c_1}{\partial x^2} \\ D_x \frac{\partial^2 c_2}{\partial x^2} \\ D_x \frac{\partial^2 c_3}{\partial x^2} \\ D_x \frac{\partial^2 c_4}{\partial x^2} \end{bmatrix} - \begin{bmatrix} D_y \frac{\partial^2 c_1}{\partial y^2} \\ D_y \frac{\partial^2 c_2}{\partial y^2} \\ D_y \frac{\partial^2 c_3}{\partial y^2} \\ D_y \frac{\partial^2 c_4}{\partial y^2} \end{bmatrix} - \begin{bmatrix} D_z \frac{\partial^2 c_1}{\partial z^2} \\ D_z \frac{\partial^2 c_2}{\partial z^2} \\ D_z \frac{\partial^2 c_3}{\partial z^2} \\ D_z \frac{\partial^2 c_4}{\partial z^2} \end{bmatrix} \\
& = \begin{bmatrix} -k_1 & 0 & 0 & 0 \\ y_2 k_1 & -k_2 & 0 & 0 \\ 0 & y_3 k_2 & -k_3 & 0 \\ 0 & 0 & y_4 k_3 & -k_4 \end{bmatrix} \begin{bmatrix} c_1 \\ c_2 \\ c_3 \\ c_4 \end{bmatrix}, \tag{4}
\end{aligned}$$

where the concentration terms  $c_1$ ,  $c_2$ ,  $c_3$ , and  $c_4$  are temporally and spatially variable unknown concentrations of the transported species.

Since the reaction coefficient matrix (**K**-matrix) on the right-hand side of equation (3) will usually have several cross-coupling terms (as shown in (4)), the set of coupled partial differential equations must be solved simultaneously to evaluate the unknown concentrations. However, for special cases when the **K**-matrix is in a diagonal form, the partial differential equations will become uncoupled and under this condition each transport equation can be solved independently. The technique simply uses a series of judiciously chosen linear transformations to equation (3) to transform the coupled system into a new domain where **K** will be in a diagonal form. In this transformed domain, the uncoupled transport equations are solved individually to compute concentrations. Later, an inverse transformation equation is used to transform the concentrations back to the original domain.

As a first step in the solution strategy, let us assume an arbitrary  $n \times n$  transformation matrix **S** and use its inverse matrix to perform the following linear transformation:

$$\hat{\mathbf{b}} = \mathbf{S}^{-1} \hat{\mathbf{c}} \tag{5}$$

Conversely, the transformation equation can also be written in an inverse form:

$$\hat{\mathbf{c}} = \mathbf{S} \hat{\mathbf{b}} \tag{6}$$

Note the transformation matrices  $\mathbf{S}^{-1}$  and **S**, respectively, are used to transform the original concentration vector  $\hat{\mathbf{c}}$  into a transformed "b" domain or to convert the transformed concentration vector  $\hat{\mathbf{b}}$  back to the original "c" domain.

Using principles of linear transformation, we can also transform the temporal derivatives of  $\hat{\mathbf{c}}$  to the "b" domain using the relation:

$$\hat{\mathbf{b}}' = \mathbf{S}^{-1} \hat{\mathbf{c}}'. \quad (7)$$

where matrix  $\mathbf{S}$  is assumed to be independent of both temporal and spatial variations. Also, spatial derivatives of the  $\mathbf{c}$  vector can be transformed using the expression:

$$\hat{\mathbf{b}}_x^2 = \mathbf{S}^{-1} \hat{\mathbf{c}}_x^2. \quad (8)$$

Similar expressions can be written for the y and z components of  $\hat{\mathbf{c}}$  and also for  $\hat{\mathbf{c}}_x^1$ . Using expressions 5 through 8, equation (3) can be transformed as:

$$\mathbf{R}\mathbf{S}\hat{\mathbf{b}}' + v\mathbf{S}\hat{\mathbf{b}}_x^1 - D_x \mathbf{S}\hat{\mathbf{b}}_x^2 - D_y \mathbf{S}\hat{\mathbf{b}}_y^2 - D_z \mathbf{S}\hat{\mathbf{b}}_z^2 = \mathbf{K}\mathbf{S}\hat{\mathbf{b}} \quad (9)$$

Pre-multiplying the inverse matrix  $\mathbf{S}^{-1}$  to every term in equation (9), we can obtain the following expression:

$$\mathbf{S}^{-1}\mathbf{R}\mathbf{S}\hat{\mathbf{b}}' + v\hat{\mathbf{b}}_x^1 - D_x \hat{\mathbf{b}}_x^2 - D_y \hat{\mathbf{b}}_y^2 - D_z \hat{\mathbf{b}}_z^2 = \mathbf{S}^{-1}\mathbf{K}\mathbf{S} \hat{\mathbf{b}} \quad (10)$$

Now, if we assume that  $\mathbf{S}^{-1}\mathbf{R} = \mathbf{R}\mathbf{S}^{-1}$  and if  $\mathbf{S}^{-1}\mathbf{K}\mathbf{S} = \tilde{\mathbf{K}}$ , where  $\tilde{\mathbf{K}}$  will be a diagonal matrix (validity of these two assumptions will be discussed later), then:

$$\mathbf{R}\hat{\mathbf{b}}' + v\hat{\mathbf{b}}_x^1 - D_x \hat{\mathbf{b}}_x^2 - D_y \hat{\mathbf{b}}_y^2 - D_z \hat{\mathbf{b}}_z^2 = \tilde{\mathbf{K}} \hat{\mathbf{b}}. \quad (11)$$

Note that the format of equation (11) is similar to equation (3); however, since  $\tilde{\mathbf{K}}$  is a diagonal matrix, equation (9) represents a set of n independent (uncoupled) transport equations that can be explicitly solved to evaluate the concentration vector  $\hat{\mathbf{b}}$  in the transformed "b" domain. A standard analytical solution can be used to solve this uncoupled advection-dispersion equation with an "appropriate" first-order decay term. The initial and boundary conditions must be transformed to the "b" domain before obtaining the analytical solution. After computing the concentrations in the "b" domain, equation (6) can be used to transform the concentrations back to the "c" domain.

At this stage, the validity of the assumptions used in deriving equation (9) must be established. The two relevant questions that need to be addressed are:

- 1) Under what conditions can we assume  $\mathbf{S}^{-1}\mathbf{R} = \mathbf{R}\mathbf{S}^{-1}$ , in order to simplify the first term in equation (9)?
- 2) How can we compute the transformation matrix  $\mathbf{S}$  that would satisfy the relationship  $\mathbf{S}^{-1}\mathbf{K}\mathbf{S} = \tilde{\mathbf{K}}$ , where  $\tilde{\mathbf{K}}$  must be a diagonal matrix?

The answer to the first question is straightforward. Since matrix multiplication is not, in general, a commutative operation  $\mathbf{S}^{-1}\mathbf{R}$  can be guaranteed to be equal to  $\mathbf{R}\mathbf{S}^{-1}$  if and only if  $\mathbf{R}$  is a diagonal matrix and the diagonal entries of  $\mathbf{R}$  are identical. This requirement implies that the solution strategy is applicable only when the transport equations have identical retardation values, which is clearly a major limitation of this solution strategy.

To answer the second question, we will use the following matrix properties related to similarity transformation of matrices [Johnson and Riess, 1981]:

- *If  $\mathbf{P}$  is a square matrix whose column vectors are the eigenvectors of a matrix  $\mathbf{A}$ , then  $\mathbf{P}^{-1}\mathbf{A}\mathbf{P} = \mathbf{D}$ , where  $\mathbf{D}$  will be a diagonal matrix; also the diagonal entries of  $\mathbf{D}$  are nothing but the eigenvalues of  $\mathbf{A}$ . The matrices  $\mathbf{A}$  and  $\mathbf{D}$  are known to be similar matrices. The process of decomposing a square matrix  $\mathbf{A}$  into a  $\mathbf{P}\mathbf{D}\mathbf{P}^{-1}$  form is known as the similarity transformation.*

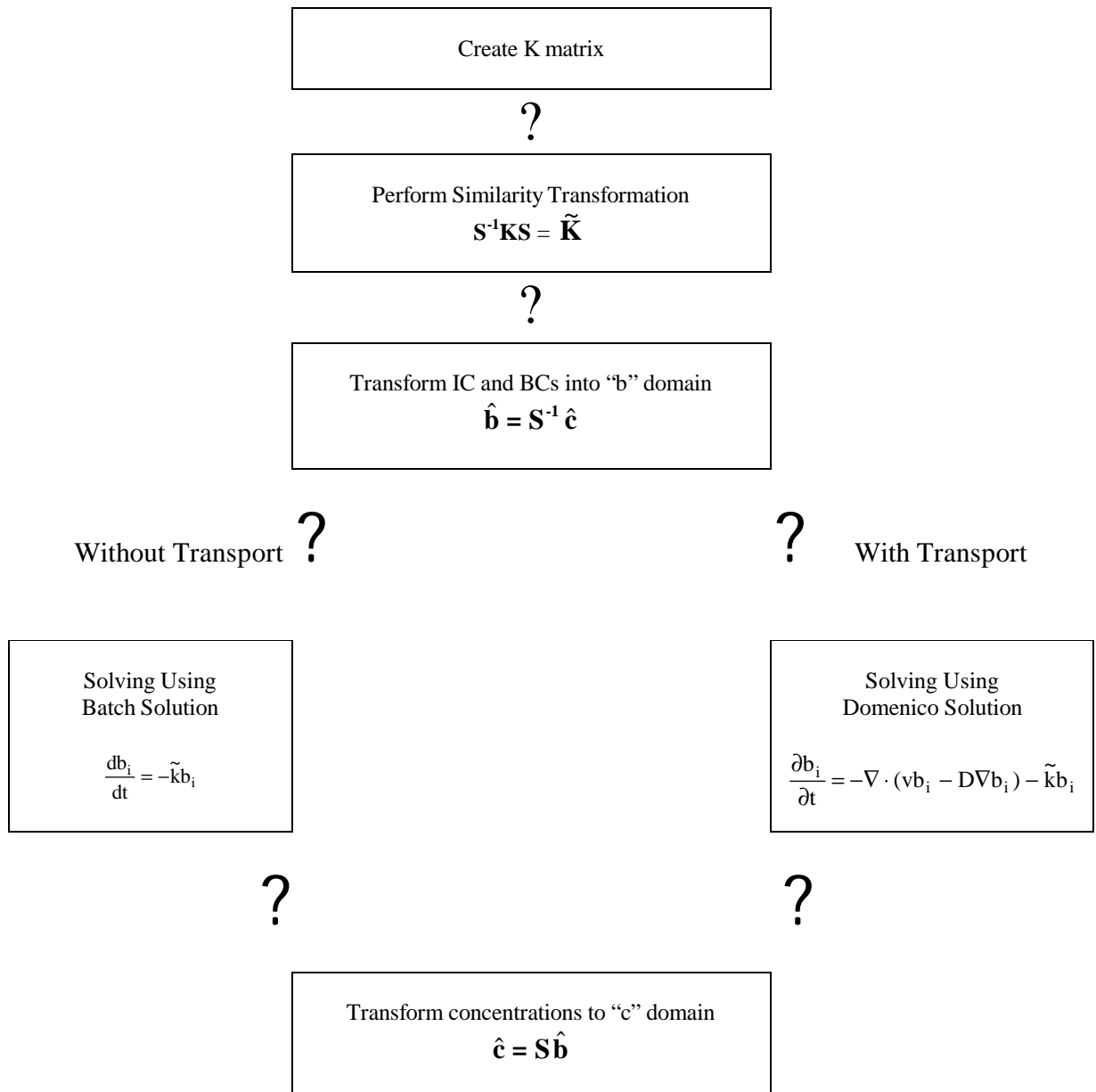
Based on these matrix properties, we can conclude that our problem of finding  $\mathbf{S}$  and  $\mathbf{S}^{-1}$  reduces to performing a similarity transformation analysis of the  $\mathbf{K}$  matrix. Several general-purpose numerical computer algorithms are available for solving the similarity transformation problem [Press et al., 1992]. One of these algorithms can be used to numerically evaluate the  $\mathbf{S}$  and  $\mathbf{S}^{-1}$  matrices for a given  $\mathbf{K}$  matrix. Once  $\mathbf{S}^{-1}$  is known, the initial and boundary conditions of the problem can be transformed to the "b" domain using equation (5), and then the uncoupled transport equations can be independently solved in the "b" domain. Later, the  $\mathbf{S}$  matrix can be used to transform the concentrations back to the "c" domain by employing equation (6). Note the  $\mathbf{K}$  matrix can be used to represent any combination of first-order reaction, including multi-parent reactions, converging, and/or reversible reactions, provided all the reaction steps follow first-order kinetics.

ART3D also solves a set of coupled partial differential equations to describe the natural attenuation reactions of some species, that is, does not exist transport of contaminants (2). The methodology utilized is exactly the same as the mention above, but to solve the system uncoupled, the Batch solution is used rather than the Domenico.

The only constraint of this procedure is that if two species are related, that is, one species is daughter of other, then they can not have the same  $k$  value (first-order rate). This would cause that the  $\mathbf{S}$  matrix does not have inverse, and hence, the equations system would not be solved. To clarify this point, we will take the reaction shown in Figure 4.1-1 as an example. For this case, PCA, 112TCA, 12DCA and CA can not have the same  $k$  value. The same situation is found in TCE, x-DCE and VC. A third group is made up by PCA, 112TCA and VC. Finally, the last set of species with this limitation is PCA, x-12DCE and VC. Conversely, x-DCE might have the same  $K$  value as 112TCA and, even so, the transformation would be successful.

A general computer algorithm for implementing this solution strategy is shown in Figure 2.2-1.

Figure 2.2-1. Algorithm used by ART3D



### 1.3 Comparison between BIOCHLOR and ART3D capabilities

There are several differences and similarities are worth to mention between these two fortran codes. In first place, the mathematical analysis done to develop both code are similar, since in both case was used a linear transformation to derive an analytical solution to equations coupled, but the methodology utilized to create ART3D is pretty more general. This is reflected in the major variability of reactions that this code can solve, for example multiparent, serial, parallel, converging, etc., whereas BIOCHLOR is limited to solve only problems of sequential reaction (e.g.,  $PCE \rightarrow TCE \rightarrow DCE \rightarrow VC$ ).

As noted previously, ART3D has an interface with GMS. This permits to have a visualization of center-line concentration distribution, a visualization of two-dimensional contours at the water table (in the x-y plane), a visualization of two-dimensional contours in cross-sections (in the x-z plane) and a visualization of three-dimensional plume. Furthermore, all the information is used to create an animation of transient plume migration patterns in multiple dimensions. As for output files generate by BIOCHLOR, they can only be used to make a plot of center-line concentration distribution, and also, to show a two-dimensional contours in x-y plane. This last graph is mainly schematic, since the amounts of points that are required to make the plot are very few, and therefore, it can not be considered to take any relevant decision.

Another positive feature of ART3D is that the data used do not need to have specific units, but they must be consistent, whereas BIOCHLOR was developed to work only with units of feet and years.

ART3D has the capability to solve problems with transport of contaminants and without it (natural attenuation reaction).

BIOCHLOR has some features that were not considered in ART3D. First, BIOCHLOR simulate the solute transport with sequential first-order decay in two zones, that is, it allows the user to use two different set of rate constants within the model area. Also, It has an input area for field data, which become quite important for calibrating the model. Finally, BIOCHLOR gives an approximate solution to variable dispersion problem.

Both models have limitations, which are worth to consider after using these tools in a real problem. As analytical models, they assume simple groundwater flow, therefore, these models should be used neither when the pumping produces a complicated flow field nor when there is a vertical flow gradients affecting the contaminant transport. Furthermore, both of them simplify the hydrogeology and the biological property that exists over the model area, since they assume constant values to represent the reality. For these reasons, when more accurate results are required, a numerical model must be applied.

Table 2.3-1 shows a list of the differences and similarities that there are between BIOCHLOR and ART3D capabilities

Table 2.3-1. Summary of Differences and Similarities

Feature	BIOCHLOR	ART3D
Solution to 3-D, transient, single-zone, sequential reactive transport system.	yes	yes
Solution to 3-D, transient, single-zone, any reactive transport system.	no	yes
Batch solution	no	yes
Approximate solution to steady-state, two reaction zone problem.	yes	no
Can It use any consistent units?	no	yes
Availability of Data bases and field data analysis utilities.	yes	no
Visualization of center-line concentration distribution	yes	yes
Visualization of two-dimensional contours at the water-table (in the x-y plane)	no	yes
Visualization of two-dimensional contours in cross sections (in the x-z plane)	no	yes
Visualization of three-dimensional plume	no	yes
Animation of transient plume migration patterns in multiple dimensions	no	yes

### 3. Example Problems of Batch Solution and Sequential Reactive Transport

#### 3.1 Batch Problem

In order to test the mode Batch of the ART3D code, a *Sequential Anaerobic Degradation* ( $\text{PCE} \rightarrow \text{TCE} \rightarrow \text{DCE} \rightarrow \text{VC}$ ) was simulated, and after, its results were compared with the results predicts using the finite difference numerical reactive transport solver RT3D. The initial concentration of all the species was fixed to be equal to 0 mg/L, except for PCE, which has a concentration equals to 1000 mg/L. The simulation period considered in this example correspond to 1000 days. Major information about the chemical parameters used in this example is shown in Table 3.1-1.

Table 3.1-1. Parameter Used in Batch Example

Parameter	Value
Reaction rate $k_1$	0.005 day <sup>-1</sup>
Reaction rate $k_2$	0.003 day <sup>-1</sup>
Reaction rate $k_3$	0.002 day <sup>-1</sup>
Reaction rate $k_4$	0.001 day <sup>-1</sup>
F (all of them)	1.0 mol mol <sup>-1</sup>
$Y_{\text{TCE/PCE}}$	0.7920
$Y_{\text{DCE/TCE}}$	0.7377
$Y_{\text{VC/DCE}}$	0.6445

Figures 3.1-1 and 3.1-2 show the predicted concentration of PCE and its degradation products, after 1000 days, calculated using the present analytical tool and by using RT3D code.

Figure 3.1-1. Analytical Solution (ART3D) Against Numerical Solution (RT3D)

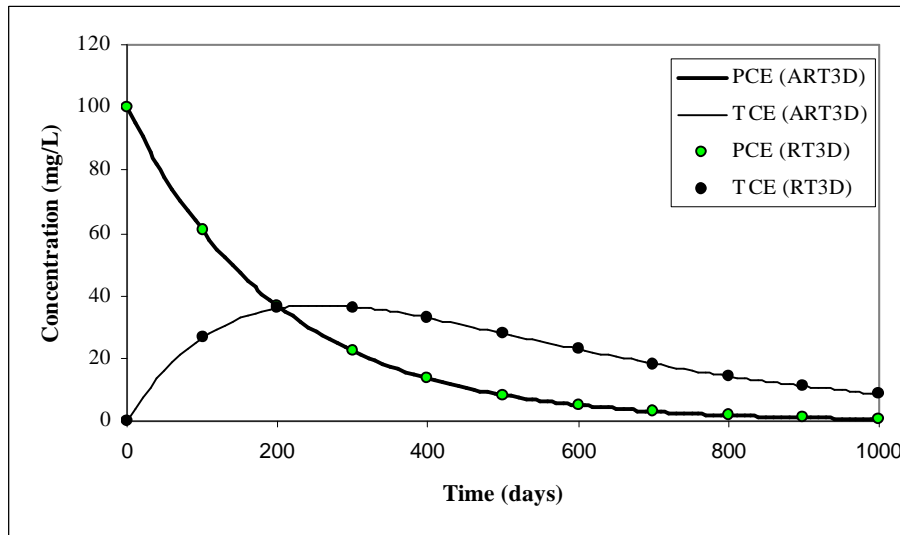
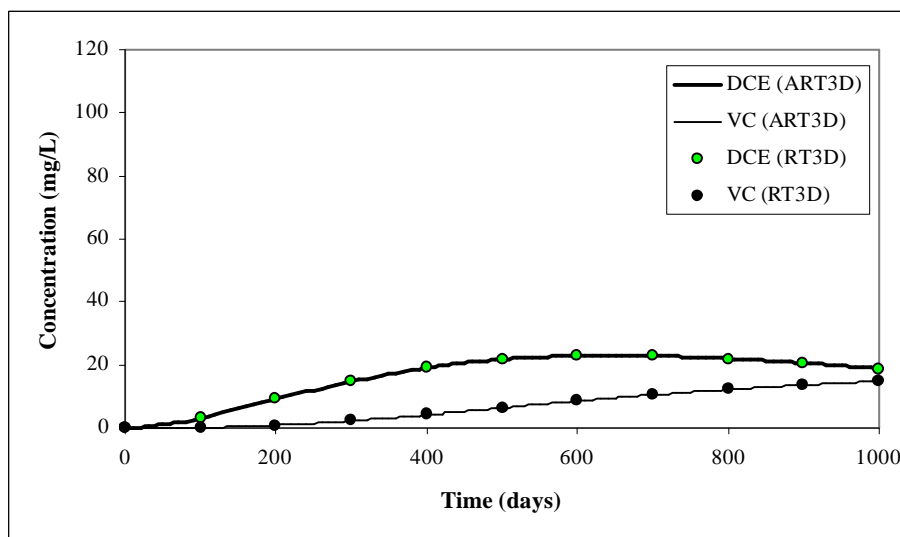


Figure 3.1-2. Analytical Solution (ART3D) Against Numerical Solution (RT3D)



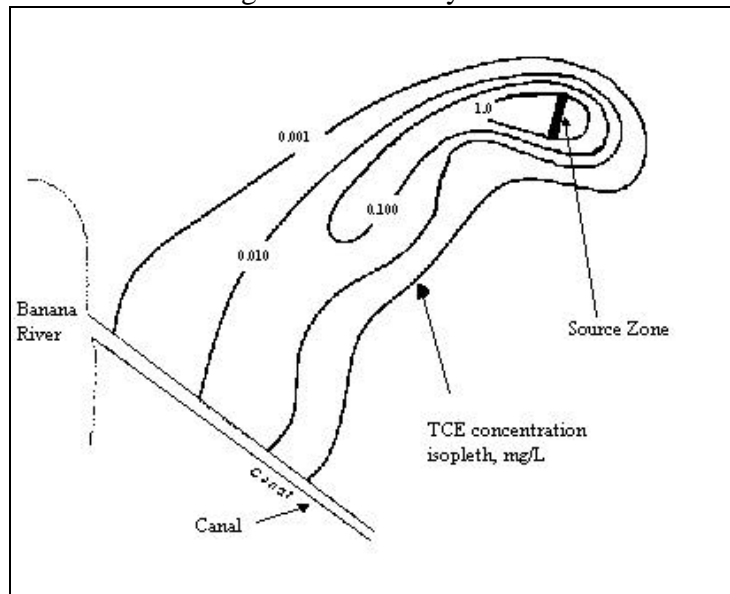
The figures above indicate that both models predict the same concentration for each species throughout the simulation period.

### 3.2 Transport Problem

The data used to test the transport mode of ART3D code were obtained from a field problem, which is reported in the BIOCHLOR manual (Version 1.0). After solving this problem by running ART3D, the results were compared with the one predicted using BIOCHLOR.

In the study zone there is a discharge of PCE and some of its daughter into the groundwater system. These solvents were released in early 1965 and the amount of contaminates discharged has stayed constant for almost 33 years (1998). All contaminates are conveyed by the groundwater flow to a canal, which, finally, converge to the Banana river. The main objective of using BIOCHLOR was to reproduce the movement of the plume throughout that period, and furthermore, to estimate the mass flux into the canal. In Figure 3.2-1 are shown the main features of this zone, that is, the locations of the river, the canal, the pollution source and the TCE concentration isopleth (1998).

Figure 3.2-1. Study Zone



The analyzed area has a length of 1085 ft and a width of 700 ft. The length is the distance from the source to the receptor (canal), and the width was chosen larger than the plume width to capture all of the mass discharging into the canal. The depth of the aquifer is 56 ft and coincides with the source thickness. The time of simulation corresponds to 33 years, from 1965 (first release) to 1998. The rest of the parameters utilized to simulate this real problem are summarized in Table 3.2-1.

Table 3.2-1. Parameter Used in Example Problem.

DATA TYPE	Parameter	Value
Hydrogeology	• Hydraulic Conductivity	$1.8 \times 10^{-2}$ (cm/s)
	• Hydraulic Gradient	0.0012
	• Effective Porosity	0.2
Dispersion	• Longitudinal Dispersivity	40 (ft)
	• Transverse Dispersivity	4 (ft)
	• Vertical Dispersivity	0 (ft)
Adsorption	• Retardation Factor	2.9
Biotransformation	• K (PCE? TCE)	2.0 (1/yr)
	• K (TCE? c-DCE)	1.0 (1/yr)
	• K (c-DCE? VC)	0.7 (1/yr)
	• K (VC? ETH)	0.4 (1/yr)
	• F (All of them)	$1.0 \text{ (mol mol}^{-1}\text{)}$
	• Y (PCE? TCE)	0.795
	• Y (TCE? c-DCE)	0.737
	• Y (c-DCE? VC)	0.645
	• Y (VC? ETH)	0.450
Source Data	• Source Thickness	56 (ft)
	• Source Width	105 (ft)
	• Source Concentrations	
	PCE	0.056 (mg/l)
	TCE	15.80(mg/l)
	c-DCE	98.50 (mg/l)
	VC	3.080 (mg/l)
ETH	0.030 (mg/l)	

In Figures 3.2-2a and 3.2-2b are shown the predicted concentrations of all four species in the centerline, after 33 years of reactive transport. Furthermore, in these Figures is presented a comparison of the results obtained using ART3D against BIOCHLOR.

Figure 3.2-2a. Concentrations of TCE and DCE.

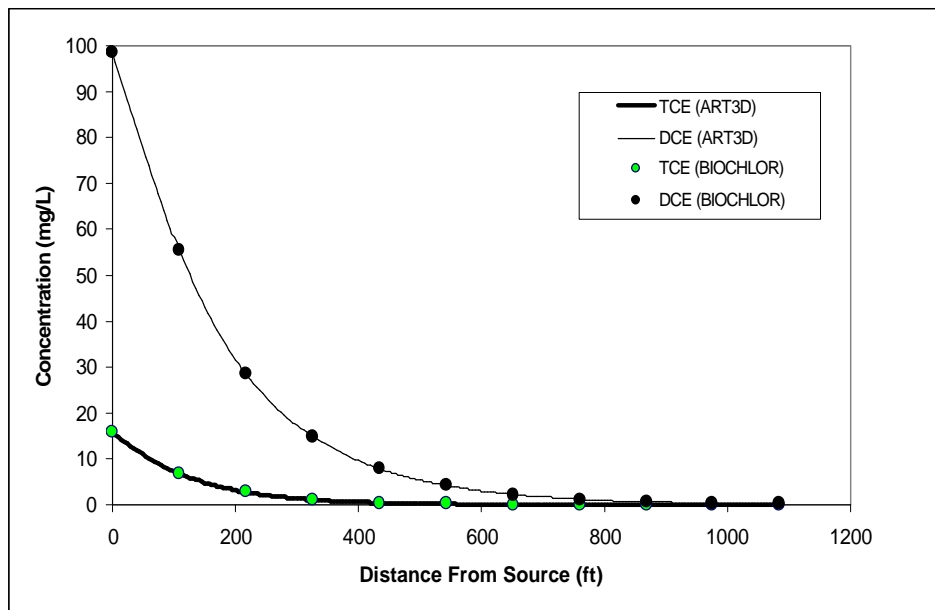
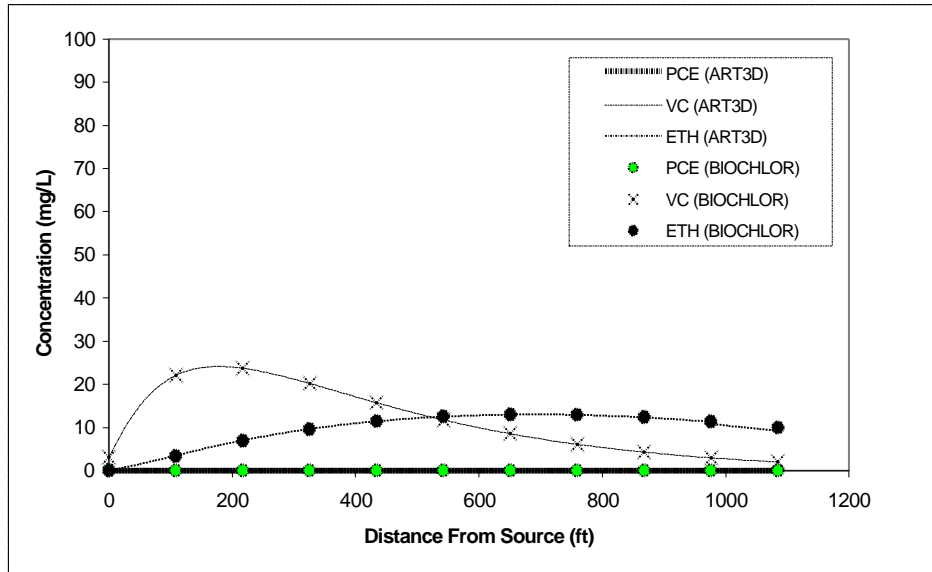


Figure 3.2-2b. Concentrations of PCE, VC and ETH.



After analyzing the graphs below, the immediate comment is that the concentrations profiles predicted by both code are equals. This should not surprise anyone, because both of them were developed applying the same algebra linear principles. For this example, the main difference is found in the manner how to show the results, since, as was mention in some item before, one of the main advantages that ART3D has is the graphic capability. In Figures 3.2-3 through 3.2-7 are given the two dimensional contours (at the water table) for each species of this example. This way of visualization of the plume is possible due to the interface that exists between ART3D and GMS.

Figure 3.2-3. Concentration of PCE at the Water Table (mg/l).

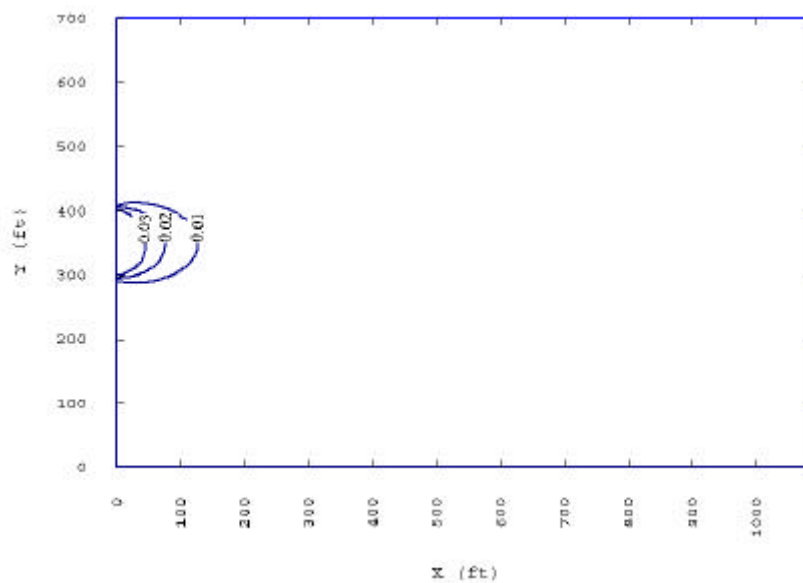


Figure 3.2-4. Concentration of TCE at the Water Table (mg/l).

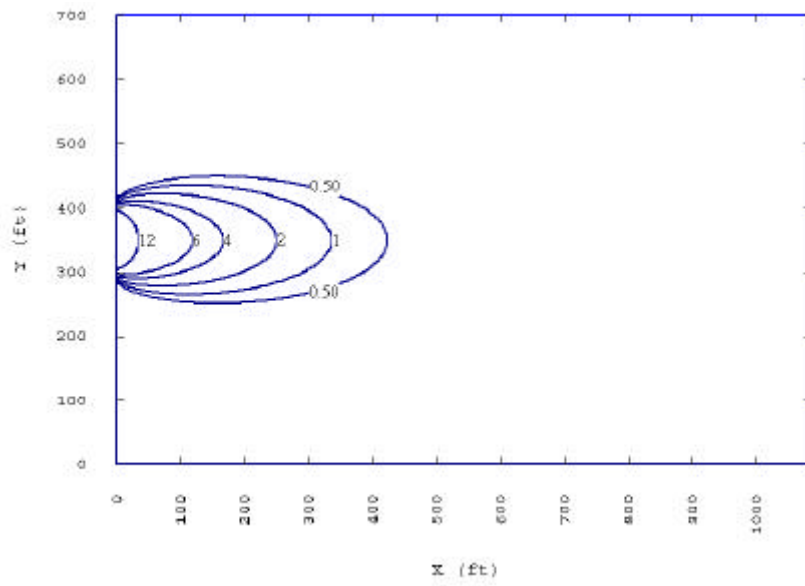


Figure 3.2-5. Concentration of DCE at the Water Table (mg/l).

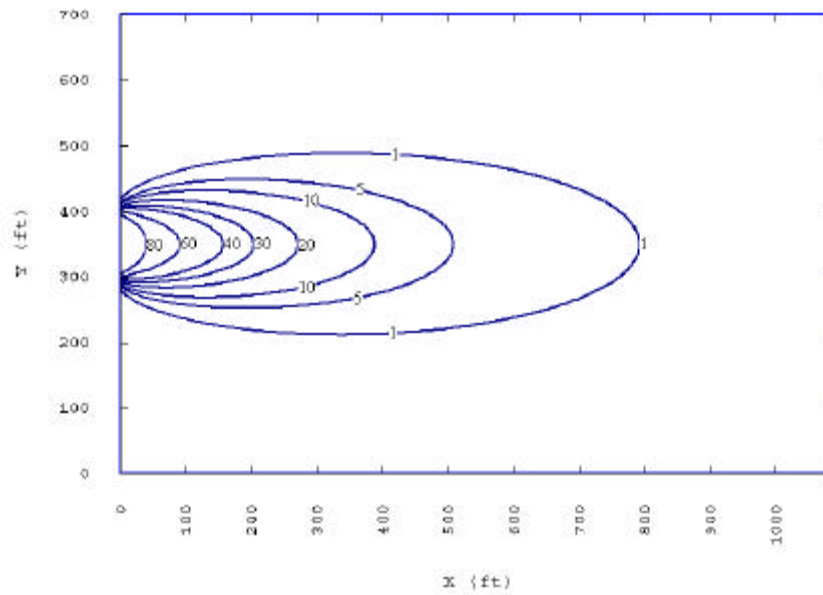


Figure 3.2-6. Concentration of VC at the Water Table (mg/l).

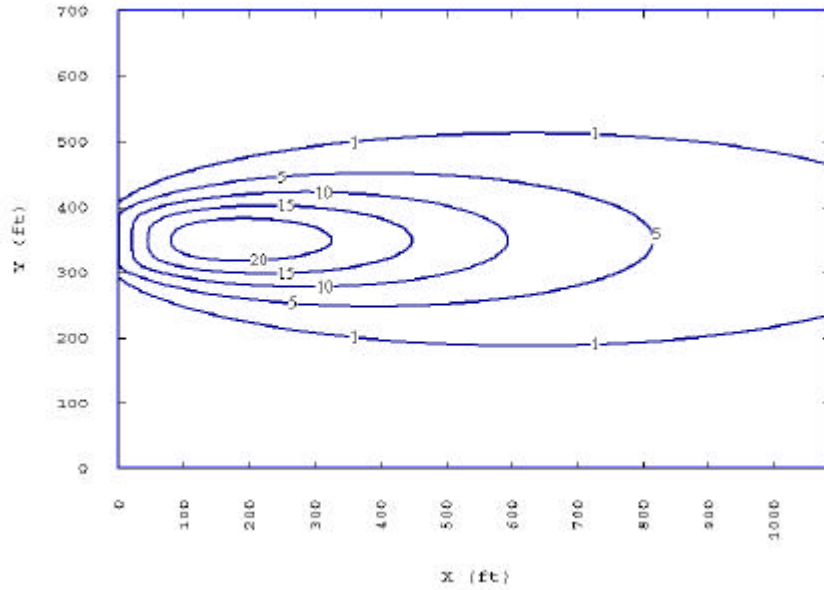
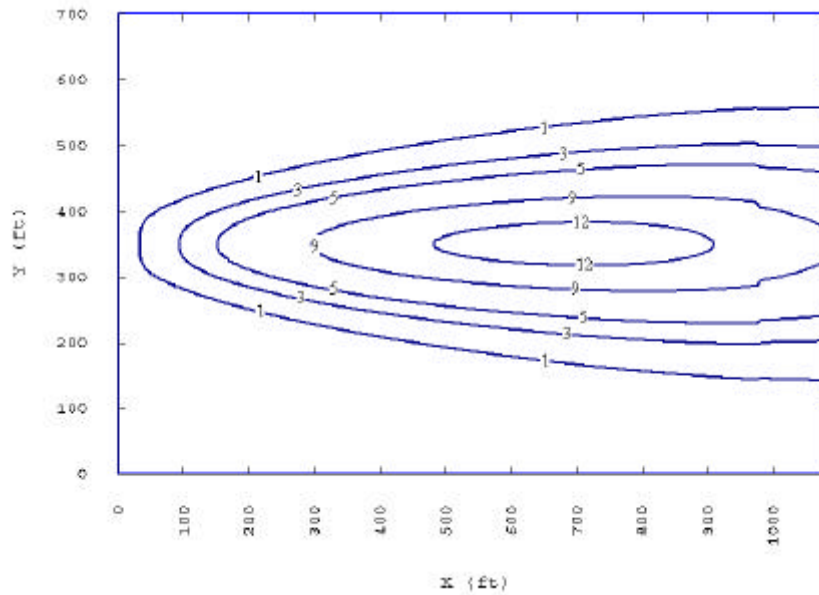


Figure 3.2-7. Concentration of ETH at the Water Table (mg/l).



ART3D also gives the users the possibility to observe the distribution of contaminates on the plane located at the centerline along the depth (x-z plane). Finally, ART3D generate a file, which can be read by GMS, and lets create a three-dimensional plot of the plume.

Owing to the fact that in this example the value of the vertical dispersivity was zero, the concentration of each species at any depth is the same as the appreciated at the water table. Therefore, despite of ART3D is able to shown a x-z plane of the aquifer, in this situation, these kind of plot are not useful. On the other hand, as a manner to summarize all the results obtained, the Figures 3.2-8 through 3.2-12 illustrate the location of the plume from a three-dimensional viewpoint.

Figure 3.2-8. Visualization three-dimensional of the PCE plume

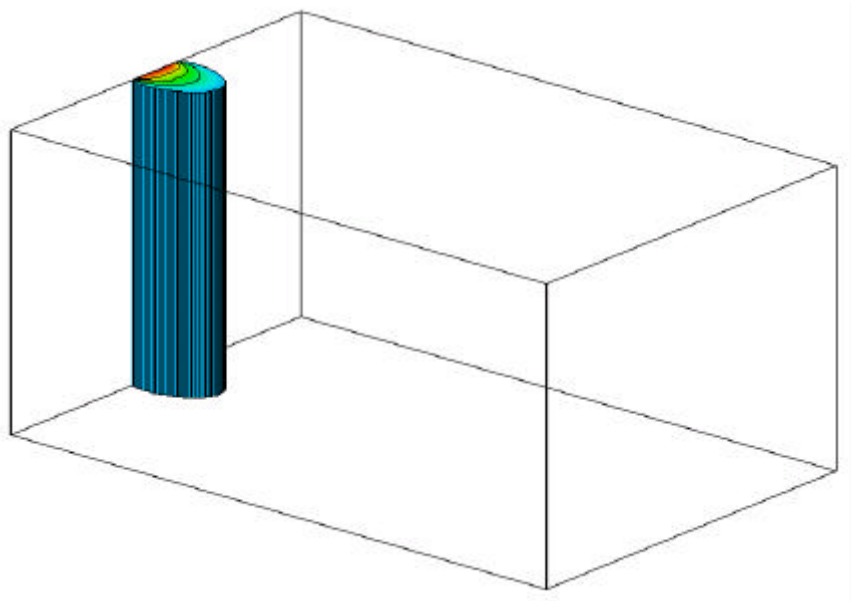


Figure 3.2-9. Visualization three-dimensional of the TCE plume

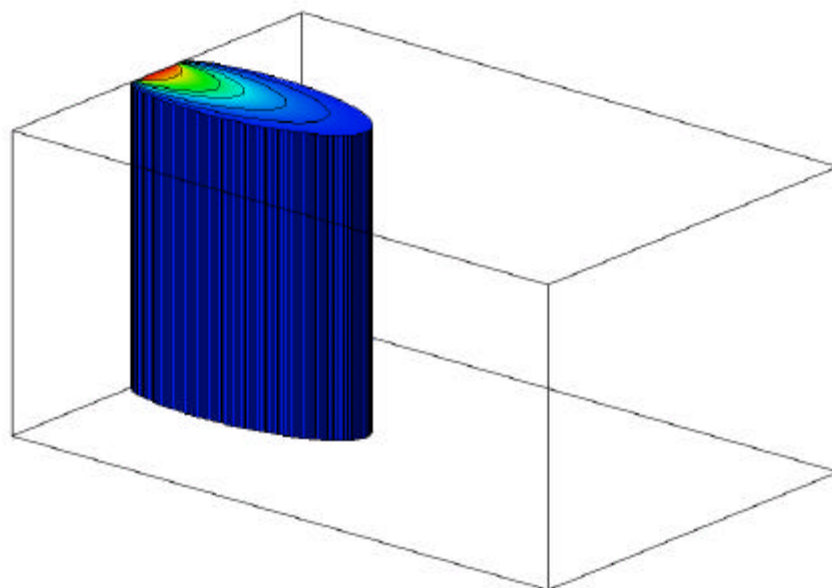


Figure 3.2-10. Visualization three-dimensional of the DCE plume

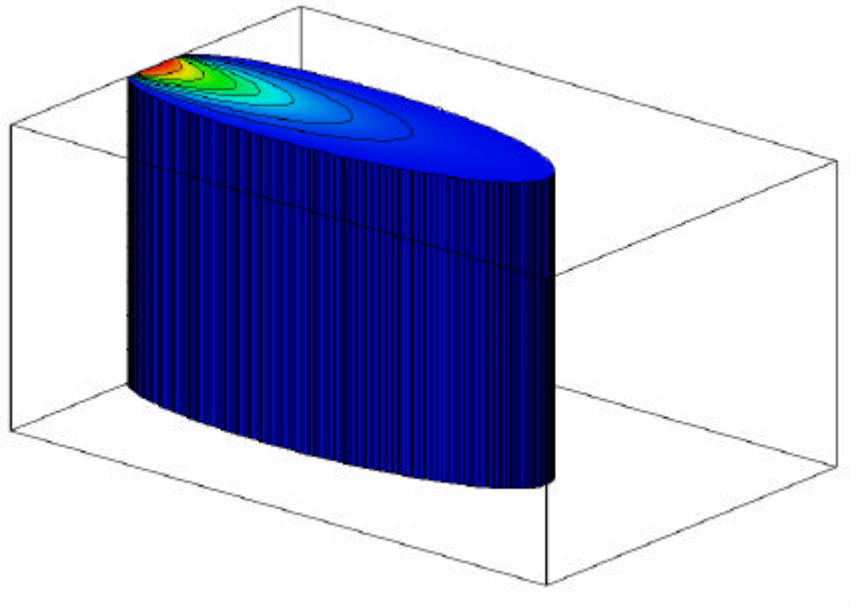


Figure 3.2-11. Visualization three-dimensional of the VC plume

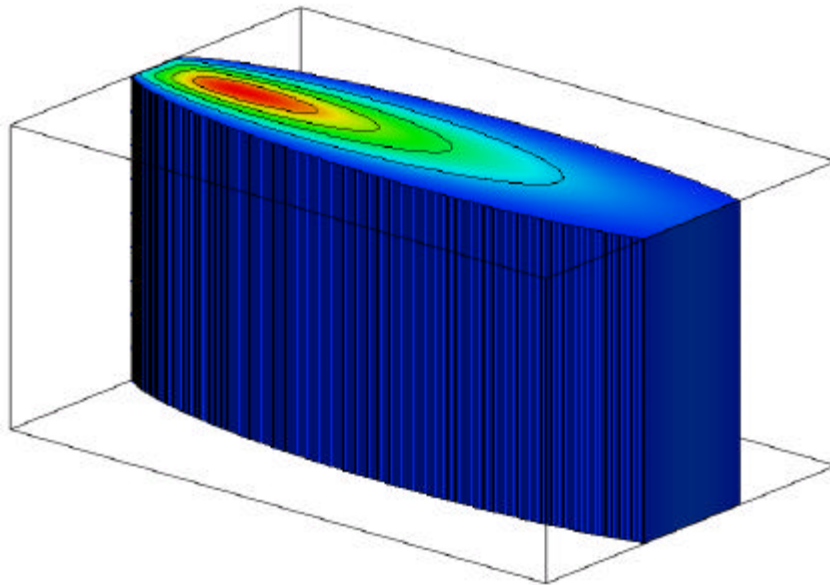
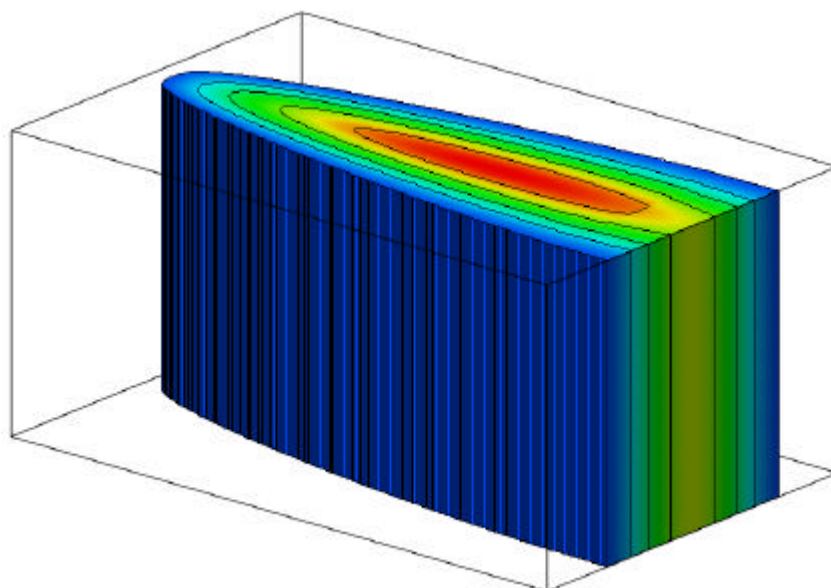


Figure 3.2-12. Visualization three-dimensional of the ETH plume



In short, although the centerline concentration distribution of all five species predicted by both code, BIOCHLOR and ART3D, turned out equals, the major spatial estimation of contaminates concentration determinate by ART3D, and its interface with GMS, become ART3D in a powerful tool. The graphs elaborated through this new code let user have a better visualization of the results, and consequently, a better understanding of the studied process.

### 3.2.1 Sensitivity Analysis

It is recommended to conduct a sensitivity analysis of each variable, when the value used comes from the literature or when the variable was estimated, but there is not certainty of its value. For example, the dispersivity values are parameters quite difficult to measure in field, then, it compulsories to understand its influence on the final results. In the transport problem developed below, most of the parameters satisfy these undesired features, therefore, in order to illustrate the response of this system to changes in the input parameter, a sensitivity analysis was carried out. The variables considered in this analysis are the following: the retardation factor, the first decay coefficient, the seepage velocity and the dispersion factors.

#### 3.2.1.1 Sensitivity Analysis-Rate Coefficient.

For this parameter, the problem was run considering values higher and smaller of the first order decay coefficient than the original situation, for all five species. In the first simulation, the parameter values were duplicated, whereas the other simulation considered a reduction of initial coefficient values in 50 %. The rest of the parameters

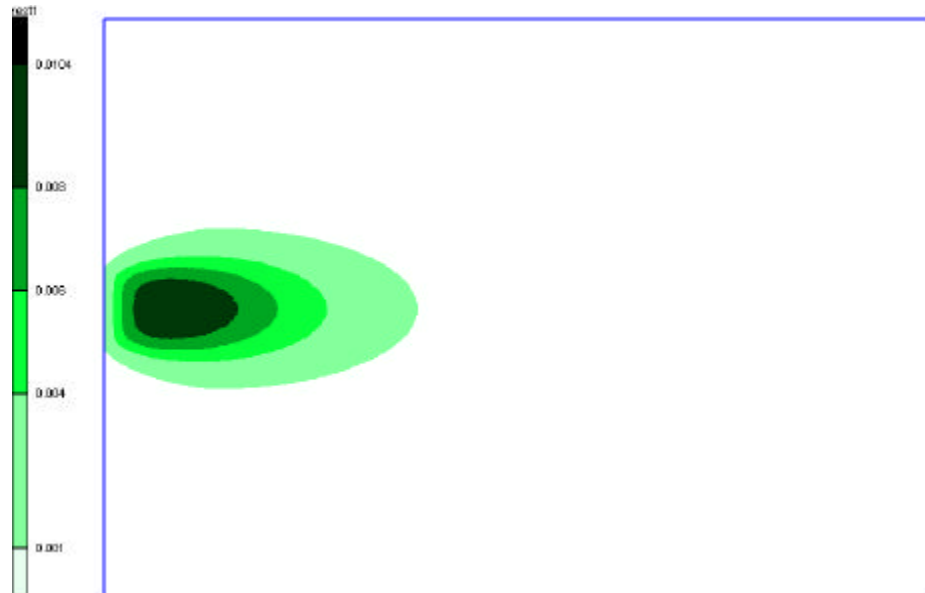
that appear in the example before did not suffer modification. Table 3.2.1.1-1 shows a summary of the values considered to conduct this analysis.

Table 3.2.1.1-1. Summary of parameter values.  
Sensitivity Analysis-Rate Coefficient

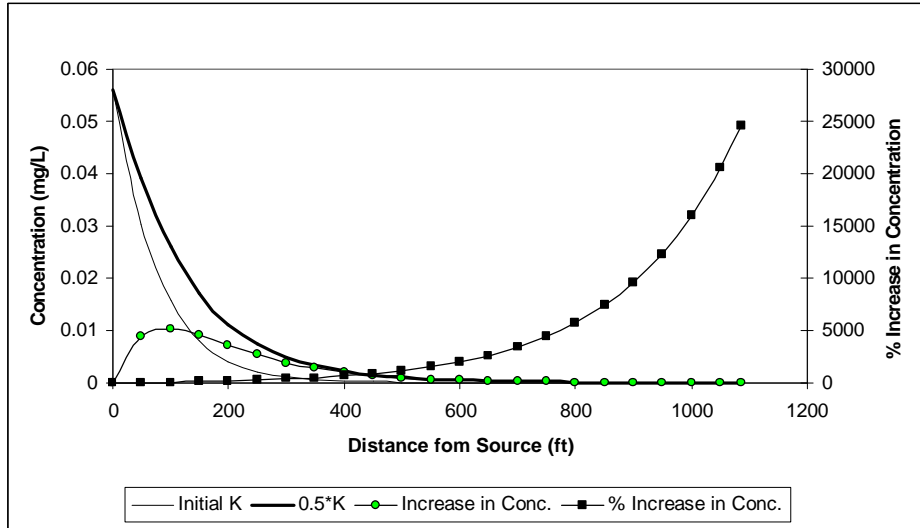
Parameter	Units	Adopted Value		
		0.5 *(Initial Value)	Initial Value	2*(Initial Value)
$K_{PCE? TCE}$	1/year	1.00	2.0	4.0
$K_{TCE? DCE}$	1/year	0.50	1.0	2.0
$K_{DCE? VC}$	1/year	0.35	0.7	1.4
$K_{VC? ETH}$	1/year	0.20	0.4	0.8
Rest of Parameters	-	No present changes		

Figures 3.2.1.1-1a through 3.2.1.1-5a illustrate the increase in the concentration of all the species on the water table (xy plane), considering that the first order decay coefficient correspond to 50 % of its initial value. These pictures permit to appreciate the influence of parameter value on the spatial distribution of the contaminant. In order to quantify the real effect of this variable on the concentration, it was necessary to analyze the change of concentration distribution in center-line. The results are shown in Figures 3.3.1-1b through 3.3.1-5b (K=50% initial value) and in Figures 3.3.1-6 to 3.3.1-10 (K=200% initial value).

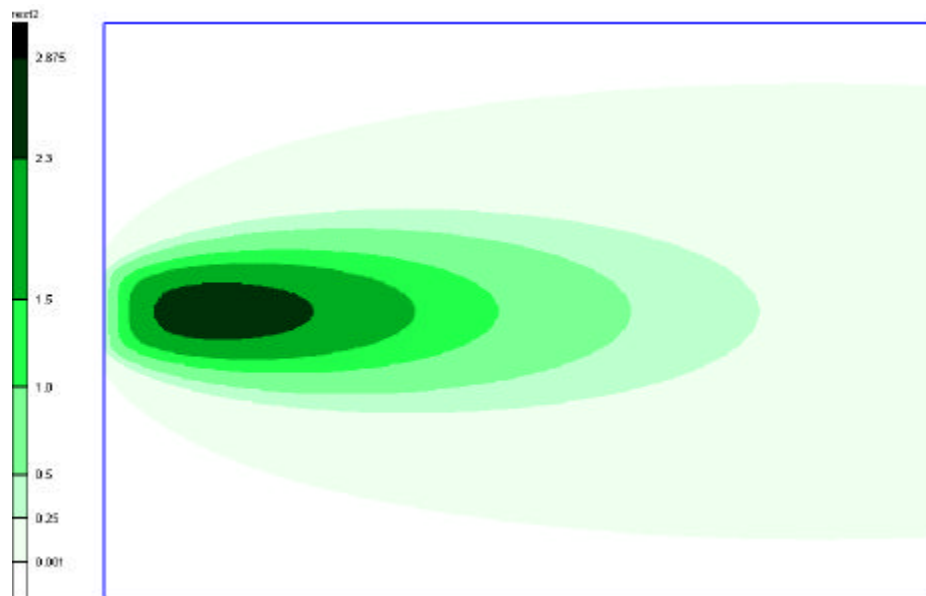
Figures 3.2.1.1-1a. Increase of PCE Concentration at the Water Table  
(K=50% Initial K)



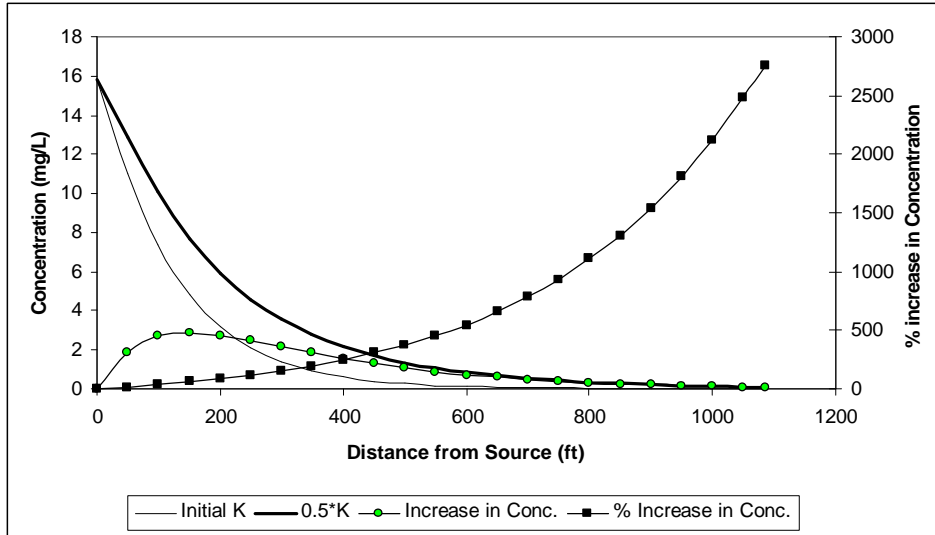
Figures 3.2.1.1-1b. Increase of PCE-Centerline (Water Table)  
(K=50% Initial K)



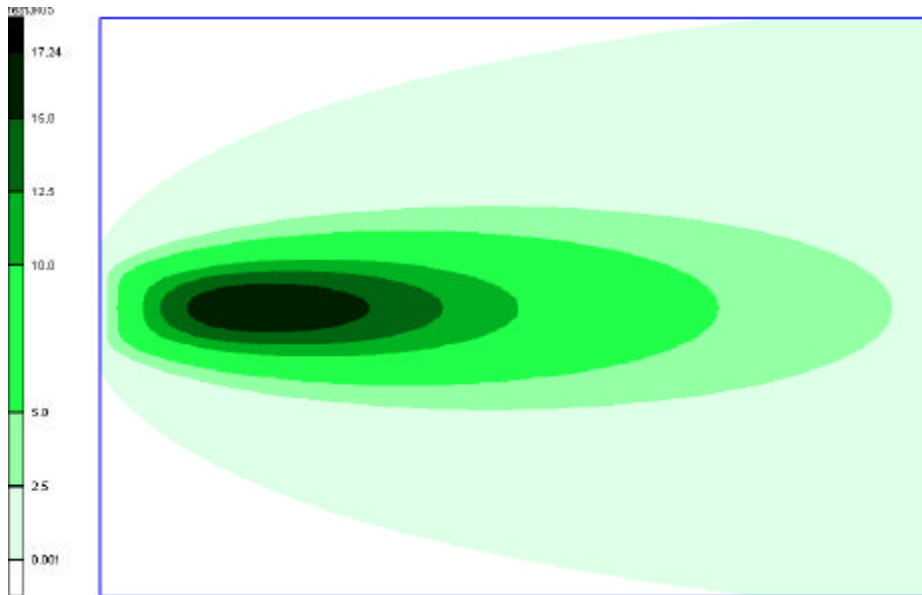
Figures 3.2.1.1-2a. Increase of TCE Concentration at the Water Table  
(K=50% Initial K)



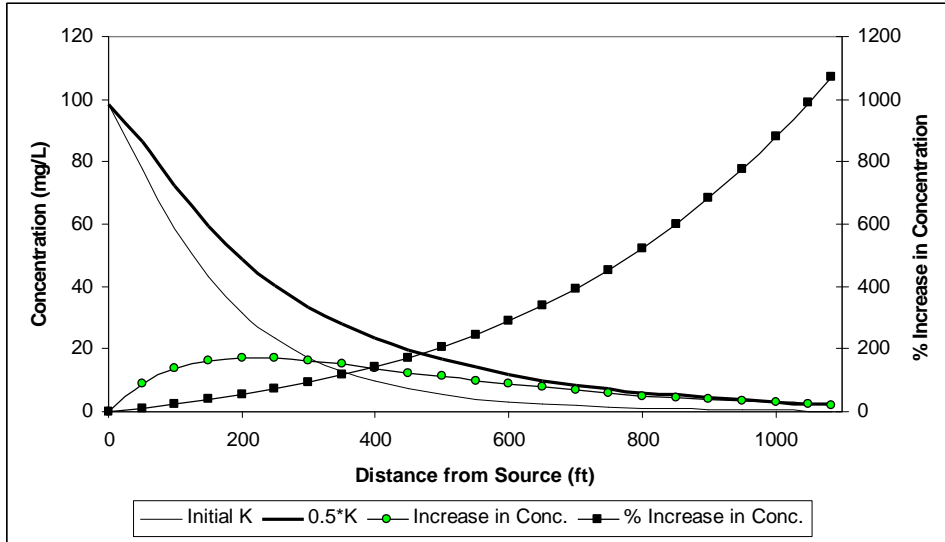
Figures 3.2.1.1-2b. Increase of TCE-Centerline (Water Table)  
(K=50% Initial K)



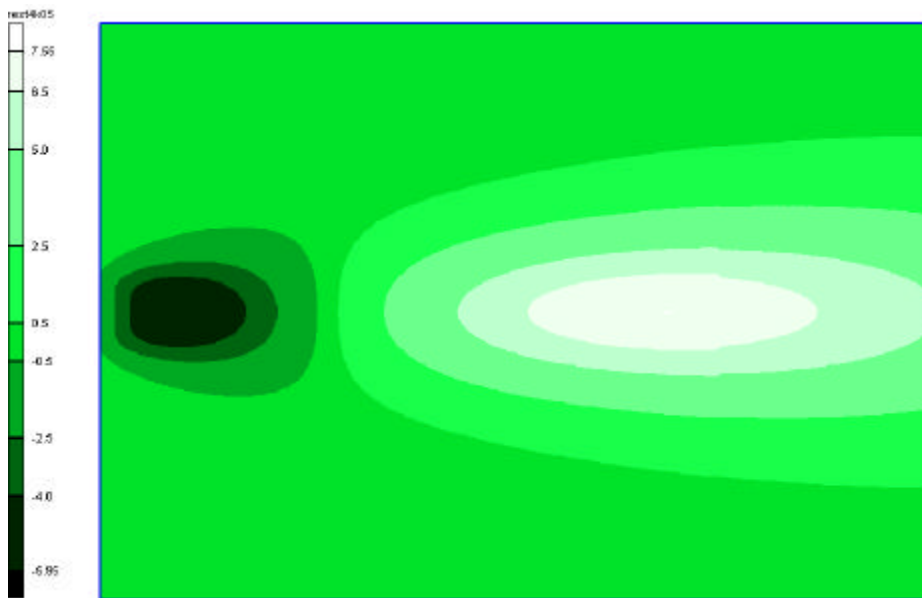
Figures 3.2.1.1-3a. Increase of DCE Concentration at the Water Table  
(K=50% Initial K)



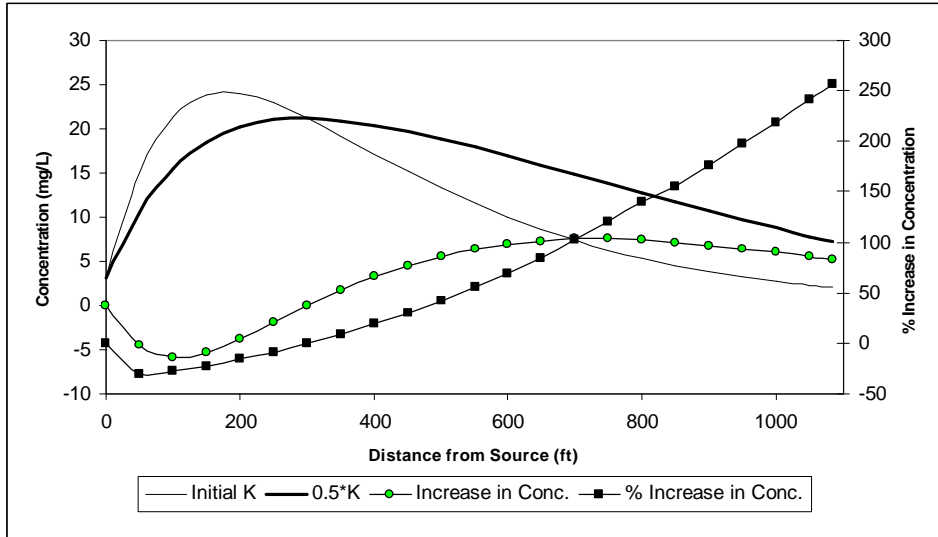
Figures 3.2.1.1-3b. Increase of DCE-Centerline (Water Table)  
(K=50% Initial K)



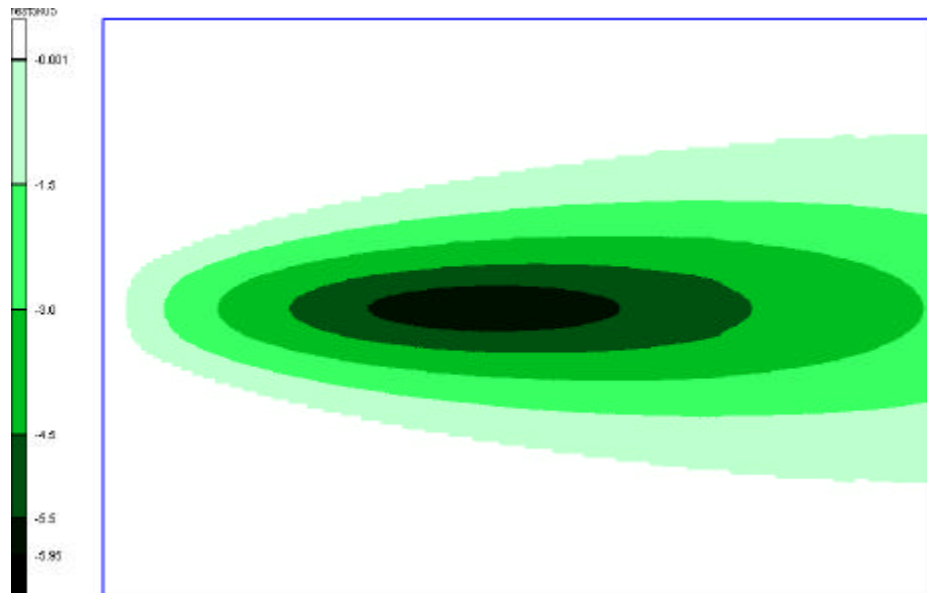
Figures 3.2.1.1-4a. Increase of VC Concentration at the Water Table  
(K=50% Initial K)



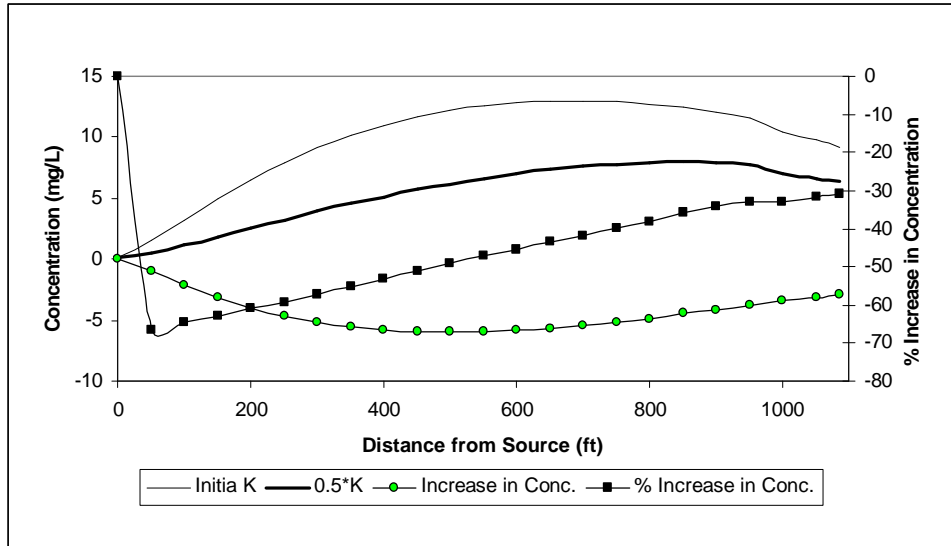
Figures 3.2.1.1-4b. Increase of VC-Centerline (Water Table)  
(K=50% Initial K)



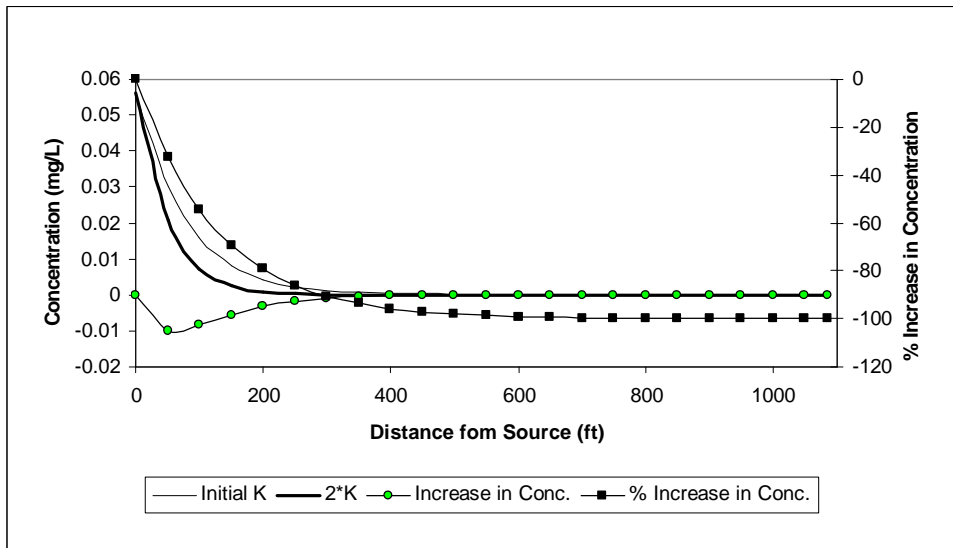
Figures 3.2.1.1-5a. Increase of ETH Concentration at the Water Table  
(K=50% Initial K)



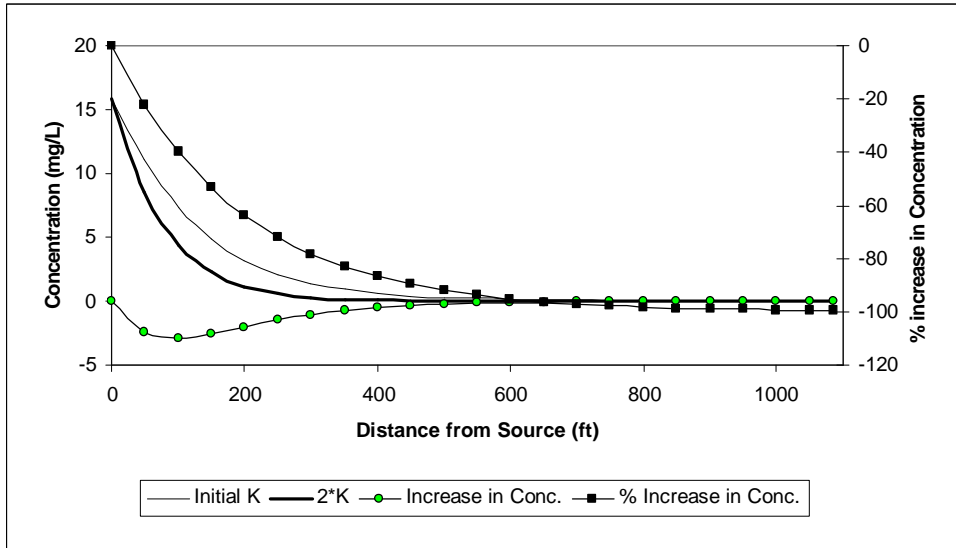
Figures 3.2.1.1-5b. Increase of ETH-Centerline (Water Table)  
(K=50% Initial K)



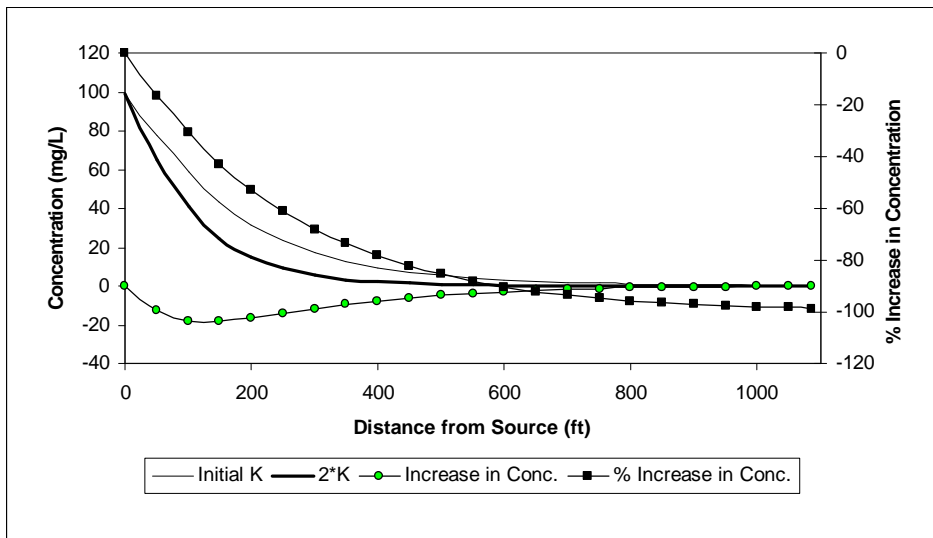
Figures 3.2.1.1-6. Increase of PCE-Centerline (Water Table)  
(K= 200% Initial K)



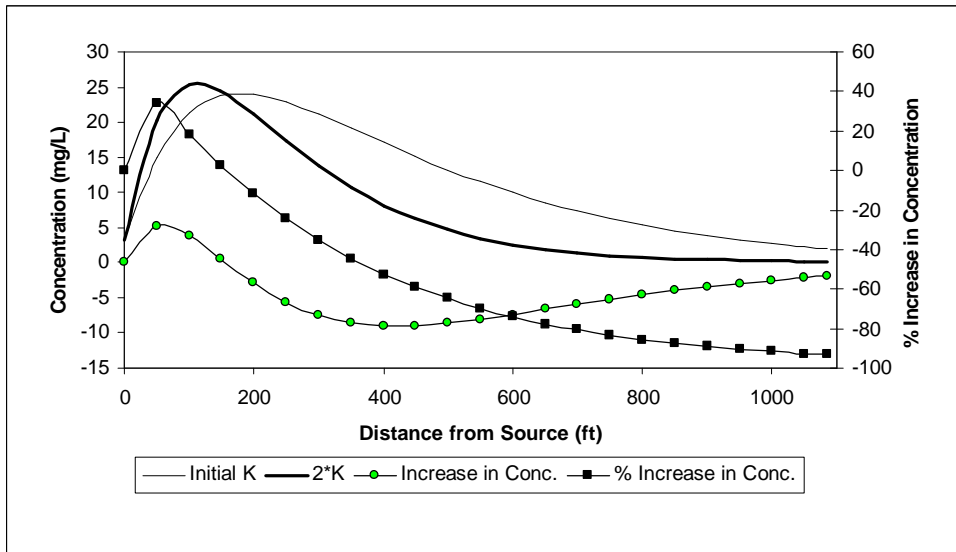
Figures 3.2.1.1-7. Increase of TCE-Centerline (Water Table)  
(K= 200% Initial K)



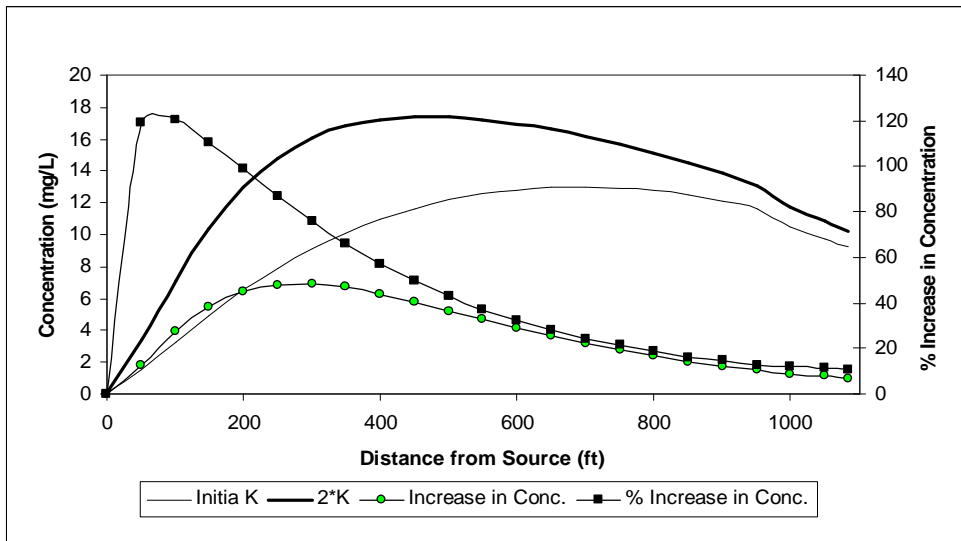
Figures 3.2.1.1-8. Increase of DCE-Centerline (Water Table)  
(K= 200% Initial K)



Figures 3.2.1.1-9. Increase of VC-Centerline (Water Table)  
(K= 200% Initial K)



Figures 3.2.1.1-10. Increase of ETH-Centerline (Water Table)  
(K= 200% Initial K)



After analyzing all the figures above, one of the observation is that the simulated concentrations at the canal location of PCE and its daughter product raise when the K value is smaller, and decrease when K value is higher than the value considerably initially. The exception to this remark is ethylene (ETH), since its concentration, just before the canal, does not change considerably to this range of K.

The increase curve shows that the major difference of concentration is reached in the stretch between the source and 500 ft from this. Although the differences of concentration obtained in both cases are almost similar, the percentage of increase in concentration, where the maximum difference is obtained, is higher when the magnitude of the rate coefficient is 0.5 times the initial value. This indicates that the election of a lower value of K produces higher variation in the concentration, and therefore, a greater error.

In Table 3.2.1.1-2 is shown the centerline concentration of all five species at the canal bank, 1085 ft from the source. Also, the maximum difference in the concentration and its the percentage of increase are summarized in this.

Table 3.2.1.1-2. Sensitivity Analysis Results- First Order Decay Coefficient

Species	Concentration – Canal Bank (mg/L)			Maximum Difference (mg/L)		% Increase in Maximum Difference	
	2*K	K	0.5*K	abs(0.5*K-K)	abs(2*K-K)	abs(0.5*K-K)/K*100	abs(2*K-K)/K*100
PCE	0.000	0.000	0.000	0.01	0.009	66	32
TCE	0.000	0.003	0.097	2.80	3.000	60	40
DCE	0.003	0.199	2.330	17.00	18.000	50	43
VC	0.136	2.010	7.160	75.00	9.000	100	52
ETH	10.200	9.210	6.350	6.00	7.000	50	75

### 3.2.1.2 Sensitivity Analysis-Retardation Factor

In order to determine the influence of retardation factor value on the concentration distribution in centerline, this example has been simulated considering two different values of this parameter. As the same way as the k parameter, the magnitude chosen to run the model are 50% and 200% of the initial value, that is, 1.5 and 4.5. In Tables 3.2.1.2-1 and 3.2.1.2-2 are shown the maximum difference in the concentration and the percentage of increase of this in the centerline.

Table 3.2.1.2-1. Sensitivity Analysis – Retardation Factor (R=1.5)

Distance From Source (ft)	% Increase in Maximum Difference [(0.5R-R)/R*100]					Maximum Difference in Concentration [(0.5R-R)] (mg/L)				
	PCE	TCE	DCE	VC	ETH	PCE	TCE	DCE	VC	ETH
	0	0.00	0.00	0.00	0.00	0.00	0.00	0.00	0.00	0.00
50	0.00	0.00	0.00	0.00	-10.68	0.00	0.00	0.00	0.00	-0.16
100	0.00	0.00	0.00	0.00	-5.38	0.00	0.00	0.00	0.00	-0.17
150	0.00	0.00	0.00	0.00	-3.34	0.00	0.00	0.00	0.00	-0.17
200	0.00	0.00	0.00	0.00	-2.26	0.00	0.00	0.00	0.00	-0.15
250	0.00	0.00	0.00	0.00	-1.59	0.00	0.00	0.00	0.00	-0.13
300	0.00	0.00	0.00	0.00	-1.12	0.00	0.00	0.00	0.00	-0.10
350	0.00	0.00	0.00	0.00	-0.75	0.00	0.00	0.00	0.00	-0.08
400	0.00	0.00	0.00	0.00	-0.43	0.00	0.00	0.00	0.00	-0.05
450	0.00	0.00	0.00	0.00	-0.09	0.00	0.00	0.00	0.00	-0.01
500	0.00	0.00	0.00	0.00	0.27	0.00	0.00	0.00	0.00	0.03
550	0.00	0.00	0.00	0.00	0.72	0.00	0.00	0.00	0.00	0.09
600	0.00	0.00	0.00	0.07	1.31	0.00	0.00	0.00	0.01	0.17
650	0.00	0.00	0.00	0.11	2.09	0.00	0.00	0.00	0.01	0.27
700	0.00	0.00	0.00	0.34	3.10	0.00	0.00	0.00	0.02	0.40
750	0.00	0.00	0.00	0.52	4.48	0.00	0.00	0.00	0.03	0.58
800	0.00	0.00	0.00	0.80	6.33	0.00	0.00	0.00	0.04	0.81
850	0.00	0.00	0.00	1.20	8.78	0.00	0.00	0.00	0.05	1.09
900	0.00	0.00	0.00	1.78	11.96	0.00	0.00	0.00	0.07	1.45
950	0.00	0.00	0.00	2.58	16.08	0.00	0.00	0.00	0.08	1.87
1000	0.00	0.00	0.00	3.69	28.03	0.00	0.00	0.00	0.10	2.93
1050	0.00	0.00	0.00	5.19	36.27	0.00	0.00	0.00	0.12	3.53
1085	0.00	0.00	0.00	6.53	43.28	0.00	0.00	0.00	0.13	3.99

Table 3.2.1.2-2. Sensitivity Analysis – Retardation Factor (R=4.5)

Distance From Source (ft)	% Increase in Maximum Difference [(2R-R)/R*100]					Maximum Difference in Concentration [(2R-R)] (mg/L)				
	PCE	TCE	DCE	VC	ETH	PCE	TCE	DCE	VC	ETH
	0	0.000	0.000	0.000	0.000	0.000	0.000	0.000	0.000	0.000
50	0.000	0.000	0.000	-0.007	-10.947	0.000	0.000	0.000	-0.001	-0.166
100	0.000	0.000	0.000	-0.009	-5.802	0.000	0.000	0.000	-0.002	-0.188
150	0.000	0.000	-0.002	-0.025	-3.992	0.000	0.000	-0.001	-0.006	-0.197
200	0.000	0.000	-0.003	-0.054	-3.289	0.000	0.000	-0.001	-0.013	-0.215
250	0.000	0.000	-0.009	-0.100	-3.185	0.000	0.000	-0.002	-0.023	-0.252
300	0.000	0.000	-0.023	-0.198	-3.557	0.000	0.000	-0.004	-0.042	-0.325
350	0.000	0.000	-0.039	-0.360	-4.405	0.000	0.000	-0.005	-0.069	-0.447
400	0.000	0.000	-0.081	-0.625	-5.792	0.000	0.000	-0.008	-0.107	-0.636
450	0.000	0.000	-0.163	-1.065	-7.792	0.000	0.000	-0.012	-0.161	-0.908
500	0.000	0.000	-0.308	-1.745	-10.489	0.000	0.000	-0.017	-0.231	-1.277
550	0.000	0.000	-0.548	-2.780	-13.972	0.000	0.000	-0.022	-0.320	-1.755
600	0.000	-0.402	-0.965	-4.263	-18.253	0.000	-0.001	-0.029	-0.425	-2.340
650	0.000	-0.710	-1.627	-6.330	-23.329	0.000	-0.001	-0.037	-0.543	-3.024
700	0.000	-1.201	-3.823	-8.546	-29.209	0.000	-0.001	-0.066	-0.629	-3.797
750	0.000	-1.959	-5.719	-11.983	-35.603	0.000	-0.001	-0.075	-0.754	-4.602
800	0.000	-3.094	-8.297	-21.091	-41.489	0.000	-0.001	-0.082	-1.130	-5.289
850	0.000	-4.730	-11.650	-26.784	-48.502	0.000	-0.001	-0.087	-1.219	-6.046
900	0.000	-6.984	-15.857	-33.143	-55.508	0.000	-0.001	-0.089	-1.278	-6.708
950	0.000	-9.982	-20.940	-40.010	-62.275	0.000	-0.001	-0.089	-1.301	-7.225
1000	0.000	-13.826	-26.858	-47.162	-72.996	0.000	-0.001	-0.086	-1.289	-7.630
1050	0.000	-18.563	-33.491	-54.368	-78.094	0.000	-0.001	-0.081	-1.243	-7.609
1085	0.000	-22.409	-38.459	-59.311	-81.283	0.000	-0.001	-0.077	-1.193	-7.485

The results indicate that the distribution of the concentration in the centerline changes slightly. The major difference appears in the ETHANE (ETH), when the

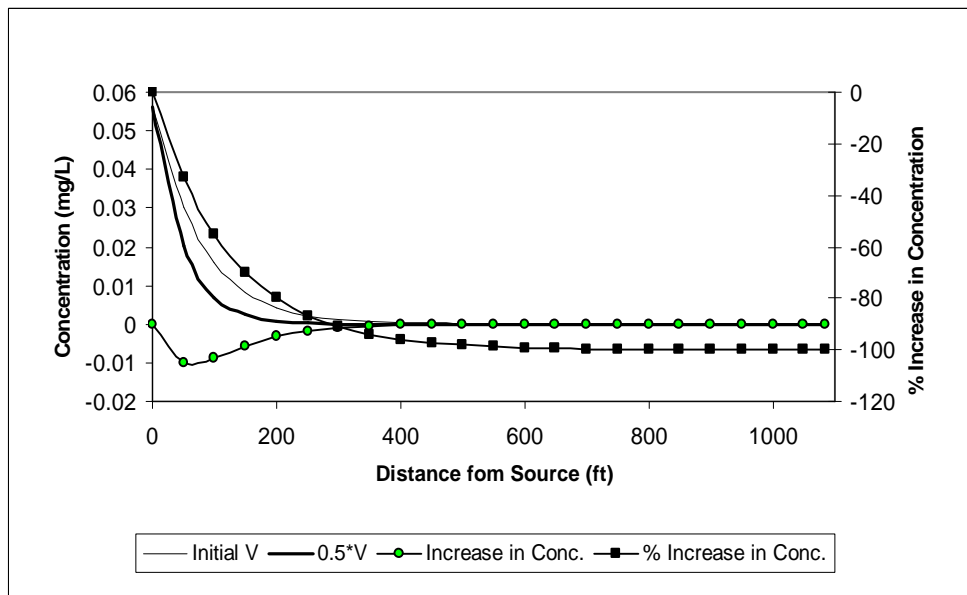
retardation factor has a higher value. The rest of the species do not suffer important alteration in the concentration.

These small variations in the concentrations indicate that, in this example, the retardation factor is not a critic parameter, since its value can be within a wide range without producing considerably changes on the final result.

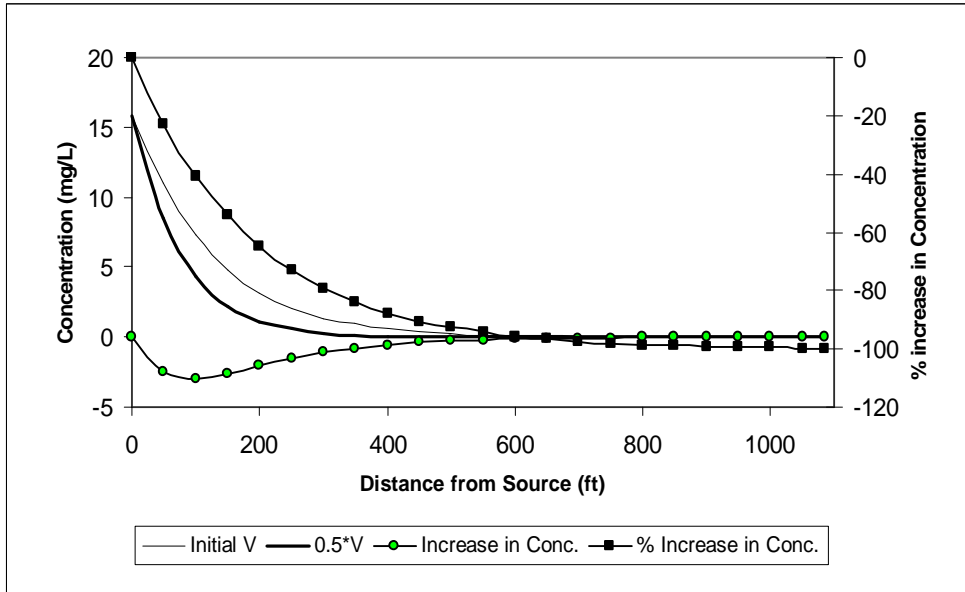
### 3.2.1.3 Sensitivity Analysis-Seepage Velocity

The seepage velocity is other parameter quite difficult to estimate with a high grade of accuracy. The hydraulic conductivity, the hydraulic gradient and the porosity are parameters that suffer modification along the aquifer, and therefore, we must work with the mean of the observed values. Any uncertainty about the magnitude of these parameters is transmitted to seepage velocity value. As the same way as the sensitivity analysis before, the magnitude chosen to run the model are 50% and 200% of the initial value, that is 55 ft/year and 220 ft/year.

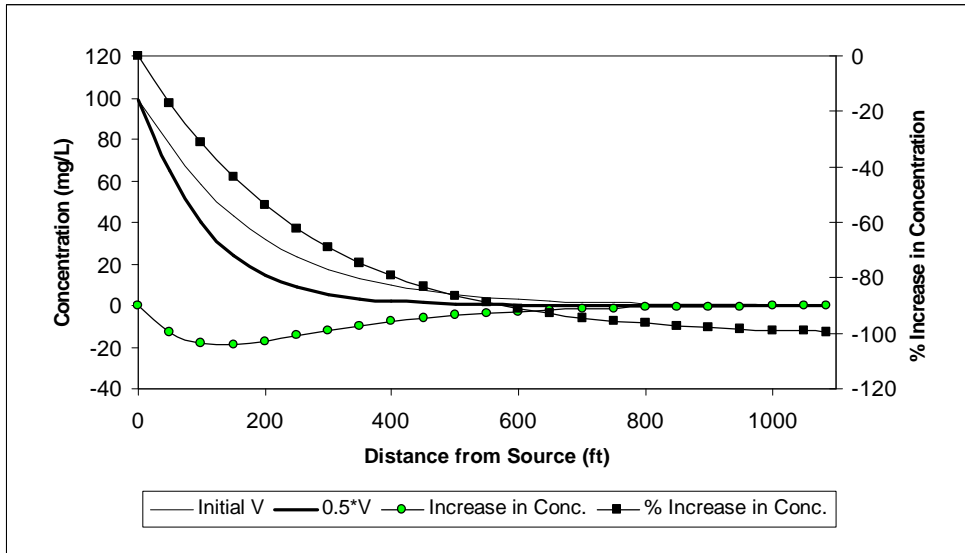
Figures 3.2.1.3-1. Increase of PCE-Centerline (Water Table)  
(V= 50% Initial V)



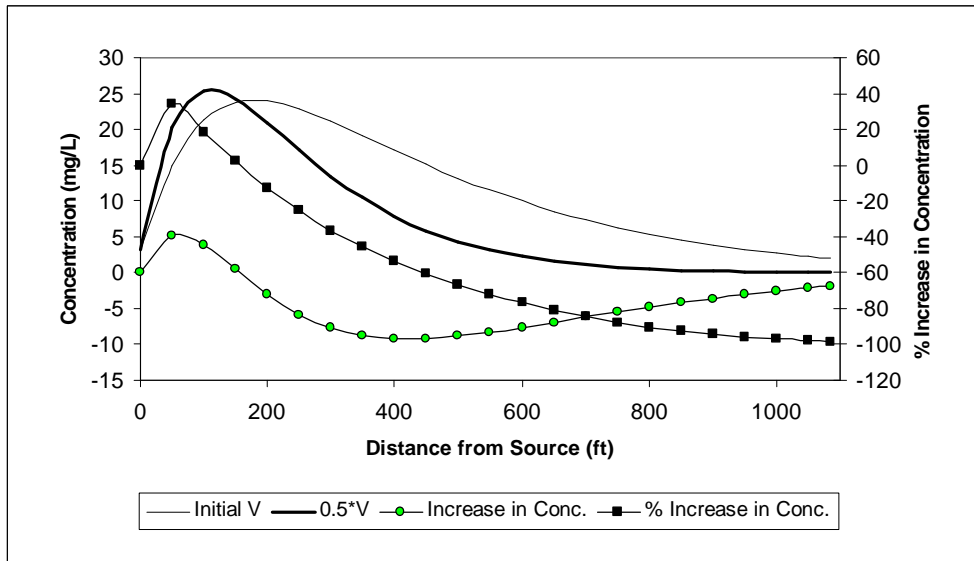
Figures 3.2.1.3-2. Increase of TCE-Centerline (Water Table)  
(V= 50% Initial V)



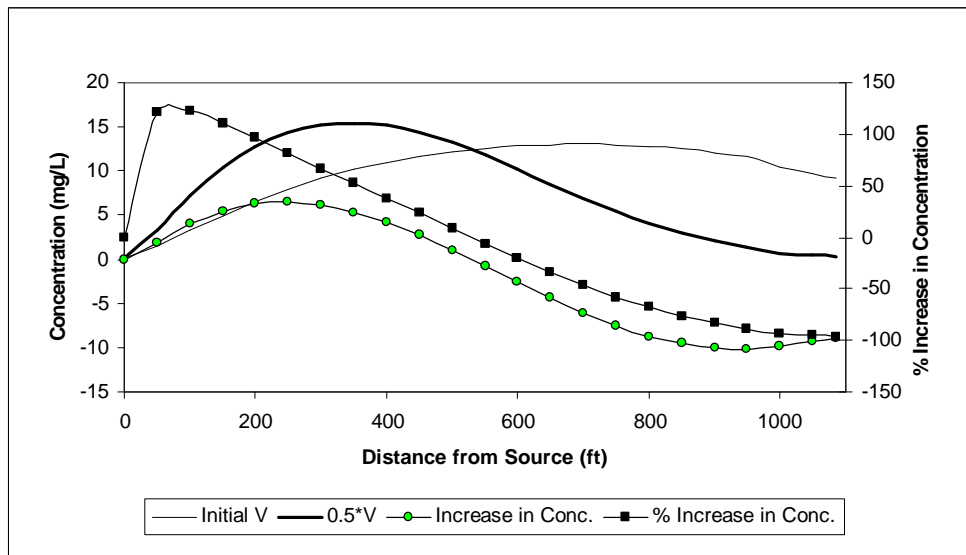
Figures 3.2.1.3-3. Increase of DCE-Centerline (Water Table)  
(V= 50% Initial V)



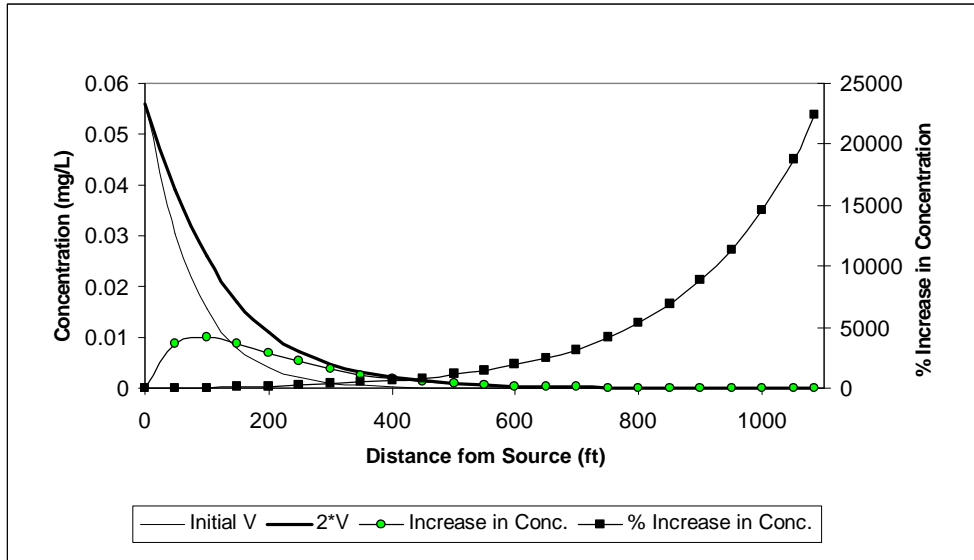
Figures 3.2.1.3-4. Increase of VC-Centerline (Water Table)  
( $V = 50\%$  Initial  $V$ )



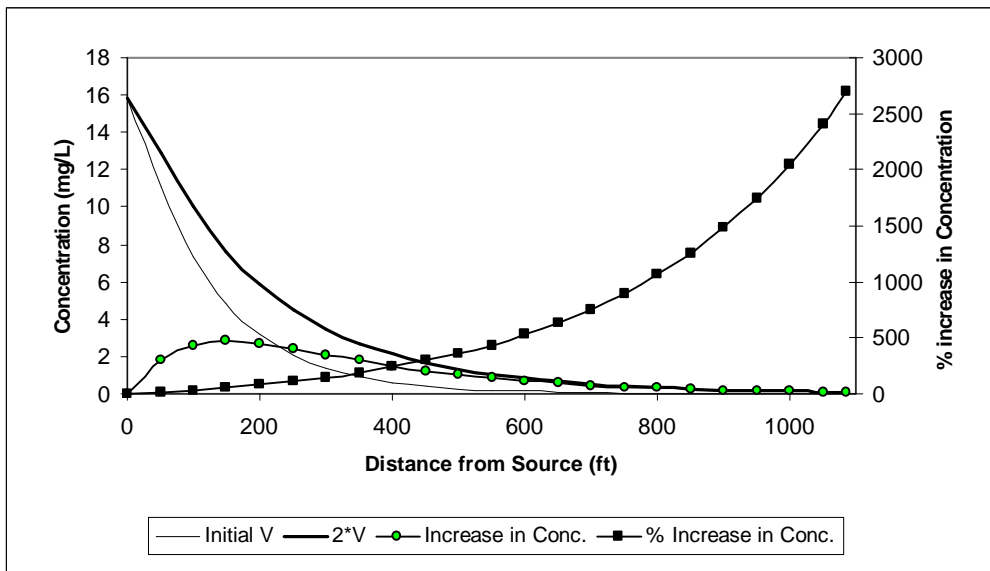
Figures 3.2.1.3-5. Increase of ETH-Centerline (Water Table)  
( $V = 50\%$  Initial  $V$ )



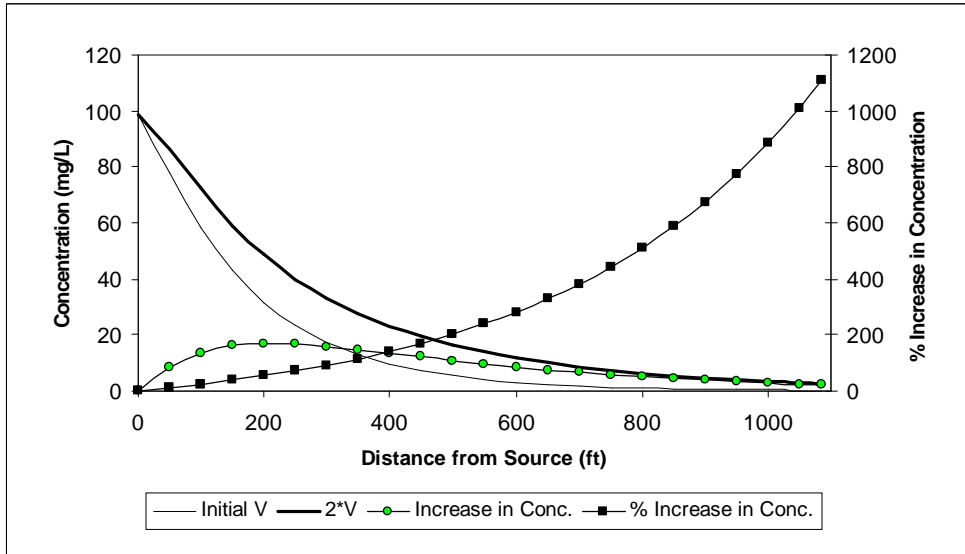
Figures 3.2.1.3-6. Increase of PCE-Centerline (Water Table)  
(V= 200% Initial V)



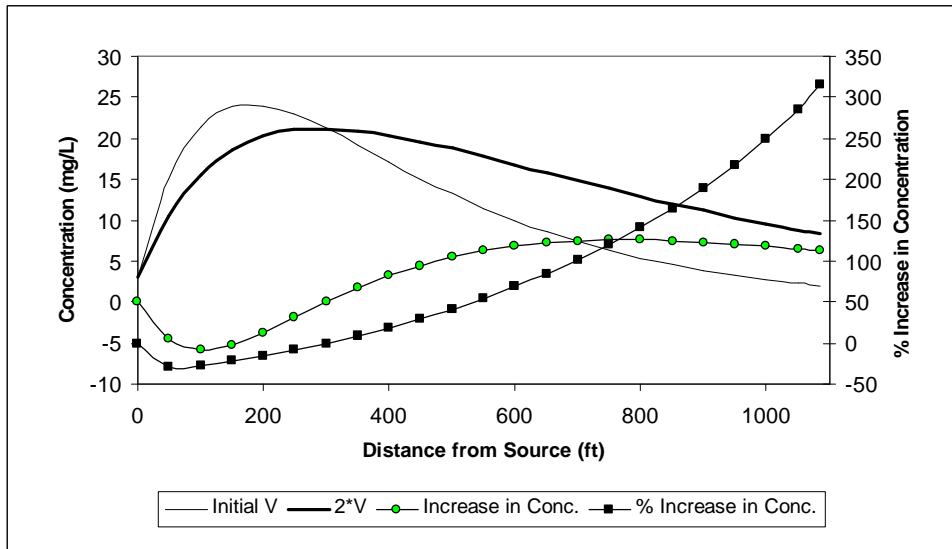
Figures 3.2.1.3-7. Increase of TCE-Centerline (Water Table)  
(V= 200% Initial V)



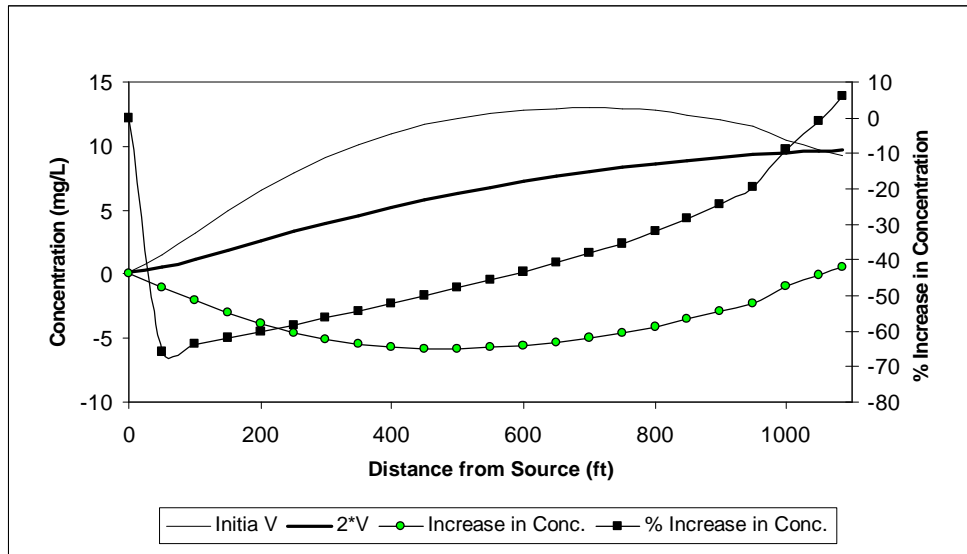
Figures 3.2.1.3-8. Increase of DCE-Centerline (Water Table)  
(V= 200% Initial V)



Figures 3.2.1.3-9. Increase of VC-Centerline (Water Table)  
(V= 200% Initial V)



Figures 3.2.1.3-10. Increase of ETH-Centerline (Water Table)  
(V= 200% Initial V)



The behavior of the model for different magnitudes of the seepage velocity is totally different to the result appreciated to several rate coefficient values. For this particular problem, there is a proportional relation between the concentration at the canal bank and the seepage velocity, since if one increase the other increase as well. In other words, the higher the seepage velocity values the higher the concentration just before the canal and vice versa. The reason is clear, when the velocity is higher, the specie reaches the canal bank earlier, and therefore, at that time, the specie has suffered the degradation process for less time. The exception of this could be ETHANE (ETH), since due to all its parents suffer less degradation, the production of ETH before the canal bank is smaller than the case with a slower flow.

#### 3.2.1.4 Sensitivity Analysis-Dispersivity

The selection of dispersivity values is not an easy process, since they present difficulty to measure in the field. There are empirical data that show a relation between the distance between source and the measurement point (Gelhar *et al.* (1992)), but they give a wide range of dispersivity. In order to do the analysis, two values of the longitudinal dispersivity have been chosen from the relation created through the empirical data, 15 ft and 70 ft.. As for the transverse dispersivity, it is, in both cases, a 10 % of the longitudinal dispersivity. Finally, the vertical dispersivity is considerate equal to 0 in all three cases.

In Tables 3.2.1.4-1 and 3.2.1.4-2 are shown the maximum difference in the concentration and the percentage of increase of this in the centerline.

Table 3.2.1.4-1. Sensitivity Analysis – Dispersivity (ax = 15 ft.)

Distance From Source (ft)	% Increase in Maximum Difference [(ax(final)-ax (initial))/ ax (initial)*100]					Maximum Difference in Concentration [ax(final)-ax (initial)] (mg/L)				
	PCE	TCE	DCE	VC	ETH	PCE	TCE	DCE	VC	ETH
	0	0.000	0.000	0.000	0.000	0.000	0.000	0.000	0.000	0.000
50	-11.428	-4.008	-1.291	12.709	-22.823	-0.003	-0.443	-1.006	1.910	-0.346
100	-17.882	-3.564	1.809	18.355	-4.952	-0.003	-0.263	1.058	3.935	-0.160
150	-23.257	-2.356	5.695	24.368	8.330	-0.002	-0.114	2.452	5.814	0.412
200	-29.028	-2.165	8.471	29.047	18.347	-0.001	-0.069	2.683	6.973	1.197
250	-35.084	-3.053	10.009	32.315	25.926	-0.001	-0.064	2.340	7.405	2.054
300	0.000	-4.764	10.526	34.423	31.722	0.000	-0.066	1.824	7.295	2.895
350	0.000	-7.039	10.280	35.661	36.222	0.000	-0.066	1.325	6.844	3.674
400	0.000	-9.699	9.448	36.243	39.796	0.000	-0.061	0.909	6.207	4.370
450	0.000	-12.600	8.200	36.334	42.719	0.000	-0.053	0.590	5.493	4.978
500	0.000	-15.645	6.642	36.056	45.191	0.000	-0.045	0.358	4.772	5.502
550	0.000	-18.758	4.853	35.493	47.385	0.000	-0.036	0.197	4.086	5.952
600	0.000	-21.887	2.900	34.740	49.485	0.000	-0.029	0.088	3.460	6.344
650	0.000	-25.009	0.837	33.839	51.585	0.000	-0.022	0.019	2.904	6.687
700	0.000	-28.084	-1.307	33.037	53.766	0.000	-0.017	-0.023	2.430	6.989
750	0.000	-31.096	-3.488	32.070	56.189	0.000	-0.013	-0.046	2.017	7.263
800	0.000	-34.033	-5.705	31.093	58.841	0.000	-0.010	-0.056	1.666	7.501
850	0.000	-36.891	-7.925	30.121	61.680	0.000	-0.007	-0.059	1.371	7.689
900	0.000	-39.656	-10.148	29.125	64.499	0.000	-0.005	-0.057	1.123	7.794
950	0.000	-42.338	-12.390	28.030	67.032	0.000	-0.004	-0.053	0.912	7.777
1000	0.000	-44.943	-14.684	26.699	78.081	0.000	-0.003	-0.047	0.730	8.161
1050	0.000	-47.490	-17.096	24.916	80.076	0.000	-0.002	-0.042	0.570	7.802
1085	0.000	-49.253	-18.906	23.254	80.356	0.000	-0.002	-0.038	0.468	7.399

Table 3.2.1.4-2. Sensitivity Analysis – Dispersivity (ax = 70 ft.)

Distance From Source (ft)	% Increase in Maximum Difference [ax(final)-ax (initial))/ ax (initial)*100]					Maximum Difference in Concentration [ax(final)-ax (initial)] (mg/L)				
	PCE	TCE	DCE	VC	ETH	PCE	TCE	DCE	VC	ETH
	0	0.000	0.000	0.000	0.000	0.000	0.000	0.000	0.000	0.000
50	4.642	-0.172	-2.060	-12.822	-7.625	0.001	-0.019	-1.605	-1.927	-0.116
100	6.243	-3.307	-6.834	-18.393	-13.592	0.001	-0.244	-3.997	-3.943	-0.440
150	10.926	-3.681	-8.787	-20.894	-17.891	0.001	-0.178	-3.783	-4.985	-0.885
200	17.680	-2.506	-9.201	-21.924	-20.576	0.001	-0.079	-2.914	-5.263	-1.342
250	25.911	-0.467	-8.781	-22.208	-22.327	0.001	-0.010	-2.053	-5.089	-1.769
300	0.000	2.131	-7.860	-22.070	-23.526	0.000	0.030	-1.362	-4.677	-2.147
350	0.000	5.121	-6.595	-21.665	-24.395	0.000	0.048	-0.850	-4.158	-2.474
400	0.000	8.427	-5.092	-21.085	-25.065	0.000	0.053	-0.490	-3.611	-2.752
450	0.000	11.998	-3.398	-20.386	-25.607	0.000	0.051	-0.244	-3.082	-2.984
500	0.000	15.810	-1.545	-19.600	-26.081	0.000	0.045	-0.083	-2.594	-3.175
550	0.000	19.843	0.440	-18.744	-26.525	0.000	0.038	0.018	-2.158	-3.332
600	0.000	24.104	2.539	-17.840	-26.942	0.000	0.032	0.077	-1.777	-3.454
650	0.000	28.568	4.753	-16.895	-27.352	0.000	0.026	0.109	-1.450	-3.546
700	0.000	33.236	7.063	-15.791	-27.767	0.000	0.020	0.122	-1.161	-3.609
750	0.000	38.126	9.475	-14.721	-28.139	0.000	0.016	0.124	-0.926	-3.637
800	0.000	43.228	11.983	-13.596	-28.459	0.000	0.012	0.118	-0.729	-3.628
850	0.000	48.551	14.595	-12.397	-28.695	0.000	0.010	0.109	-0.564	-3.577
900	0.000	54.107	17.208	-11.080	-28.831	0.000	0.007	0.097	-0.427	-3.484
950	0.000	59.909	20.016	-9.661	-28.807	0.000	0.006	0.085	-0.314	-3.342
1000	0.000	65.952	22.961	-8.076	-24.670	0.000	0.004	0.074	-0.221	-2.579
1050	0.000	72.295	26.076	-6.283	-23.561	0.000	0.003	0.063	-0.144	-2.296
1085	0.000	76.910	28.377	-4.869	-22.573	0.000	0.003	0.057	-0.098	-2.079

The result of this simulation shown that the first three species, PCE, TCE and DCE, are slightly affected by the value of the dispersivity, whereas the other two species, VC and ETH, present a considerably variation on their concentration. When the

dispersivity coefficient is equal to 70 ft. the fall of the concentration is between 20 % and 30 %. On the other hand, if the  $\alpha_x$  is reduced to 15 ft., VC raises in the same percentage as before, but ETH increases its amount in about 80 %.

As a general observation, it is important to emphasize that in this example the spatial distribution of the concentration is quite sensible to rate coefficient value and the seepage velocity. Different values of the dispersivity parameter produce modifications in the concentration distribution, mainly in VC and ETH. Finally, in this example, ART3D is less sensitive to changes in the retardation factor than any parameter.

### **3.3 BIOCHLOR example, with x-z visualization**

The example before permitted to compare BIOCHLOR capabilities against ART3D capabilities. Most the characteristics of ART3D were shown an exception for the possibility of having a visualization of two-dimensional contours in cross sections (in x-y plane). For this example, this sort of figures did not contribute to the understanding of the movement of the plume, since the assumption that depth of source is approximate depth of aquifer produced as a result that the concentration distribution reached on the water table is the same at any depth. This behavior can be observed on figures where the three dimensional plume is shown.

On account of the features of this real transport problem, the marvelous graph display of ART3D and its ability of predicting the contaminant concentration in any point within the aquifer were not appreciated properly. Considering this situation, a new example problem was solved to illustrate all the capabilities of this new code. This new problem is fairly similar to the example before, where the difference is in that the source thickness has been reduced from 56 ft. to 5 ft. and the vertical dispersivity increased its value to 0.4 ft.

In Figures 3.3-1 through 3.3-4 are given the two dimensional contours in cross section for each species of this example. Furthermore, as a manner to summarize all the results obtained, the Figures 3.3-5 to 3.3-8 illustrate the location of the plume from a three-dimensional viewpoint.

Figure 3.1-1. Concentration of PCE in Cross Section (mg/l).

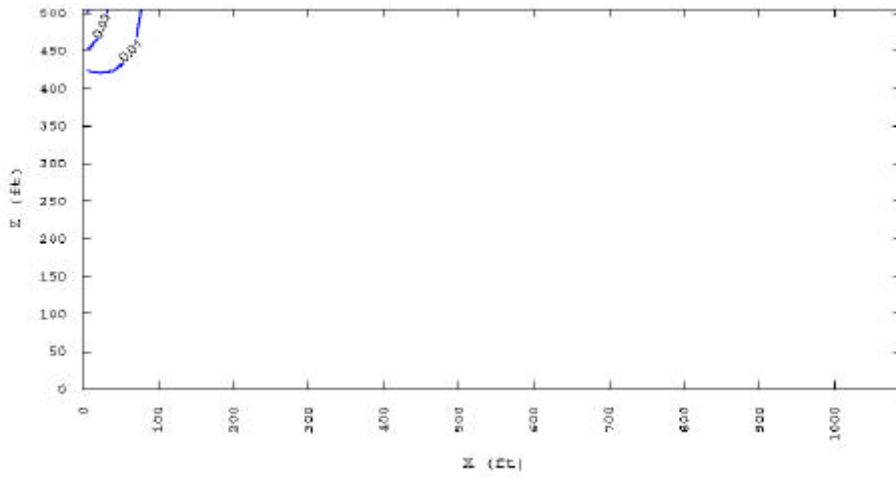


Figure 3.1-2. Concentration of TCE in Cross Section (mg/l).

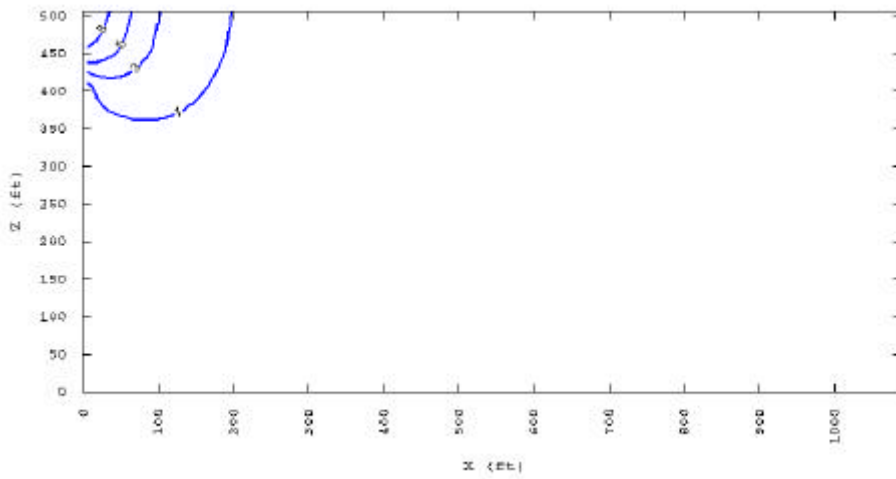


Figure 3.1-3. Concentration of DCE in Cross Section (mg/l).

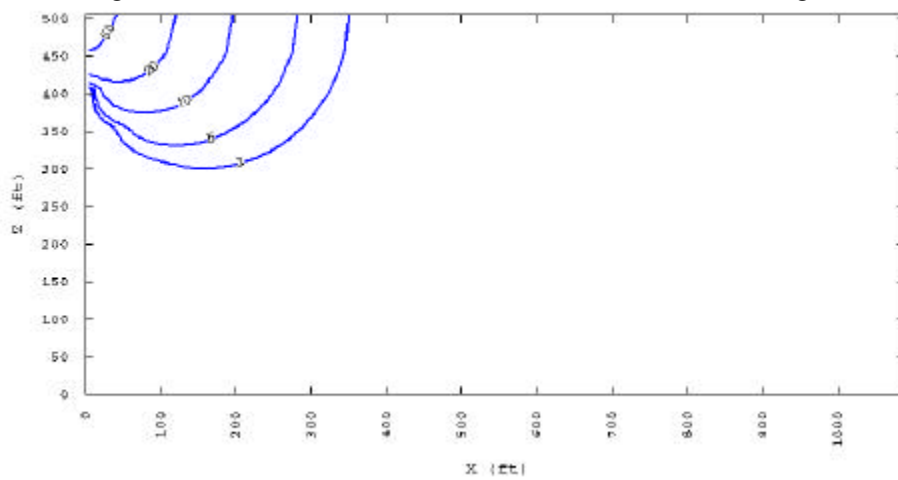


Figure 3.1-4. Concentration of VC in Cross Section (mg/l).

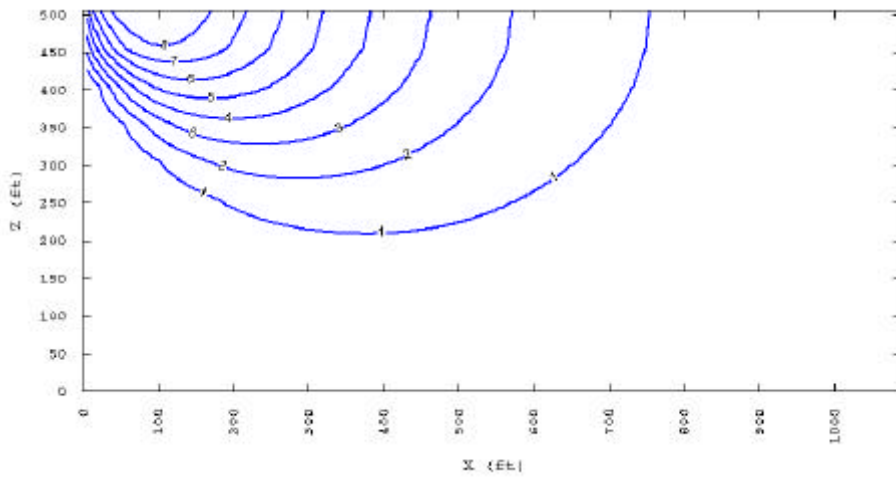


Figure 3.1-5. Visualization three-dimensional of the PCE plume

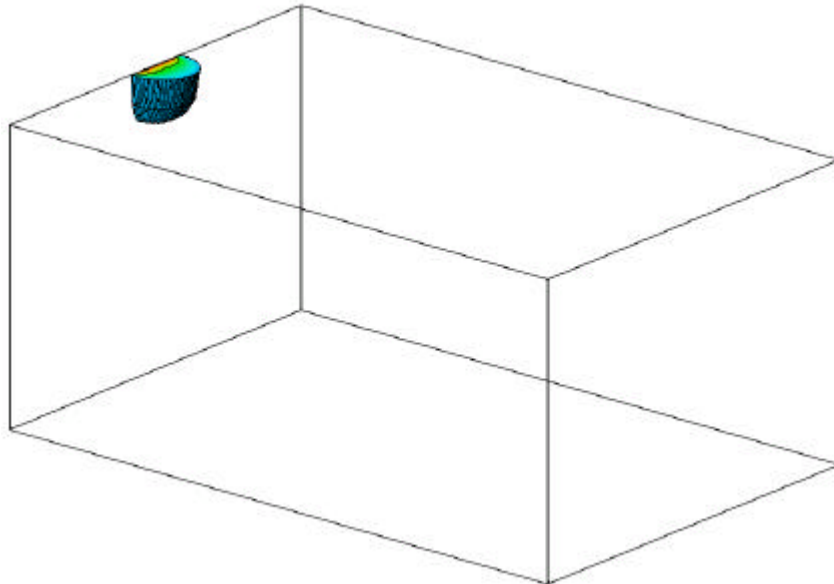


Figure 3.1-6. Visualization three-dimensional of the TCE plume

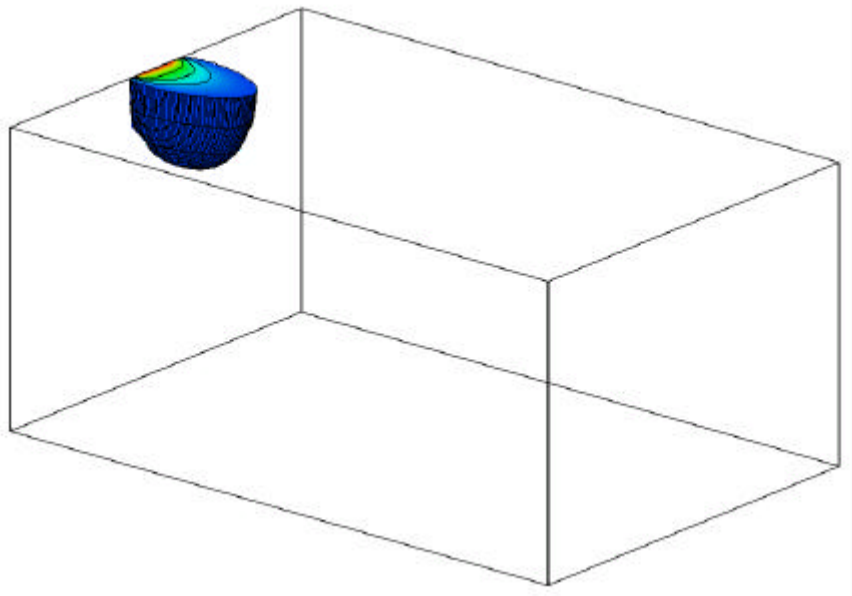


Figure 3.1-7. Visualization three-dimensional of the DCE plume

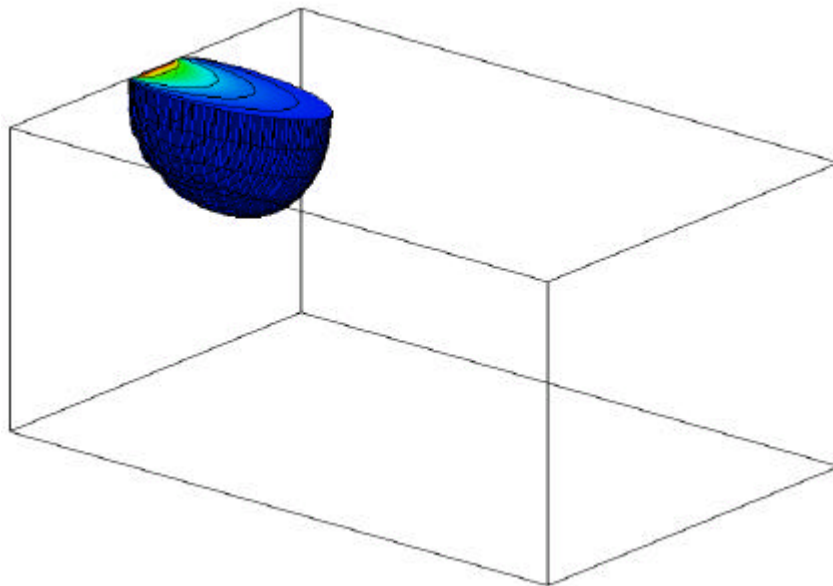
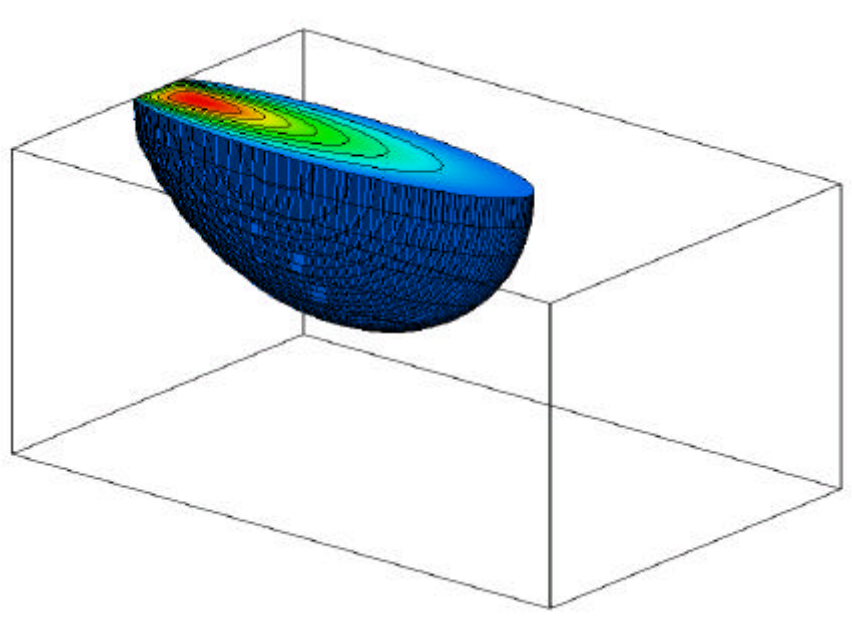


Figure 3.1-8. Visualization three-dimensional of the VC plume



All these graphs show clearly that ART3D is a 3 dimensional tool, since it allows make an estimate of the contaminant concentration at any depth of the aquifer. This characteristic is unavailable in BIOCHLOR, which is only able to predict the concentration distribution at the water table (2 dimensional code).

#### **4. Example Problems with PCE and PCA together**

##### **4.1 Anaerobic degradation for PCA and PCE.**

PCA is a common groundwater contaminant, but its fate in the environment is not well known. Nowadays, there are three types of degradation reactions possible for PCA, hydrogenolysis, dichloroelimination and dehydrochlorination (Figure 4.1-1). Hydrogenolysis entails the sequential replacement of a chlorine atom by hydrogen. The second degradation reactions, dichloroelimination, entails the release of two chlorine simultaneously from the parent species. This degradation reaction is possible for PCA and 1,1,2-trichloroethane. The last possible transformation for PCA is called dehydrochlorination, where a hydrogen atom and a chlorine atom are released from the parent species.

The studies made until now have not be able to determinate which of these degradation reactions is dominant or has the highest chances to occur. One of the reasons is found in that TCE is disposed quite often at the same place as PCA, which generate mistakes in the measurements of the contaminants, since TCE can produce the same daughter as PCA. The other motive, more general than the one before, indicates that the

dominant pathway would depend on the geochemical and microbiological features of the site.

The kinetics of the degradation pathways of PCA is different to the PCE degradation. Although, the degradation kinetics of PCA can be approximated as first order reaction, its degradation pathway is away of been a sequential reaction (Figure 4.1-1).

According to the mention before and the degradation pathways shown in Figure 4.1-1, the governing equations for this reactive transport system are:

$$R_{PCE} \frac{\partial c_{PCE}}{\partial t} + v \frac{\partial c_{PCE}}{\partial x} - D_x \frac{\partial^2 c_{PCE}}{\partial x^2} - D_y \frac{\partial^2 c_{PCE}}{\partial y^2} - D_z \frac{\partial^2 c_{PCE}}{\partial z^2} = -k_{PCE} \cdot C_{PCE} \quad (12)$$

$$R_{Teca} \frac{\partial c_{Teca}}{\partial t} + v \frac{\partial c_{Teca}}{\partial x} - D_x \frac{\partial^2 c_{Teca}}{\partial x^2} - D_y \frac{\partial^2 c_{Teca}}{\partial y^2} - D_z \frac{\partial^2 c_{Teca}}{\partial z^2} = -k_{Teca} \cdot C_{TeCA} \quad (13)$$

$$R_{TCE} \frac{\partial c_{TCE}}{\partial t} + v \frac{\partial c_{TCE}}{\partial x} - D_x \frac{\partial^2 c_{TCE}}{\partial x^2} - D_y \frac{\partial^2 c_{TCE}}{\partial y^2} - D_z \frac{\partial^2 c_{TCE}}{\partial z^2} = y_{\frac{TCE}{PCE}} \cdot k_{TCE} \cdot C_{TCE} + \\ + y_{\frac{TCE}{TeCA}} \cdot F_{\frac{TCE}{TeCA}} \cdot k_{TCE} \cdot C_{TCE} - k_{TCE} \cdot C_{TCE} \quad (14)$$

$$R_{TCA} \frac{\partial c_{TCA}}{\partial t} + v \frac{\partial c_{TCA}}{\partial x} - D_x \frac{\partial^2 c_{TCA}}{\partial x^2} - D_y \frac{\partial^2 c_{TCA}}{\partial y^2} - D_z \frac{\partial^2 c_{TCA}}{\partial z^2} = \\ = y_{\frac{TCA}{TeCA}} \cdot F_{\frac{TCA}{TeCA}} \cdot k_{TeCA} \cdot C_{TeCA} - k_{TCA} \cdot C_{TCA} \quad (15)$$

$$R_{11DCE} \frac{\partial c_{11DCE}}{\partial t} + v \frac{\partial c_{11DCE}}{\partial x} - D_x \frac{\partial^2 c_{11DCE}}{\partial x^2} - D_y \frac{\partial^2 c_{11DCE}}{\partial y^2} - D_z \frac{\partial^2 c_{11DCE}}{\partial z^2} = \\ = y_{\frac{DCE}{TCE}} \cdot F_{\frac{DCE}{TCE}} \cdot k_{TCE} \cdot C_{TCE} - k_{11DCE} \cdot C_{11DCE} - ka_{11DCE} \cdot C_{11DCE} \quad (16)$$

$$R_{cDCE} \frac{\partial c_{cDCE}}{\partial t} + v \frac{\partial c_{cDCE}}{\partial x} - D_x \frac{\partial^2 c_{cDCE}}{\partial x^2} - D_y \frac{\partial^2 c_{cDCE}}{\partial y^2} - D_z \frac{\partial^2 c_{cDCE}}{\partial z^2} = \\ = y_{\frac{DCE}{TeCA}} \cdot F_{\frac{cDCE}{TeCA}} \cdot k_{TeCA} \cdot C_{TeCA} + y_{\frac{DCE}{TCE}} \cdot F_{\frac{cDCE}{TCE}} \cdot k_{TCE} \cdot C_{TCE} -$$

$$-k_{cDCE} \cdot C_{cDCE} - ka_{cDCE} \cdot C_{cDCE} \quad (17)$$

$$\begin{aligned} R_{iDCE} \frac{\partial c_{iDCE}}{\partial t} + v \frac{\partial c_{iDCE}}{\partial x} - D_x \frac{\partial^2 c_{iDCE}}{\partial x^2} - D_y \frac{\partial^2 c_{iDCE}}{\partial y^2} - D_z \frac{\partial^2 c_{iDCE}}{\partial z^2} = \\ = y_{DCE} \cdot \frac{F_{iDCE}}{TeCA} \cdot k_{TeCA} \cdot C_{TeCA} + y_{DCE} \cdot \frac{F_{iDCE}}{TCE} \cdot k_{TCE} \cdot C_{TCE} - \\ - k_{iDCE} \cdot C_{iDCE} - ka_{iDCE} \cdot C_{iDCE} \end{aligned} \quad (18)$$

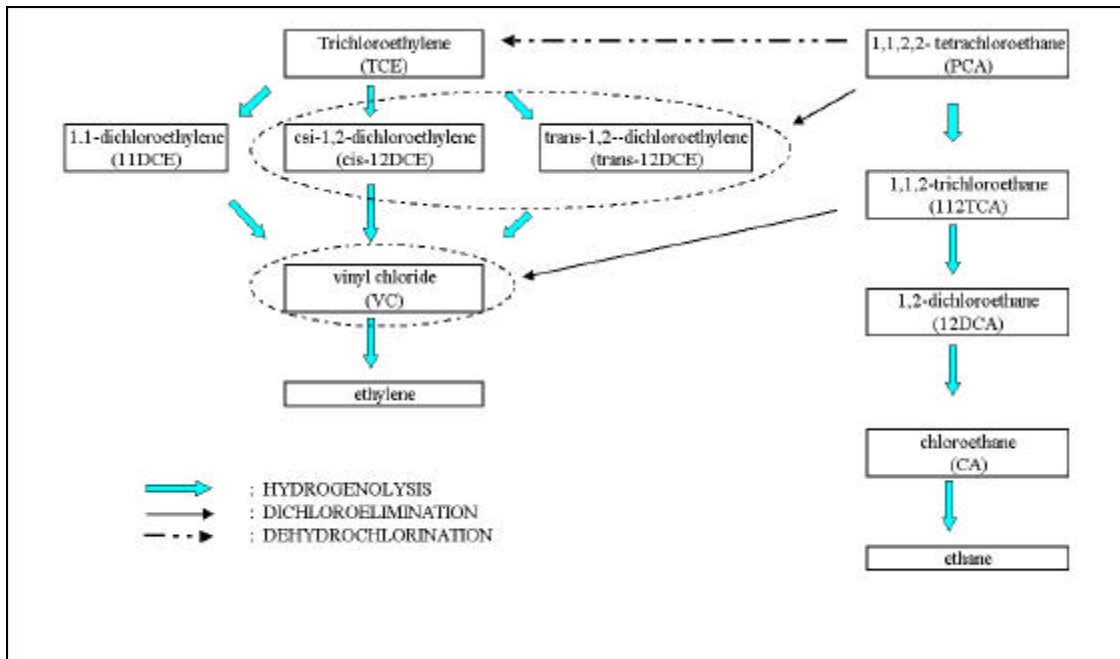
$$\begin{aligned} R_{DCA} \frac{\partial c_{DCA}}{\partial t} + v \frac{\partial c_{DCA}}{\partial x} - D_x \frac{\partial^2 c_{DCA}}{\partial x^2} - D_y \frac{\partial^2 c_{DCA}}{\partial y^2} - D_z \frac{\partial^2 c_{DCA}}{\partial z^2} = \\ = y_{DCA} \cdot \frac{F_{DCA}}{TCA} \cdot k_{TCA} \cdot C_{TCA} - k_{DCA} \cdot C_{DCA} - ka_{DCA} \cdot C_{DCA} \end{aligned} \quad (19)$$

$$\begin{aligned} R_{VC} \frac{\partial c_{VC}}{\partial t} + v \frac{\partial c_{VC}}{\partial x} - D_x \frac{\partial^2 c_{VC}}{\partial x^2} - D_y \frac{\partial^2 c_{VC}}{\partial y^2} - D_z \frac{\partial^2 c_{VC}}{\partial z^2} = \\ = y_{VC} \cdot \frac{F_{VC}}{TCA} \cdot k_{TCA} \cdot C_{TCA} + y_{VC} \cdot \frac{k_{11DCE}}{DCE} \cdot C_{11DCE} + y_{VC} \cdot \frac{k_{cDCE}}{DCE} \cdot C_{cDCE} \\ + y_{VC} \cdot \frac{k_{iDCE}}{DCE} \cdot C_{iDCE} - k_{VC} \cdot C_{VC} - ka_{VC} \cdot C_{VC} \end{aligned} \quad (20)$$

$$\begin{aligned} R_{CA} \frac{\partial c_{CA}}{\partial t} + v \frac{\partial c_{CA}}{\partial x} - D_x \frac{\partial^2 c_{CA}}{\partial x^2} - D_y \frac{\partial^2 c_{CA}}{\partial y^2} - D_z \frac{\partial^2 c_{CA}}{\partial z^2} = \\ = y_{CA} \cdot \frac{F_{CA}}{DCA} \cdot k_{DCA} \cdot C_{DCA} - k_{CA} \cdot C_{CA} - ka_{CA} \cdot C_{CA} \end{aligned} \quad (21)$$

It should be point out that all the variables utilized in the equations system above have the same meaning that the ones used in the general expression (1), a exception for  $y_{d/p}$ . In this particular case, the effective yield factor is represented by  $F_{d/p} \cdot Y_{d/p}$ , where  $Y_{d/p}$  represents the amount of daughter species “d” produced by degrading a unit mass of parent species “p” [MM<sup>-1</sup>] (assuming that a parent specie “p” exclusively produces a specific daughter product “d”) and  $F_{d/p}$  is the mole fraction of a parent species “p” that will degrade and produce a specific daughter product “d”. If there is a sequential reactive system, the F values are equals to 1.

Figure 4.1-1. Anaerobic Degradation Pathways for PCA and TCE.



## 4.2 Example Batch Problem

In this chapter, two examples have been developed to test the ART3D code (Batch mode). Both of them correspond to experiments done in laboratory with the goal of observing the attenuation of PCA and its subsequent degradation products. The explanation of each experiment and the comparison of their results against ART3D are presented next.

### 4.2.1 First problem-Lorah and Olsen (1999)

#### 4.2.1.1 Description Problem

The objective of this study was to give an evidence of PCA degradation for a wetland that receives contaminated groundwater discharge. The methodology used by the author consisted of taking samples of the wetland sediment from the upper peat unit, between 0 and 25 cm depth. Subsequently, these samples were sieved to eliminate the particles greater than 4.75 mm. Also, groundwater was collected from the same place as the sediment. Once at the laboratory, microcosms were constructed in 162-ml serum bottles using 1.5:1 volumetric ratio of groundwater to wetland sediments. In order to increase the concentration of PCA in these microcosms, a certain amount of this specie was put into them. The behavior of PCA and all its daughters were monitored for almost 35 days. The results obtained from this experiment were used in this ART3D example.

### 4.2.1.2 Simulation

Before simulating this problem, it was necessary to estimate the degradation rate and the decay fraction of all species, in order to fit the concentration predicted by the model into the experimental data. The result of this procedure is summarized in Table 4.2.1.2-1.

Table 4.2.1.2-1. Summary Degradation Parameters Estimated from Experimental Data

Parameter	Value	Parameter	Value
$K_{PCE}$	NA	$K_{CA}$	$0.15 \text{ day}^{-1}$
$K_{TeCA}$	$0.14 \text{ day}^{-1}$	$Ka_{CA}$	NA
$K_{TCE}$	$0.13 \text{ day}^{-1}$	$Y_{\text{all species/all species}}$	1.0
$K_{TCA}$	$0.13 \text{ day}^{-1}$	$F_{TCE/TeCA}$	0.02
$K_{cDCE}$	$0.15 \text{ day}^{-1}$	$F_{TCA/TeCA}$	0.33
$Ka_{cDCE}$	NA	$F_{cDCE/TeCA}$	0.45
$K_{dDCE}$	$0.09 \text{ day}^{-1}$	$F_{dDCE/TeCA}$	0.18
$Ka_{dDCE}$	NA	$F_{cDCE/TCE}$	0.85
$K_{11DCE}$	$0.05 \text{ day}^{-1}$	$F_{dDCE/TCE}$	0.1
$Ka_{11DCE}$	NA	$F_{11DCE/TCE}$	0.05
$K_{DCA}$	$0.001 \text{ day}^{-1}$	$F_{DCA/TCA}$	0.2
$Ka_{DCA}$	NA	$F_{VC/TCA}$	0.8
$K_{VC}$	$0.045 \text{ day}^{-1}$	$F_{CA/DCA}$	NA
$Ka_{VC}$	NA		

NA: Not applicable. The lab data used is not useful for evaluating these parameters

In Figures 4.2.1.2-1 through 4.2.1.2-4 are shown the predicted concentrations obtained after using ART3D, and furthermore, the data reported in Lora and Olsen (1999), for each specie.

Figure 4.2.1.2-1. Distribution of PCA and the Sum of Daughter Products

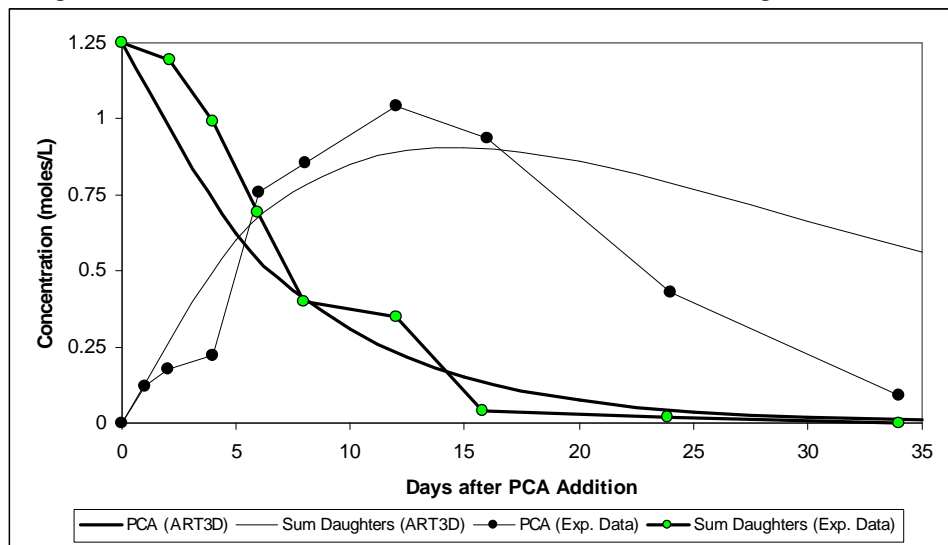


Figure 4.2.1.2-2. Distribution of TCA and DCA

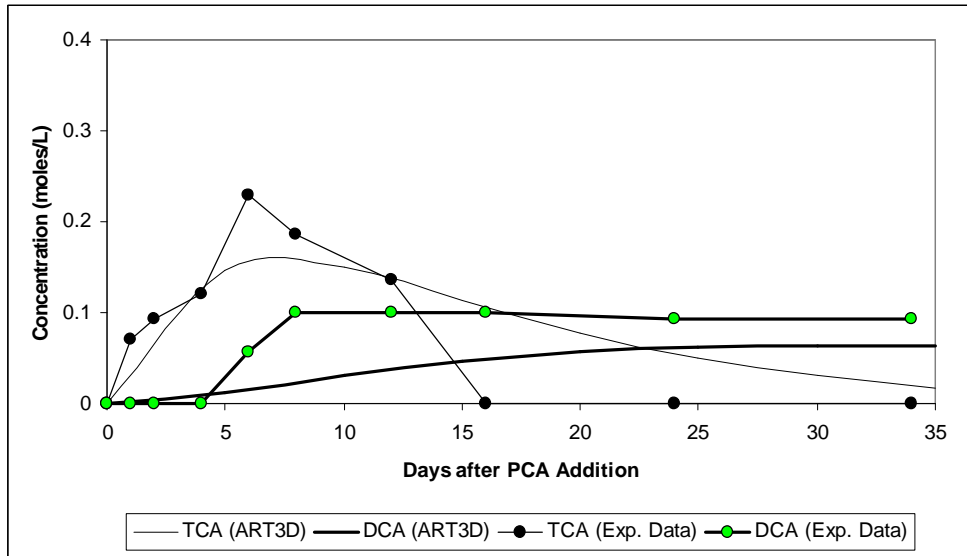


Figure 4.2.1.2-3. Distribution of VC and DCE

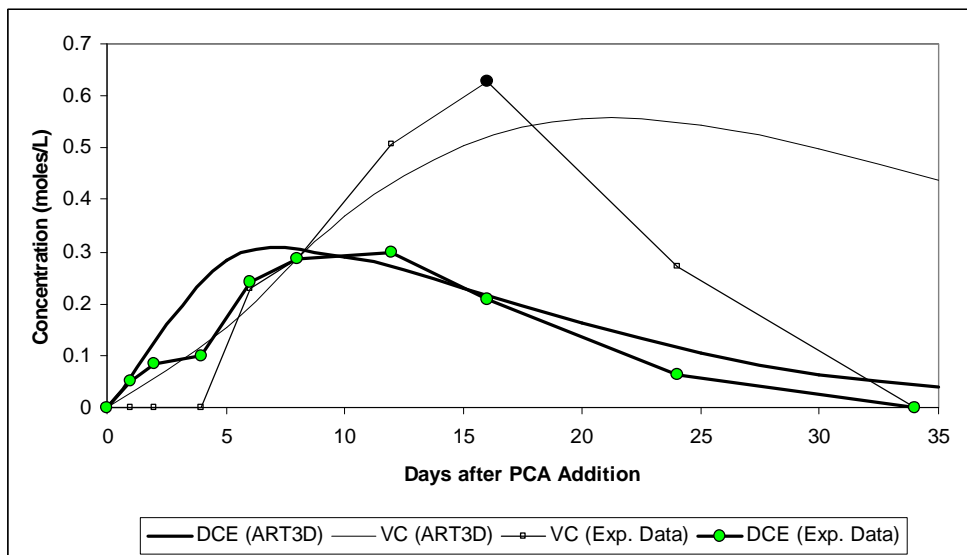
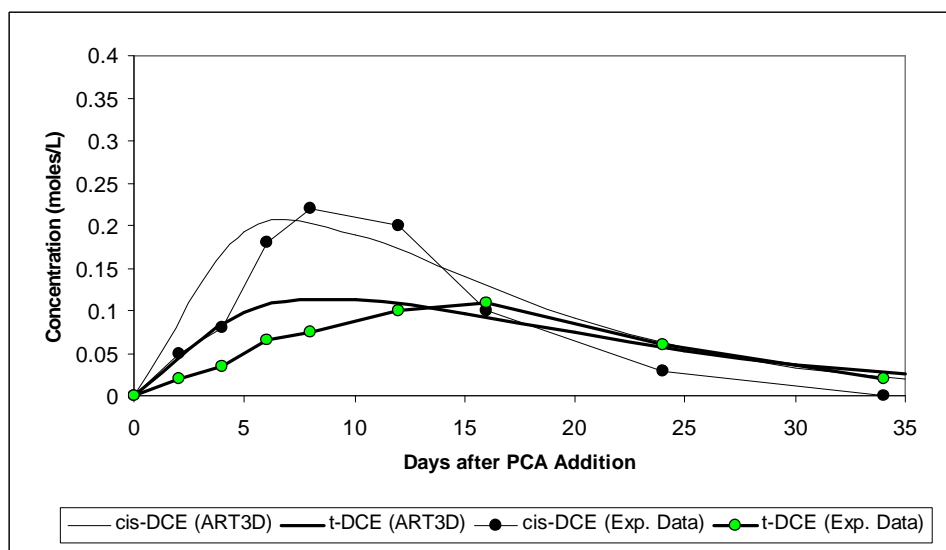


Figure 4.2.1.2-3. Distribution of cis- and trans-DCE isomers



It can be observed from these figures that the model can reproduce fairly well the behavior of all the species monitored, except for VC. ART3D predicted satisfactory the trend of the experimental data recorder for VC throughout the first fifteen days, but after this period of time, the model indicated that the VC degradation is slower than the one indicated by the experimental data. The explanation of this difference seems to be that VC presented two different degradation rate, one applied to the first fortnight, and a second one applied to the rest of the period. In order to fit the result from the simulation into the laboratory data, it must be considered a degradation rate value for the second period higher than the first one, but ART3D has not the capability of using different parameter values for one single variable.

In this particular example, given the features geochemical and microbiological of the wetland sediments, the main degradation pathway is the Dichloroelimination. This statement can be confirmed from the Figures 4.2.2-2 and 4.2.2-3, where the DCE concentration produced from TeCA is higher than the TCA concentration. Similar situation is found in the concentration of DCA and VC, where this last specie presents a greater concentration. VC and DCE come from a Dichloroelimination and TeCA and DCA from a Hydrogenolysis.

## 4.2.2 Second problem-NPC services, Inc. (2000)

### 4.2.2.1 Description Problem

This experiment had as objective to observe the natural attenuation of PCA and its subsequent degradation products at the NPC Services Inc. Brooklawn Site. Some samples of clay and alluvial sediments were collected from this site in order to conduct some microcosm tests. These sediment samples, clay and alluvial, were tested in separated

microcosms to evaluate the variability in natural attenuation activity between the geologic setting. Several experimental conditions were evaluated in this study, three of which were established with both TeCA and PCE to assess the effects of having both chlorinated ethenes and ethanes in the same microcosms. The behavior of PCA and all its daughters were monitored for almost 90 days.

#### 4.2.2.2 Simulation

The experimental data obtained from this study were used as input data for ART3D. Owing to the fact that some parameter values were not estimated in that study, it was necessary to assign them certain proper magnitudes before running the model. Table 4.2.2.2-1 presents the associated rate coefficients and decay fractions estimated from the microcosm data, besides the values utilized in ART3D.

Table 4.2.2.2-1. Summary Degradation Parameters Estimated from Experimental Data and Values Used in ART3D.

Parameter	Units	Estimated Reaction Parameters	
		Alluvium Microcosms	Values used in ART3D
$K_{PCE}$	day <sup>-1</sup>	ND <sup>a</sup>	0.20
$K_{TECA}$	day <sup>-1</sup>	0.14 ± 0.004	0.14
$K_{TCE}$	day <sup>-1</sup>	ND <sup>a</sup>	0.21
$K_{TCA}$	day <sup>-1</sup>	= 0.10 ± 0.005 <sup>b</sup>	0.10
$K_{CDCE}$	day <sup>-1</sup>	0.09 ± 0.02 <sup>b</sup>	0.07
$K_{TDCE}$	day <sup>-1</sup>	= 0.067 ± 0.007 <sup>b</sup>	0.06
$K_{DCA}$	day <sup>-1</sup>	= 0.12 ± 0.003	0.12
$K_{VC}$	day <sup>-1</sup>	0.06	0.06
$F_{TCE/TECA}$	mol/mol	0.0	0.00
$F_{CDCE/TECA}$	mol/mol	0.3	0.30
$F_{TDCE/TECA}$	mol/mol	0.7	0.70
$F_{TCA/TECA}$	mol/mol	ND <sup>a</sup>	0.00
$F_{CDCE/TCE}$	mol/mol	ND <sup>a</sup>	0.50
$F_{TDCE/TCE}$	mol/mol	ND <sup>a</sup>	0.50
$F_{T11DCE/TCE}$	mol/mol	ND <sup>a</sup>	0.00
$F_{VC/TCA}$	mol/mol	1.0	1.00
$F_{DCA/TCA}$	mol/mol	ND <sup>a</sup>	0.00
$F_{VC/DCA}$	mol/mol	= 0.18 <sup>b</sup>	0.18

<sup>a</sup> ND denotes no data is available

<sup>b</sup> The “greater than” symbol denotes that the compound was depleted over the period the rate was determined. Hence, the actual values may be higher than estimated.

In Figures 4.2.2.2-1 through 4.2.2.2-2 are presented the predicted concentrations obtained after using ART3D, and furthermore, the data reported in NPC services (2000) for each species.

Figure 4.2.2.2-1. Distribution of TeCA and PCE

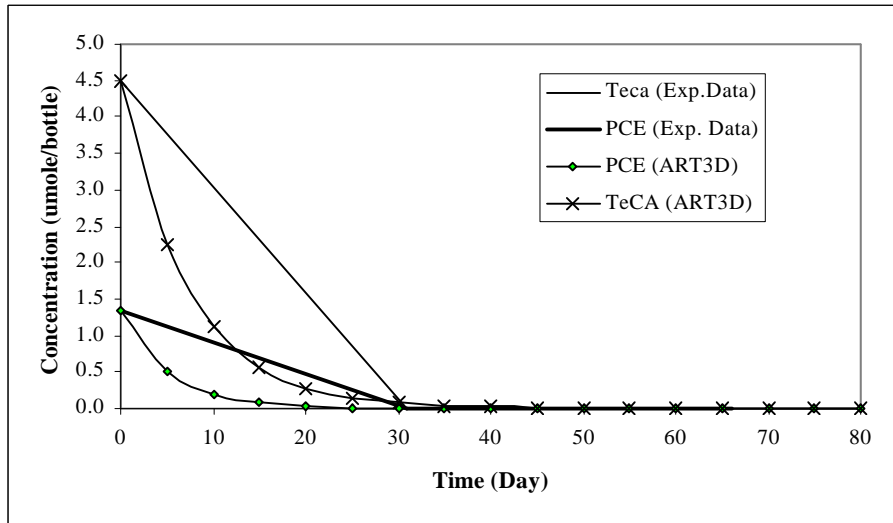
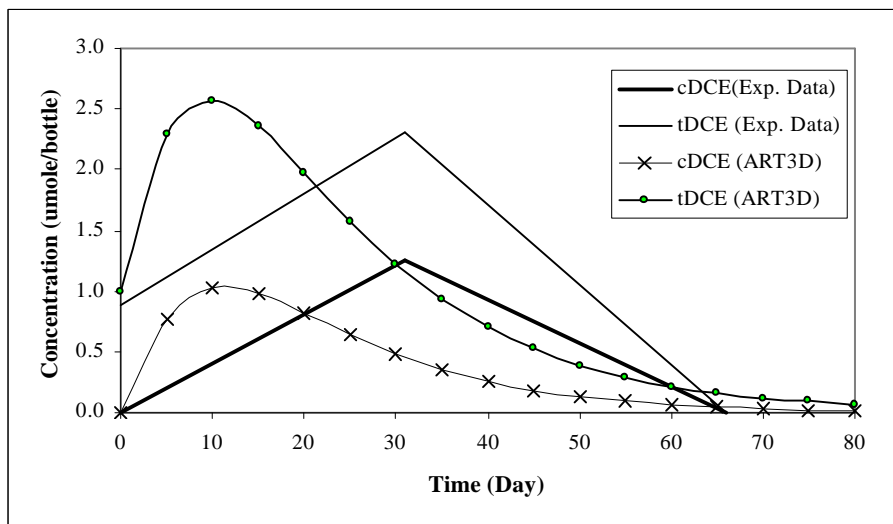
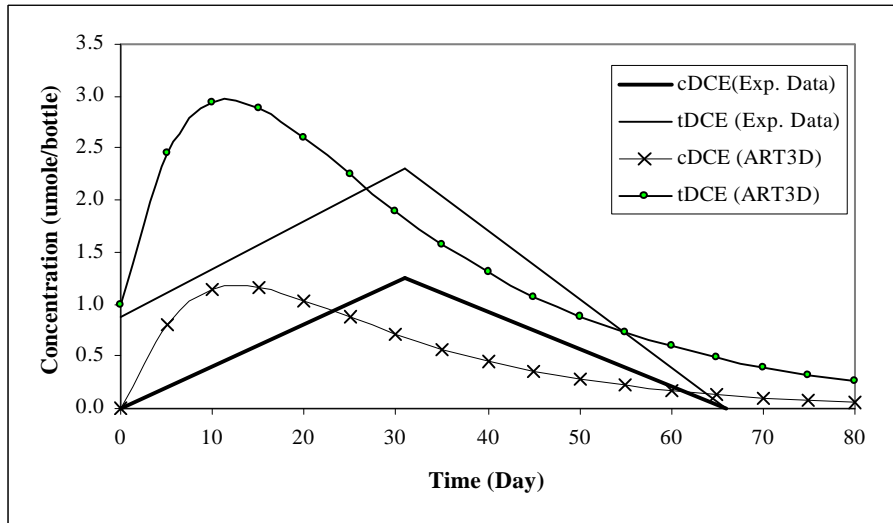


Figure 4.2.2.2-2. Distribution of cDCE and tDCE



It can be appreciated from the graphs that the predicted concentrations by the model fit pretty well for TeCA and PCE species, whereas for cDCE and tDCE, the simulated trend is long away from matching up with the experimental data. The explanation seems to be in the degradation rate value, which might not be constant throughout the period of monitoring. For example, a smaller degradation rate within the first 30 days would produce a greater concentration of both species during this period. This can be observed in Figure 4.2.2.2-3, where the degradation rate for cDCE and tDCE are  $0.05 \text{ day}^{-1}$  and  $0.04 \text{ day}^{-1}$  respectively.

Figure 4.2.2.2-3. Distribution of cDCE and tDCE - New Degradation Rates.



Although the degradation rates are fairly similar to the estimated in the study, the final results are better. If a higher K value could be used after the 30<sup>th</sup> day of monitoring, the predicted trend would follow the same behavior as the experimental data.

#### 4.2.3 Sensitivity Analysis-Initial PCA Concentration.

In order to know the influence of the initial PCA concentration on the other species, two new magnitudes of this parameter were considered to simulate the first example. The greatest value corresponds to 60 % higher than the initial concentration (2.0 moles/L) and the smallest one is equal to 0.75 moles/L (60 % initial concentration). Figures 4.2.3-1 through 4.2.3-8 show the predicted concentrations by the model for these two new initial PCA concentrations.

Figure 4.2.3-1. Increase of PCA and Sum Daughter (PCA: 2 mol/L)

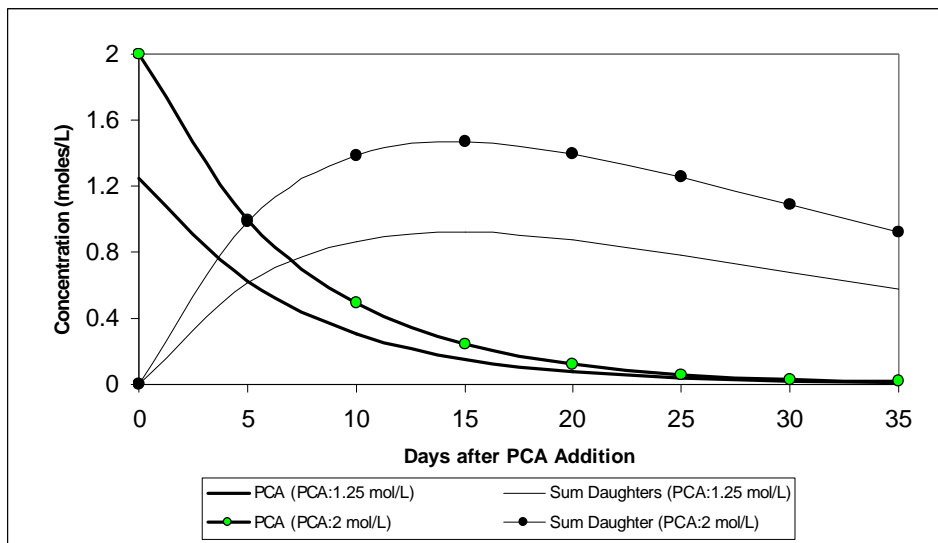


Figure 4.2.3-2. Increase of TCA and DCA (PCA: 2 mol/L)

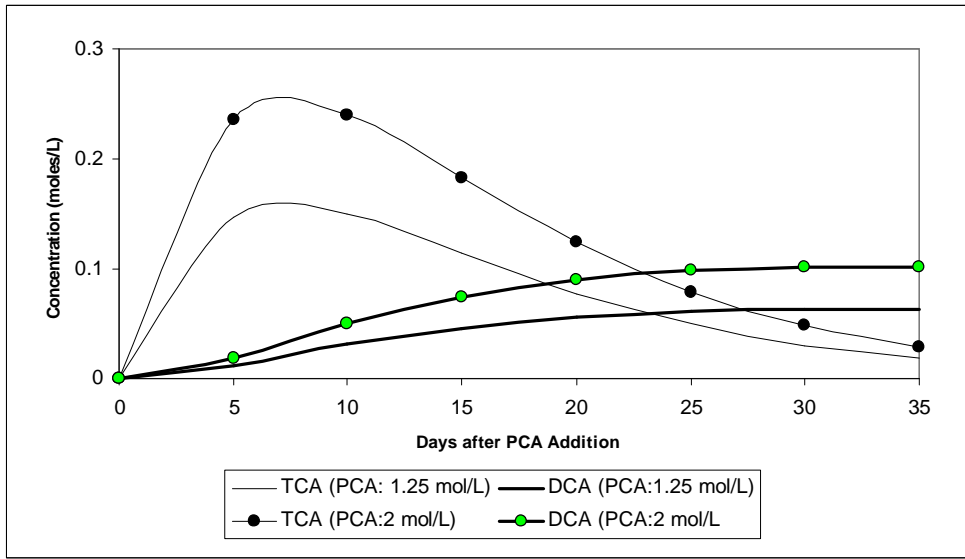


Figure 4.2.3-3. Increase of DCE and VC (PCA: 2 mol/L)

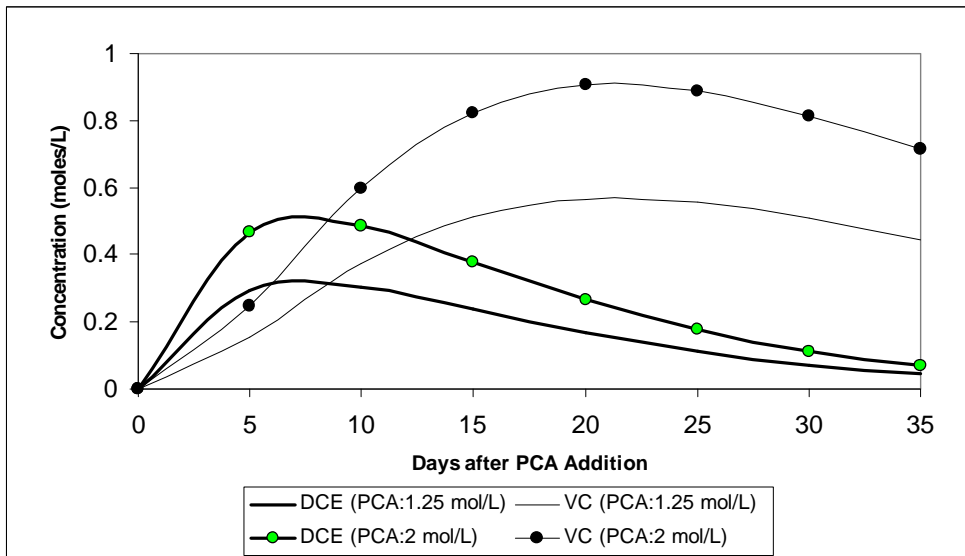


Figure 4.2.3-4. Increase of cis- and t-DCE (PCA: 2 mol/L)

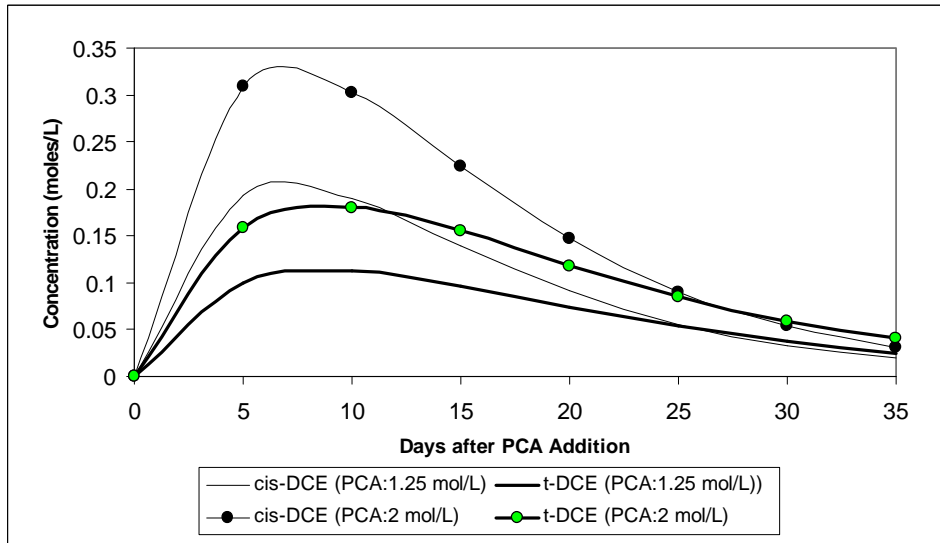


Figure 4.2.3-5. Increase of PCA and Sum Daughter (PCA: 0.75 mol/L)

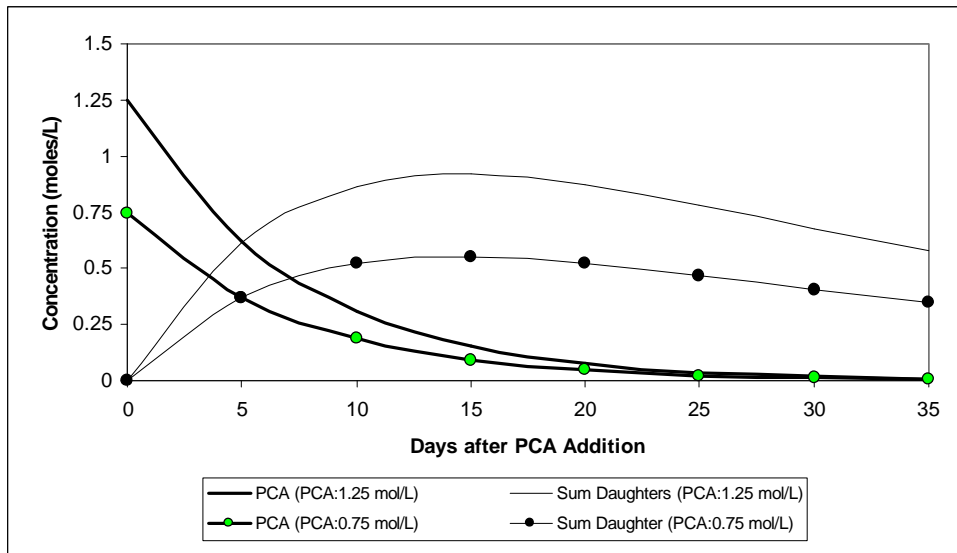


Figure 4.2.3-6. Increase of TCA and DCA (PCA: 2 mol/L)

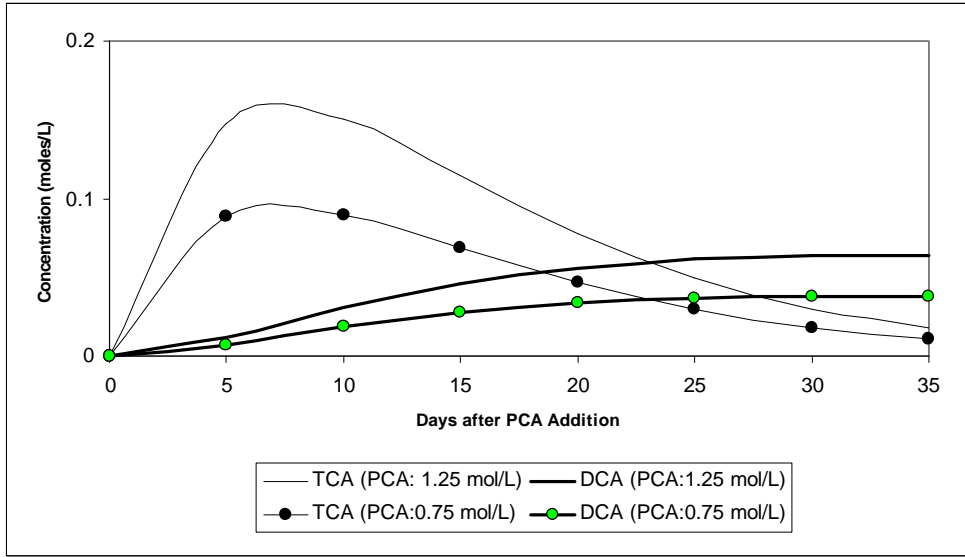


Figure 4.2.3-7. Increase of DCE and VC (PCA: 2 mol/L)

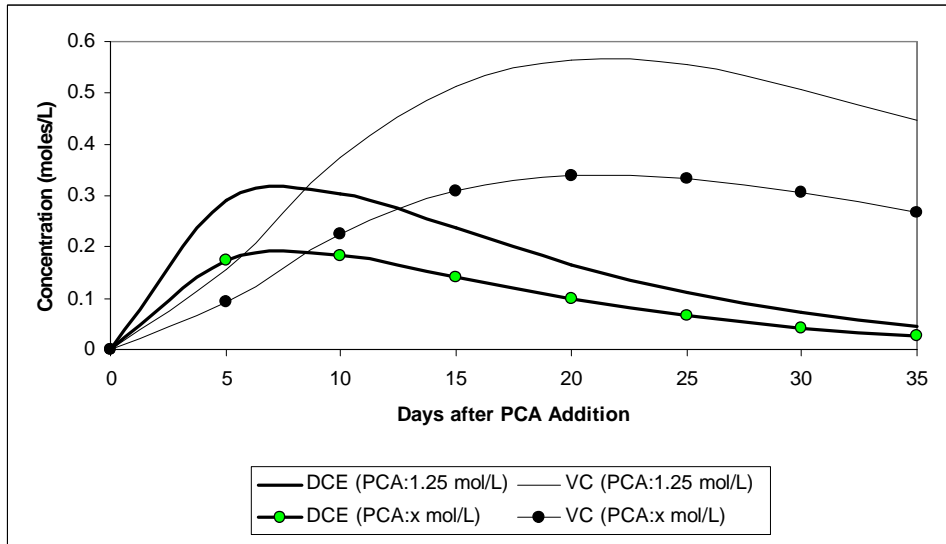
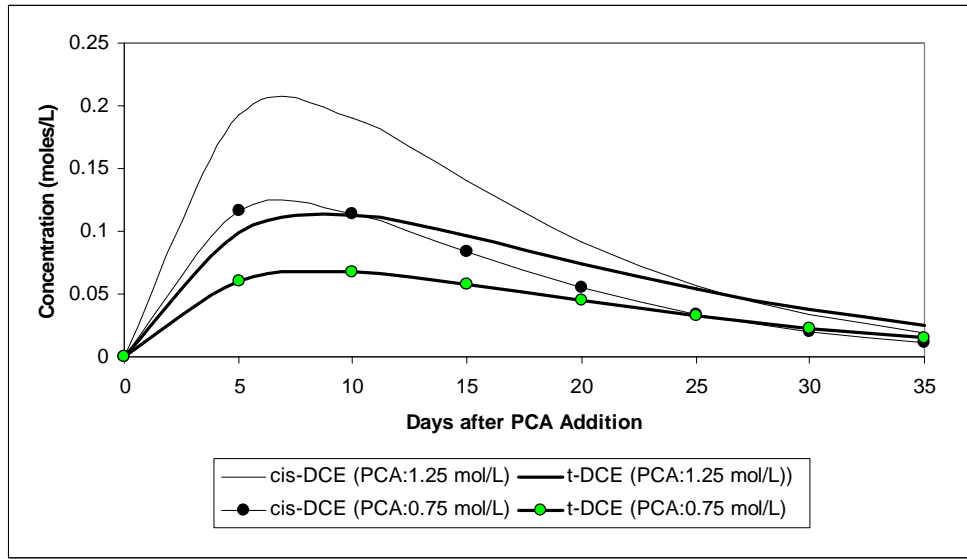


Figure 4.2.3-8. Increase of cis- and t-DCE (PCA: 2 mol/L)



In both cases, when PCA initial concentration equal to 2.0 mol/l and equal to 0.75 mol/L, the predicted concentration followed the same rules. The results indicate that when the PCA concentration swells in 60 %, the predicted concentration of the all the species suffer the same **porcentual** increase. In the case of a reduction of the initial concentration, the rest of the species reduce their concentration in the same percentage as PCA. This behavior can be observed throughout the period of monitoring, for example, the original concentration of TCA, 15 days after the PCA addition, was of 0.114 mol/L.. After applying the new two values of PCA, the predicted concentrations of TCA were 0.183 mol/L and 0.069 mol/L, that is, 160 % and 40 % of the original value.

The immediately consequence of this result is that it will be possible to know the concentration of all the species, for all the possible values of the PCA initial concentration, at any time, without running the model. Although this seems to be a great discovery, exist an explanation to these results. As noted previously, the decay fraction  $F_{D/P}$  is the mole fraction of a parent species "p" that will degrade and produce a specific daughter product "d". In order to conserve mass balance, the value of this parameter must be constrained by the following relations:

$$\frac{F_{TCE}}{TeCA} + \frac{F_{TCA}}{TeCA} + \frac{F_{tDCE}}{TeCA} + \frac{F_{cDCE}}{TeCA} = 1 \quad (22)$$

$$\frac{F_{1tDCE}}{TCE} + \frac{F_{tDCE}}{TCE} + \frac{F_{cDCE}}{TCE} = 1 \quad (23)$$

$$\frac{F_{DCA}}{TCA} + \frac{F_{VC}}{TCA} = 1 \tag{24}$$

$$\frac{F_{CA}}{DCA} \leq 1 \tag{25}$$

After analyzing the expressions before, it is clear that any increase or reduction on the PCA initial concentration will be distributed into its daughters considering a constant proportion. Therefore, in this example, when PCA concentration swelled in 60 %, all its daughters increased their concentration in the same percentage.

### 4.3 Transport Problem Example

#### 4.3.2 Problem Description and Simulation

The data used to test the transport mode of ART3D, when PCE, PCA and their daughters are disposed of at the same sites, correspond to the information utilized in the PCE example (Cape Canaveral Air Station, Florida). The features of the field and the hydrogeology were kept exactly as in that example, but, in this new application, the source presents discharges of PCA, TCA and DCA, beside PCE, TCE, DCE and VC. In order to know the influence of PCA and the product of its degradation on the degradation of PCE, the source concentrations of PCE and its daughters were not modified. This let us quantify the changes on their concentration distribution because of the presence of PCA in the aquifer system. A summary of the parameters utilized to simulate this problem is shown in Table 4.3.1-1.

Table 4.3.1-1. Parameter Used in Example.

DATA TYPE	Parameter	Value
Hydrogeology	• Hydraulic Conductivity	1.8e-2 (cm/sec)
	• Hydraulic Gradient	0.0012
	• Effective Porosity	0.2
Dispersion	• Longitudinal Dispersivity	40 (ft)
	• Transverse Dispersivity	4.0 (ft)
	• Vertical Dispersivity	0.0 (ft)
Adsorption	• Retardation Factor	2.9
Biotransformation	• Kpce	0.0055 (1/day)
	• Kteca	0.004 (1/day)
	• Ktce	0.0027 (1/day)
	• Ktca	0.0125(1/day)
	• Kcdce	0.0019 (1/day)
	• Kacdce	0.0 (1/day)
	• Ktdce	0.009 (1/day)
	• Katdce	0.0 (1/day)
	• K11dce	0.005 (1/day)
	• Ka11dce	0.0 (1/day)
	• Kdca	0.005 (1/day)
	• Kadca	0.0 (1/day)
	• Kvc	0.0011 (1/day)
	• Kavc	0.0 (1/day)
	• Kca	0.0014 (1/day)
	• Kaca	0.0 (1/day)
• Ytcepce	0.79	

	<ul style="list-style-type: none"> <li>• YtceTeca</li> <li>• YtcaTeca</li> <li>• YdceTeca</li> <li>• YdceTeca</li> <li>• Ydcatca</li> <li>• Yvcdce</li> <li>• Yvctca</li> <li>• Ycadca</li> <li>• FtceTeca</li> <li>• FtcaTeca</li> <li>• FcdceTeca</li> <li>• FtdceTeca</li> <li>• FcdceTeca</li> <li>• FtdceTeca</li> <li>• F11dceTeca</li> <li>• Fdcatca</li> <li>• Fvctca</li> <li>• Fcadca</li> </ul>	<ul style="list-style-type: none"> <li>0.78</li> <li>0.8</li> <li>0.74</li> <li>0.58</li> <li>0.74</li> <li>0.64</li> <li>0.47</li> <li>0.65</li> <li>0.02</li> <li>0.35</li> <li>0.45</li> <li>0.18</li> <li>0.85</li> <li>0.1</li> <li>0.05</li> <li>0.2</li> <li>0.8</li> <li>1.0</li> </ul>
Source Data	<ul style="list-style-type: none"> <li>• Source Thickness</li> <li>• Source Width</li> <li>• Source Concentrations</li> <li>PCE</li> <li>Teca</li> <li>TCE</li> <li>TCA</li> <li>t-DCE</li> <li>cis-DCE</li> <li>1,1-DCE</li> <li>DCA</li> <li>VC</li> <li>CA</li> </ul>	<ul style="list-style-type: none"> <li>56 (ft)</li> <li>105 (ft)</li> <li>(mg/L)</li> <li>0.056</li> <li>57.0</li> <li>15.8</li> <li>100.0</li> <li>0.8</li> <li>98.5</li> <li>0.0</li> <li>50.0</li> <li>3.08</li> <li>0.0</li> </ul>

In Figures 4.3.1-1 through 4.3.1-3 are shown the predicted concentrations of all eight species in the centerline, after 33 years of reactive transport.

Figure 4.3.1-1. Centerline Concentration of Teca, TCA, VC and DCE (Total)

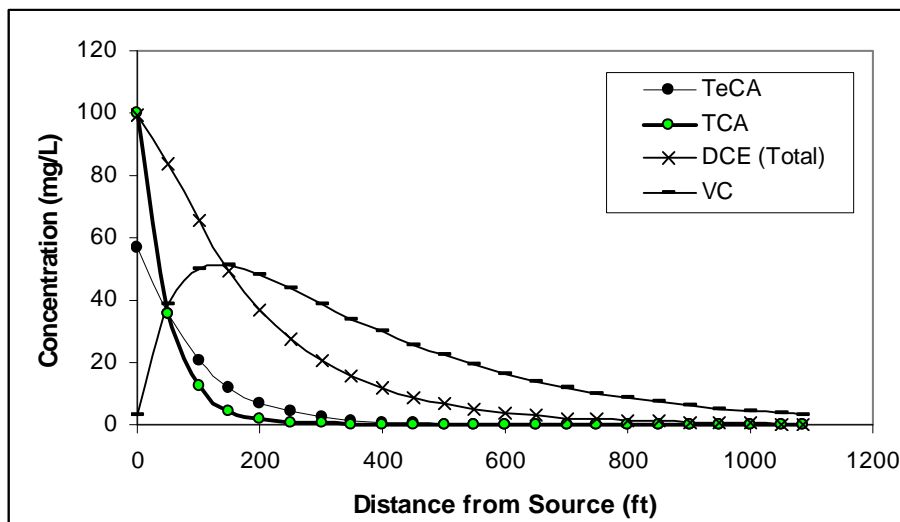


Figure 4.3.1-2. Centerline Concentration of TCE, DCA and CA

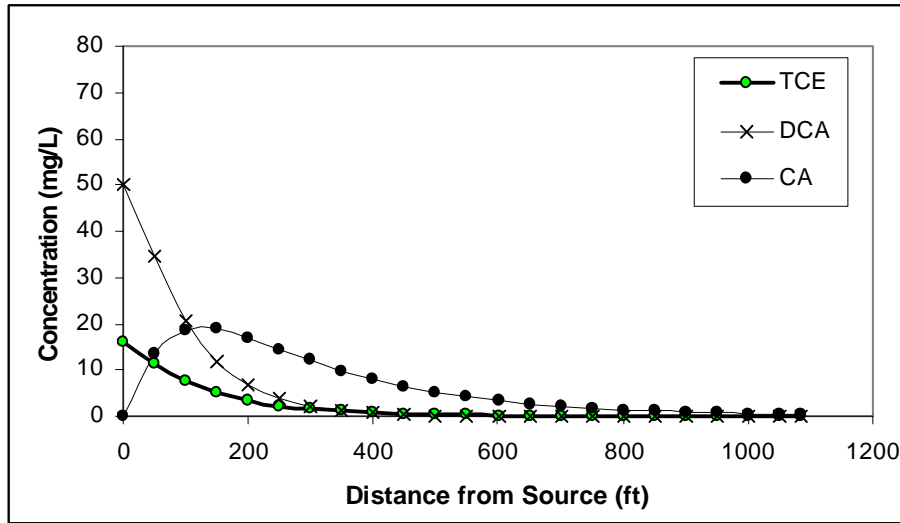
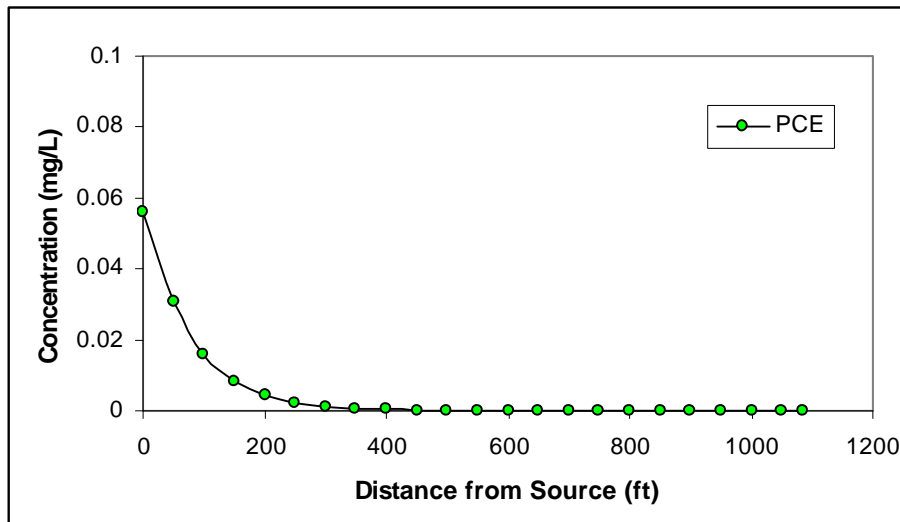
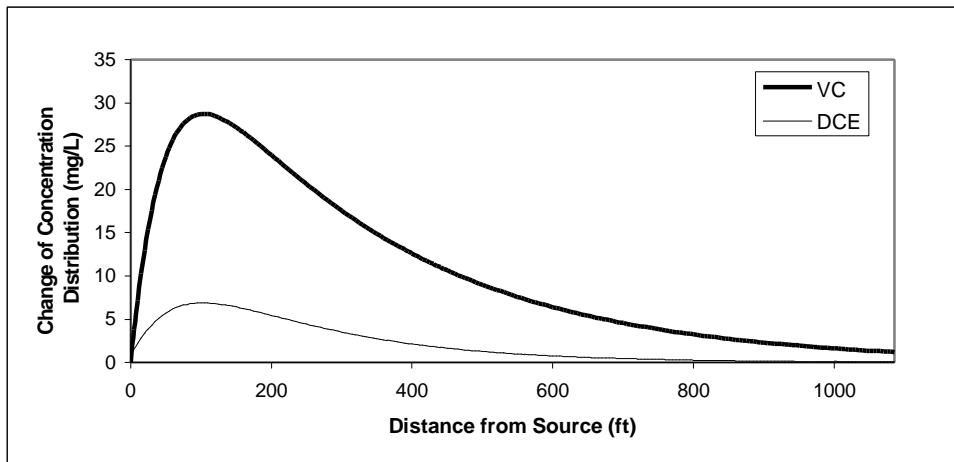


Figure 4.3.1-3. Centerline Concentration of PCE



After comparing the results obtained in this situation against the results of the simulation without PCA, it is easy to note that the influence of this last specie on PCE degradation is appreciated mainly in the final concentration of DCE and VC. Both of them have swelled their concentration in the studied site, and furthermore, the major increase was observed in the area located within the source and 400 ft from this (Figure 4.3.1-4). Also, TCE suffered some changes of concentration, but in a smaller scale.

Figure 4.3.1-4. Increase of concentration of DCE and VC.



The reason of this rise in the concentration of DCE and VC, and the distribution of this increase can be explained through the Figure 4.1-1. Initially, when PCA was not present in the aquifer system, the DCE concentration only depended on the TCE degradation. When PCA was put into the aquifer, the production of DCE swelled, since TeCA and TCE produce it in their degradation process. Owing to the fact that DCE is the first daughter of TeCA, beside TCA, its concentration started to augment immediately after the source. Conversely, if DCE was produced at the end of the PCA degradation process, the transport of the species created earlier, by the groundwater flow, would produce that the DCE concentration swell more far from the source than the original example.

The factors that affected the VC concentration and its distribution are quite similar to the mention before. In this case, VC is produce by TCA and DCE, whose concentration is influenced by TeCA.

In short, the existence of PCA and TCA at the same place of PCE and its daughters will produce an increase of the concentration of these last species. The magnitude of this influence will depend on the concentration of PCA and TCA at the source.

In Figures 4.3.1-5 through 4.3.1-12 are given the two dimensional contours (at the water table) for each species of this example.

Figure 4.3.1-5. Concentration of PCE at the Water Table (mg/l).

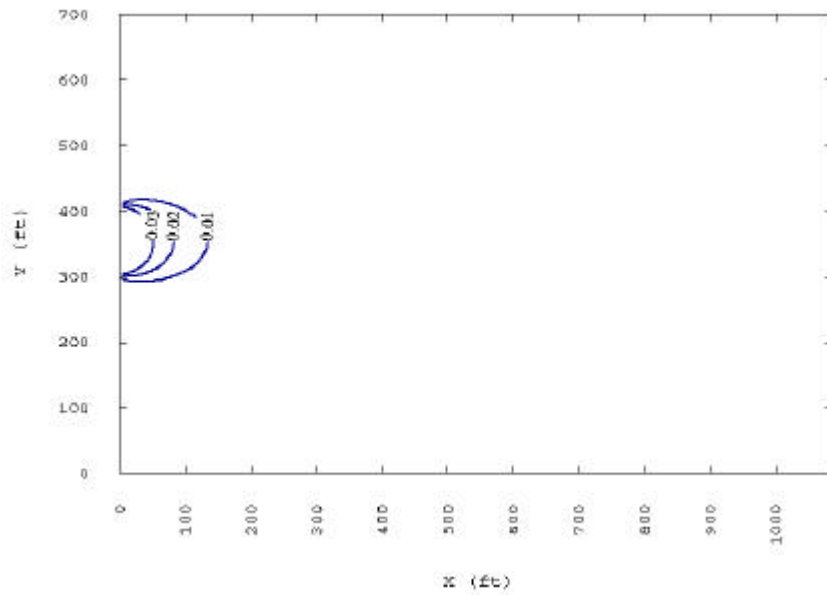


Figure 4.3.1-6. Concentration of TeCA at the Water Table (mg/l).

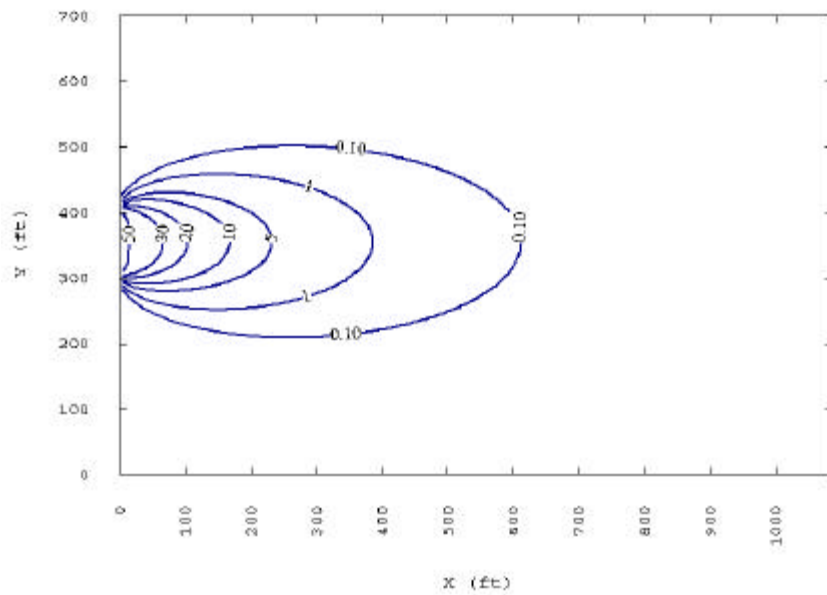


Figure 4.3.1-7. Concentration of TCE at the Water Table (mg/l).

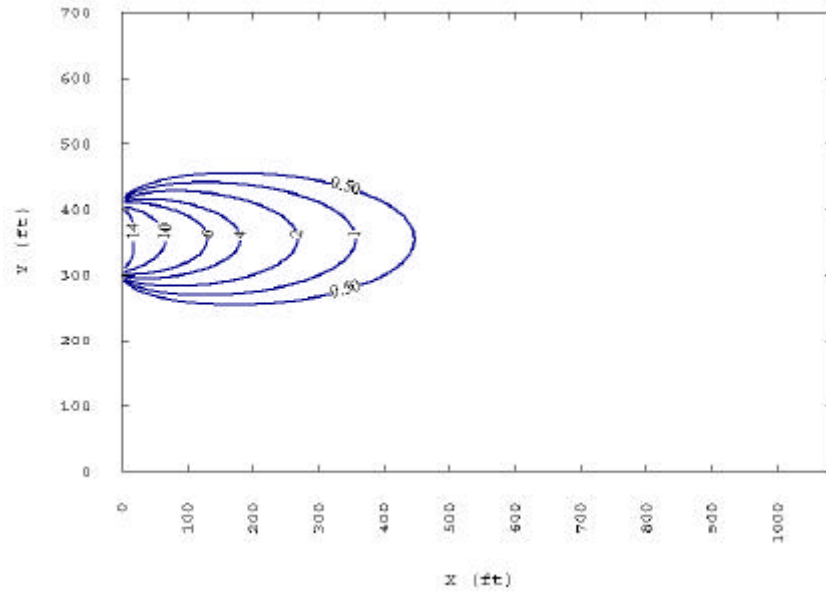


Figure 4.3.1-8. Concentration of TCA at the Water Table (mg/l).

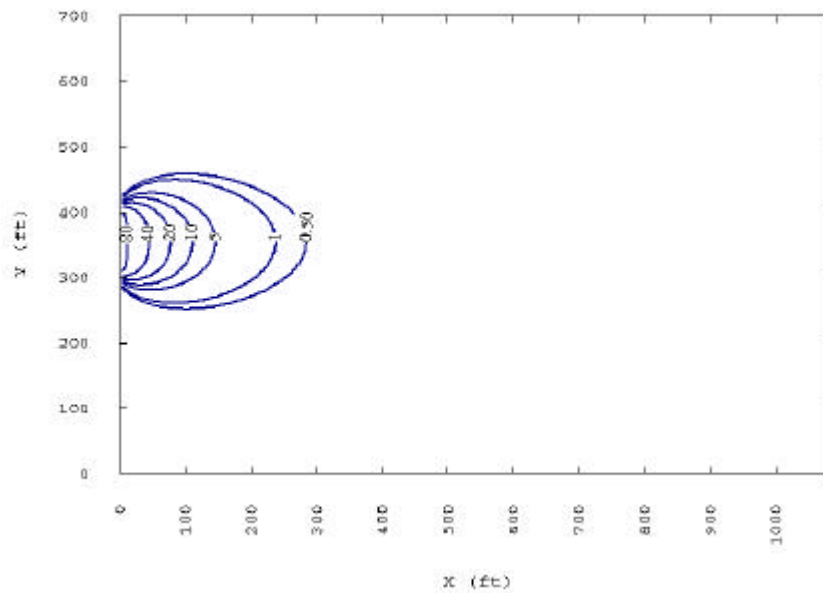


Figure 4.3.1-9. Concentration of DCE (Total) at the Water Table (mg/l).

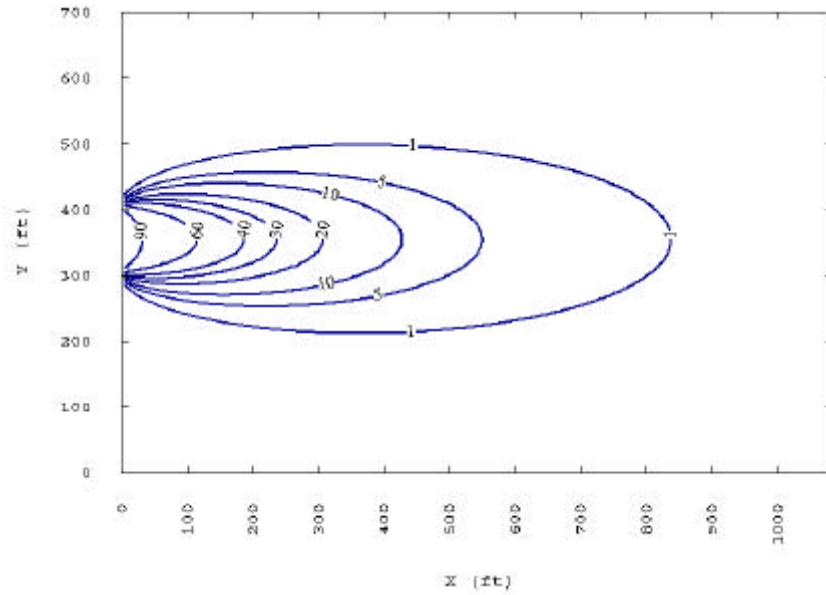


Figure 4.3.1-10. Concentration of DCA at the Water Table (mg/l).

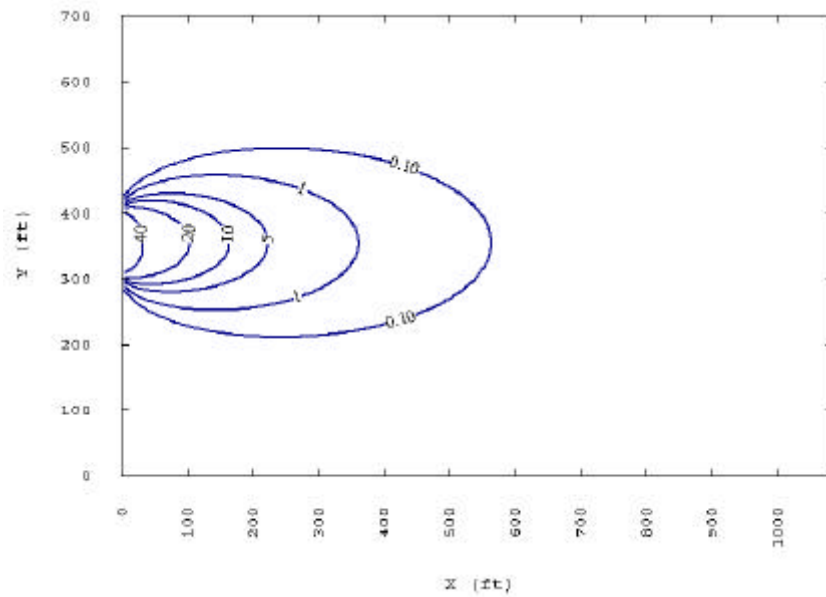


Figure 4.3.1-11. Concentration of VC at the Water Table (mg/l).

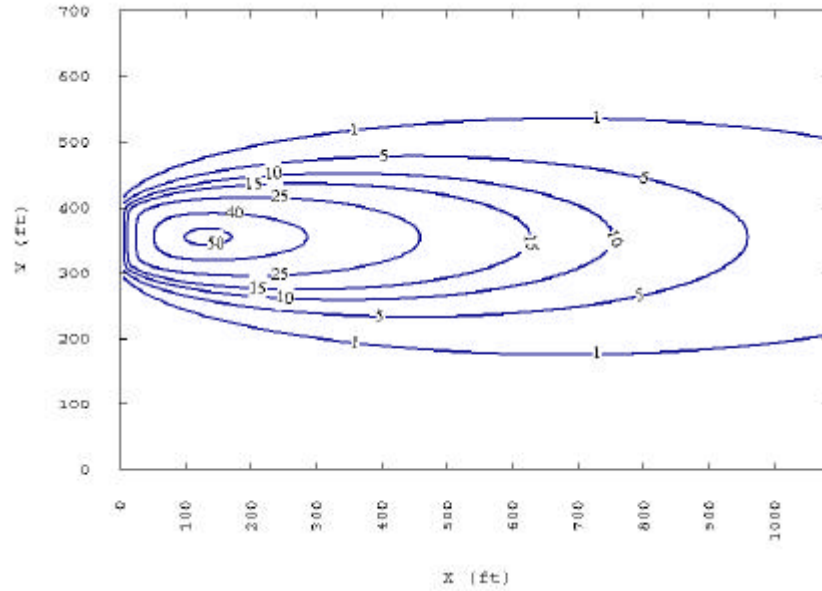
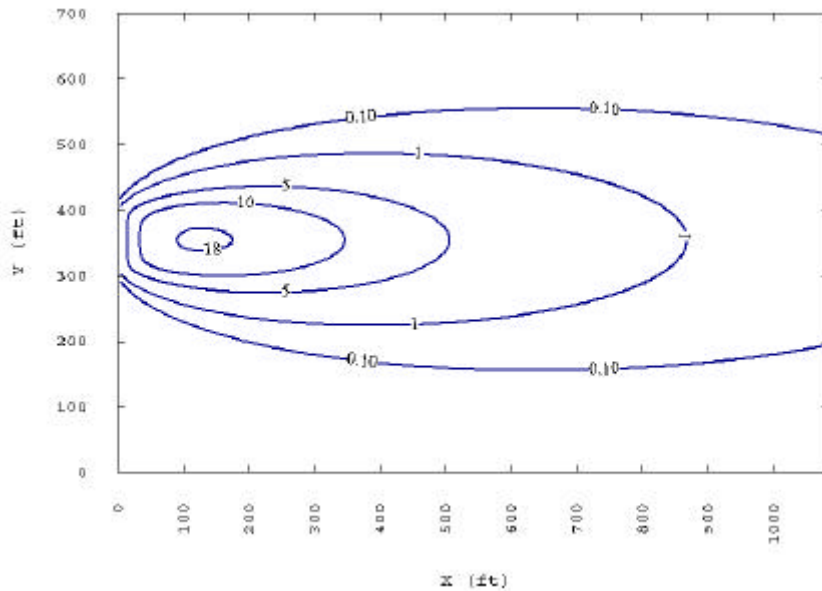


Figure 4.3.1-12. Concentration of CA at the Water Table (mg/l).



### 4.3.3 Sensitivity Analysis-Initial PCA concentration

According to the results obtained previously, as for the influence of the PCA and TCA on the concentration distribution of DCE and VC, the direct consequence is that ART3D model is quite sensible to the concentrations of PCA and TCA. As was mentioned in Batch example, changes on magnitudes of PCA and TCA concentrations produce that ART3D predicts increase of the concentration proportional to these changes.

It is important to emphasize that, in this example, the highest rise in the concentrations is found near the source, and, as the contaminant approaches the canal, its concentration starts falling slowly until to reach a magnitude pretty similar to the initial case. This remark is important, since if we want to evaluate the concentration near the canal, the magnitude obtained will not change considerably to different values of the concentration of PCA and TCA, unless these are so high.

As a result of the mention in the paragraph before, the sensibility of ART3D, for this example, will depend on the aim desired, that is, if the objective is to calculate the amount of contaminant at the canal location, the results will not present high changes. On the other hand, if the main goal is to predict the concentration nearer the source, any small variation of PCA and TCA concentrations will generate significant changes in the concentration of the other species.

### 4.3.4 Sensitivity Analysis-Rate Coefficient

In order to know the importance of PCA and TCA rate coefficients on the behavior of the other species, the case study problem was run with two different values of this parameter. The first magnitude corresponded to original values multiply by 2, and in the other simulation, the rate coefficients were 0.5 fold those used in the original example. In Table 4.3.3-1 is shown a summary of the values considered to conduct this analysis.

Table 4.3.3-1. Summary of Rate Coefficient

Specie	First order decay coefficient		
	0.5*K (1/day)	K (1/day)	2*K (1/day)
PCA	0.002	0.004	0.008
TCA	0.00625	0.0125	0.025
Others	They do not present modification		

The results obtained from both simulations are given in Tables 4.3.3-1a through 4.3.3-2b. These Tables show the maximum difference in the concentration and the percentage of increase of this in the centerline after comparing both simulations against the original one.

Table 4.3.3-1a. Increase of the concentration – 0.5\*K  
[Final simulation-Initial Simulation]

Distance (ft)	PCE (mg/L)	TeCA (mg/L)	TCE (mg/L)	TCA (mg/L)	Total DCE (mg/L)	DCA (mg/L)	VC (mg/L)	CA (mg/L)
0	0.000	0.000	0.000	0.000	0.000	0.000	0.000	0.000
50	0.000	7.961	-0.089	17.361	-2.049	-1.781	-6.896	-0.584
100	0.000	10.470	-0.093	14.544	-2.149	-0.915	-5.783	-0.786
150	0.000	10.192	-0.067	9.282	-1.593	-0.153	-3.631	-0.655
200	0.000	8.870	-0.038	5.484	-0.967	0.194	-2.004	-0.425
250	0.000	7.305	-0.015	3.196	-0.454	0.288	-0.952	-0.214
300	0.000	5.829	0.001	1.893	-0.087	0.272	-0.296	-0.059
350	0.000	4.562	0.011	1.157	0.150	0.222	0.111	0.041
400	0.000	3.525	0.016	0.734	0.289	0.169	0.363	0.099
450	0.000	2.700	0.018	0.484	0.358	0.125	0.514	0.128
500	0.000	2.056	0.018	0.330	0.380	0.091	0.599	0.137
550	0.000	1.559	0.017	0.231	0.372	0.067	0.638	0.135
600	0.000	1.179	0.015	0.165	0.346	0.049	0.645	0.126
650	0.000	0.889	0.013	0.120	0.312	0.036	0.630	0.114
700	0.000	0.670	0.011	0.088	0.274	0.026	0.599	0.102
750	0.000	0.504	0.009	0.065	0.237	0.019	0.561	0.089
800	0.000	0.379	0.007	0.048	0.201	0.014	0.516	0.077
850	0.000	0.285	0.006	0.036	0.169	0.011	0.469	0.066
900	0.000	0.214	0.005	0.027	0.141	0.008	0.422	0.055
950	0.000	0.161	0.004	0.020	0.116	0.006	0.375	0.047
1000	0.000	0.121	0.003	0.015	0.095	0.005	0.330	0.039
1050	0.000	0.091	0.002	0.011	0.077	0.003	0.288	0.032
1085	0.000	0.074	0.002	0.009	0.067	0.003	0.260	0.028

Table 4.3.3-1b. Percentage of increase – 0.5\*K  
[(Final Sim.-Initial Sim.)/Initial. Sim.]\*100

Distance (ft)	PCE %	TeCA %	TCE %	TCA %	Total DCE %	DCA %	VC %	CA %
0	0.0	0.0	0.0	0.0	0.0	0.0	0.0	0.0
50	0.0	22.5	-0.8	48.7	-2.5	-5.2	-17.8	-4.4
100	0.0	50.1	-1.2	115.3	-3.3	-4.4	-11.5	-4.3
150	0.0	83.9	-1.3	198.9	-3.2	-1.3	-7.1	-3.5
200	0.0	125.4	-1.1	292.2	-2.6	2.9	-4.2	-2.5
250	0.0	176.1	-0.6	384.0	-1.6	7.8	-2.2	-1.5
300	0.0	238.3	0.1	467.1	-0.4	13.3	-0.8	-0.5
350	0.0	314.5	1.0	543.7	1.0	19.4	0.3	0.4
400	0.0	407.8	2.2	622.5	2.5	26.3	1.2	1.2
450	0.0	522.1	3.7	715.3	4.1	34.5	2.0	2.0
500	0.0	662.3	5.4	831.6	5.7	44.3	2.7	2.7
550	0.0	834.0	7.4	979.3	7.4	57.3	3.3	3.3
600	0.0	1044.6	9.6	1166.8	9.1	73.3	3.9	3.8
650	0.0	1301.6	12.1	1407.7	10.9	93.9	4.5	4.3
700	0.0	1617.8	14.9	1706.1	12.7	117.7	5.0	4.8
750	0.0	2003.3	17.6	2076.9	14.5	148.7	5.5	5.3
800	0.0	2476.0	19.9	2522.3	16.2	188.9	6.0	5.7
850	0.0	3055.8	24.7	3105.9	18.0	254.9	6.5	6.1
900	0.0	3760.9	29.7	3818.6	19.8	317.4	6.9	6.3
950	0.0	4632.3	34.4	4631.3	21.5	406.3	7.3	6.7
1000	0.0	5693.6	37.2	5681.0	23.2	576.1	7.6	7.0
1050	0.0	6996.2	35.8	6806.9	24.9	586.4	7.9	7.2
1085	0.0	8017.9	46.3	7849.3	26.3	847.6	8.1	7.4

Table 4.3.3-2a. Increase of the concentration – 2.0\*K  
[Final simulation-Initial Simulation]

Distance (ft)	PCE (mg/L)	TeCA (mg/L)	TCE (mg/L)	TCA (mg/L)	Total DCE (mg/L)	DCA (mg/L)	VC (mg/L)	CA (mg/L)
0	0.000	0.000	0.000	0.000	0.000	0.000	0.000	0.000
50	0.000	-9.715	0.111	-15.717	2.569	1.700	6.645	0.544
100	0.000	-9.905	0.085	-8.371	1.955	0.398	3.806	0.580
150	0.000	-7.514	0.039	-3.605	0.928	-0.181	1.698	0.379
200	0.000	-5.119	0.005	-1.551	0.203	-0.292	0.599	0.178
250	0.000	-3.316	-0.012	-0.715	-0.194	-0.253	0.027	0.039
300	0.000	-2.090	-0.019	-0.359	-0.366	-0.186	-0.277	-0.042
350	0.000	-1.298	-0.020	-0.193	-0.412	-0.128	-0.434	-0.084
400	0.000	-0.798	-0.018	-0.110	-0.392	-0.086	-0.504	-0.099
450	0.000	-0.488	-0.015	-0.064	-0.344	-0.057	-0.523	-0.100
500	0.000	-0.298	-0.012	-0.038	-0.289	-0.037	-0.509	-0.094
550	0.000	-0.181	-0.010	-0.023	-0.236	-0.024	-0.477	-0.084
600	0.000	-0.110	-0.007	-0.014	-0.189	-0.015	-0.436	-0.072
650	0.000	-0.067	-0.005	-0.008	-0.149	-0.010	-0.393	-0.061
700	0.000	-0.041	-0.004	-0.005	-0.117	-0.006	-0.348	-0.051
750	0.000	-0.025	-0.003	-0.003	-0.091	-0.004	-0.305	-0.043
800	0.000	-0.015	-0.002	-0.002	-0.070	-0.002	-0.266	-0.035
850	0.000	-0.009	-0.001	-0.001	-0.054	-0.002	-0.230	-0.029
900	0.000	-0.006	-0.001	-0.001	-0.041	-0.001	-0.198	-0.023
950	0.000	-0.003	-0.001	0.000	-0.032	-0.001	-0.169	-0.019
1000	0.000	-0.002	-0.001	0.000	-0.024	0.000	-0.144	-0.015
1050	0.000	-0.001	0.000	0.000	-0.019	0.000	-0.122	-0.012
1085	0.000	-0.001	0.000	0.000	-0.015	0.000	-0.108	-0.011

Table 4.3.3-2b. Percentage of increase – 2.0\*K  
[(Final Sim.-Initial Sim.)/Initial. Sim.]\*100

Distance (ft)	PCE %	TeCA %	TCE %	TCA %	Total DCE %	DCA %	VC %	CA %
0	0.0	0.0	0.0	0.0	0.0	0.0	0.0	0.0
50	0.0	-27.5	1.0	-44.1	3.1	4.9	17.1	4.1
100	0.0	-47.4	1.1	-66.4	3.0	1.9	7.6	3.1
150	0.0	-61.9	0.8	-77.3	1.9	-1.5	3.3	2.0
200	0.0	-72.3	0.1	-82.7	0.5	-4.4	1.2	1.0
250	0.0	-80.0	-0.5	-85.9	-0.7	-6.9	0.1	0.3
300	0.0	-85.4	-1.2	-88.6	-1.8	-9.1	-0.7	-0.3
350	0.0	-89.5	-1.9	-90.7	-2.6	-11.2	-1.3	-0.9
400	0.0	-92.3	-2.5	-93.3	-3.3	-13.4	-1.7	-1.2
450	0.0	-94.4	-3.1	-94.6	-3.9	-15.7	-2.0	-1.6
500	0.0	-96.0	-3.6	-95.8	-4.3	-18.0	-2.3	-1.8
550	0.0	-96.8	-4.4	-97.5	-4.7	-20.5	-2.5	-2.0
600	0.0	-97.5	-4.5	-99.0	-5.0	-22.4	-2.7	-2.2
650	0.0	-98.1	-4.6	-93.8	-5.2	-26.1	-2.8	-2.3
700	0.0	-99.0	-5.4	-96.9	-5.4	-27.2	-2.9	-2.4
750	0.0	-99.4	-5.9	-95.9	-5.6	-31.3	-3.0	-2.5
800	0.0	-98.0	-5.7	-105.1	-5.6	-27.0	-3.1	-2.6
850	0.0	-96.5	-4.1	-86.3	-5.8	-46.3	-3.2	-2.7
900	0.0	-105.4	-5.9	-141.4	-5.8	-39.7	-3.2	-2.6
950	0.0	-86.3	-8.6	0.0	-5.9	-67.7	-3.3	-2.7
1000	0.0	-94.1	-12.4	0.0	-5.9	0.0	-3.3	-2.7
1050	0.0	-76.9	0.0	0.0	-6.1	0.0	-3.4	-2.7
1085	0.0	-108.3	0.0	0.0	-5.9	0.0	-3.4	-2.9

The Tables indicate that changes of the first order decay coefficient in PCA and TCA do not modify to a large extent the concentration distribution of the other species. From the Tables 4.3.3.1a and 4.3.3.2b it is observed that the species with the highest percentage of increase are PCA and TCA, the rest of the species present a small variation. Although DCA registered a big percentage of increase in some place, the rise in its concentration in those locations is pretty small, therefore, the influence of PCA and TCA first order decay coefficient on DCA concentration can be considered negligible.

In short, the results indicated that, in this example, the model is more sensitive to changes in the PCA and TCA concentration at the source and less sensitive to changes in the first order decay coefficient of these species.

## 5 Conclusions

A new fortran code called ART3D is presented for solving multispecies equations coupled, considering or not transport, with multiparent, serial, parallel, converging, diverging, and/or reversible first-order reactions. This code lets solve the equations that describe the natural attenuation reactions (Batch solution), and also, the reactive transport of some chlorinated solvent species, such as PCA and PCE, in saturated groundwater systems. This new code has an interface with GMS, which help visualize two- or three-dimensional plume patterns.

ART3D solves coupled reactive transport problems using linear transformation techniques. Due to some constraints on matrixes operation, the developed methodology is limited to use the same retardation factor value for all the species. A second consequence of the mathematics procedure used is that if two species are related, that is, one species is daughter of other, then they can not have the same first order decay coefficient. Although this last consequence is not really a limitation of the model, certain warnings must be taken.

In order to test ART3D code in a sequential reactive system, two examples were solved and the results of these simulations compared with the solution obtained by other models. The first problem was a Batch example and the comparison was done with the results from a numerical solution obtained using RT3D. The second example corresponded to a real transport problem, which had already been solved using BIOCHLOR. In both cases, the concentrations distribution predicted by ART3D are quite similar to the obtained by the other models.

As was mention before, ART3D is capable to solve complex multispecies problems under first order reactive conditions. This feature permits reproduce the biotic and abiotic degradation pathways of both ethenes and ethanes contaminats. Laboratory data reported by Lorah and Olsen (1999) about this issue were used to test this new fortran code. The results indicated that ART3D predicted the observed trend of the majority of the chlorinated ethene and ethane.

Several sensitivity analyses were done for all the examples mention before, however, the results obtained from them must not be applied as a general rule.

The capabilities of ART3D and the results obtained after comparing its results against solution from other known methods and from laboratory data, permit to define ART3D as a useful tool to solve any multispecies equations coupled under first-order reactive conditions.

# **APPENDIX A**

## **(Input Files)**

### Batch\_RT3D.txt

```

Unit: mg/l, days
4      !number of species
0      !Used Code (0: Batch; 1: Transport)
Geometric Information
0      0      0      0      !nx,ny,nz,nt
0      0      0      !dx,dy,dz
K matrix
-0.005  0.00  0.00  0.00  !pce
0.00396 -0.003  0.00  0.00  !tce
0.00  0.002211 -0.002  0.00  !dce
0.00  0.00  0.00129 -0.001  !vc
Observation Time
1000   !observation time
Adsorption-Dispersion-Hydrogeology-Source
0      0      0      0      0      ! Retard,vel,alphax,alphay,alphaz
0      0      !Source-Dimensions
Initial Concentration
100.0  !pce
0.0    !tce
0.0    !dce
0.0    !vc
    
```

### Batch\_lorah.txt

```

Unit: mol/L, days
9      !number of species
0      !Used Code (0: Batch; 1: Transport)
Geometric Information
0      0      0      0      !nx,ny,nz,nt
0      0      0      !dx,dy,dz
K matrix
-0.14  0      0      0      0      0      0      0      0      !TeCA
0.0028 -0.13  0      0      0      0      0      0      0      !TCE
0.0462  0      -0.13  0      0      0      0      0      0      !TCA
0      0.0065  0      -0.05  0      0      0      0      0      !11DCE
0.063  0.1105  0      0      -0.15  0      0      0      0      !cDCE
0.0252  0.013  0      0      0      -0.09  0      0      0      !dDCE
0      0      0.026  0      0      0      -0.001  0      0      !DCA
0      0      0.104  0.05  0.15  0.09  0      -0.045  0      !VC
0      0      0      0      0      0      0.001  0      -0.15  !CA
Observation Time
35     !observation time
Adsorption-Dispersion-Hydrogeology-Source
0      0      0      0      0      ! Retard,vel,alphax,alphay,alphaz
0      0      !Source-Dimensions
Initial Concentration
1.25   !TeCA
0.0    !TCE
0.0    !TCA
0.0    !11DCE
0.0    !cDCE
0.0    !dDCE
0.0    !DCA
0.0    !VC
0.0    !CA
    
```

**Batch\_NPC.txt**

```

Unit: mg/l, days
9          !number of species
0          !Used Code (0: Batch; 1: Transport)
Geometric Information
0          0          0          0          !nx,ny,nz,nt
0          0          0          !dx,dy,dz
K matrix
-0.2      0          0          0          0          0          0          0          0          !PCE
0          -0.14     0          0          0          0          0          0          0          !TeCA
0.2       0          -0.21    0          0          0          0          0          0          !TCE
0          0          0          -0.1     0          0          0          0          0          !TCA
0          0          0          0          -0.05    0          0          0          0          !11DCE
0          0.042     0.105   0          0          -0.07    0          0          0          !cDCE
0          0.098     0.105   0          0          0          -0.06    0          0          !tDCE
0          0          0          0          0          0          0          -0.12    0          !DCA
0          0          0          0.1      0.05     0.07     0.06     0          -0.065   !VC
Observation Time
80        !observation time
Adsorption-Dispersion-Hydrogeology-Source
0          0          0          0          0          ! Retard,vel,alphax,alphay,alphaz
0          0          !Source-Dimensions
Initial Concentration
1.35      !PCE
4.5       !TeCA
0.169    !TCE
0.0       !TCA
0.0       !1.1DCE
0.0       !cDCE
0.99     !tDCE
0.0       !DCA
0.0       !VC
    
```

**Transp\_Pce (ex1).txt**

```

units:ft,years,mg/l
5          !number of species
1          !Used Code (0: Batch; 1: Transport)
Geometric Information
218       141       10        1          !nx,ny,nz,nt
5.0       5.0       5.6       !delx,dely,delz
K matrix
-2.00     0.0       0.0       0.0       0.0       !pce
1.58984   -1.00     0.0       0.0       0.0       !tce
0.0       0.73744   -0.7      0.0       0.0       !DCE
0.0       0.0       4.51E-01  -4.00E-01 0.0       !VC
0.0       0.0       0.0       0.17984   -1.00E-99 !ETH
Observation Time
33.0      !observation time
Adsorption-Dispersion-Hydrogeology-Source
2.9       111.7     40.0      4.0       1e-99     !retard,vel,alphax,alphay,alphaz
105.0     56.0      !ys and zs, source dimensions
Initial Concentration
0.056     !concentration specie 1 (PCE)
15.8      !concentration specie 2 (TCE)
98.5      !concentration specie 3 (DCE)
3.08      !concentration specie 4 (VC)
0.03      !concentration specie 5 (ETH)
    
```

### Transp\_Pce (ex2).txt

```

units:ft,years,mg/l
5          !number of species
1          !Used Code (0: Batch; 1: Transport)
Geometric Information
218      141      11      1          !nx,ny,nz,nt
5.0      5.0      5.0      !delx,dely,delz
K matrix
-2.00    0.0      0.0      0.0      0.0      !pce
1.58984  -1.00    0.0      0.0      0.0      !tce
0.0      0.73744  -0.7      0.0      0.0      !DCE
0.0      0.0      4.51E-01  -4.00E-01  0.0      !VC
0.0      0.0      0.0      0.17984  -1.00E-99 !ETH
Observation Time
33.0     !observation time
Adsorption-Dispersion-Hydrogeology-Source
2.9      111.7    40.0     4.0      0.4      !retard,ve1,alphax,alphay,alphaz
105.0    5.0      !ys and zs, source dimensions
Initial Concentration
0.056    !concentration specie 1 (PCE)
15.8     !concentration specie 2 (TCE)
98.5     !concentration specie 3 (DCE)
3.08     !concentration specie 4 (VC)
0.03     !concentration specie 5 (ETH)

```

### Transp\_Pca.txt

```

units:ft,days,mg/l
10       !number of species
1        !Used Code (0: Batch; 1: Transport)
Geometric Information
218      141      10      1          !nx,ny,nz,nt
5.0      5.0      5.6      !delx,dely,delz
K matrix
-0.005479452  0      0      0      0      0      0      0      0      0      !PCE
0      -0.004  0      0      0      0      0      0      0      0      !TeCA
0.004328767  0.0000624  -0.002739726  0      0      0      0      0      0      0      !TCE
0      0.001056  0      -0.0125  0      0      0      0      0      0      !TCA
0      0      0.00010137  0      -0.005  0      0      0      0      0      !11DCE
0      0.001044  0.001723288  0      0      -0.001917808  0      0      0      0      !cDCE
0      0.000464  0.00020274  0      0      0      -0.009  0      0      0      !dDCE
0      0      0      0.00185  0      0      0      -0.005  0      0      !DCA
0      0      0      0.0047  0.0032  0.001227397  0.00576  0      -0.00109589  0      !VC
0      0      0      0      0      0      0      0.00325  0      -0.0014  !CA
Observation Time
12045.0 !observation time
Adsorption-Dispersion-Hydrogeology-Source
2.9      0.31     40.0     4.0      1e-99    !retard,ve1,alphax,alphay,alphaz
105.0    56.0     !ys and zs, source dimensions
Initial Concentration
0.056    !PCE
57.0     !TeCA
15.8     !TCE
100.0    !TCA
0.0      !11DCE
98.5     !cDCE
0.8      !dDCE
50.0     !DCA
3.08     !VC
0.0      !CA

```